

**TELEVISION RECEIVER
DESIGN**

**FLYWHEEL SYNCHRONIZATION
OF SAW-TOOTH GENERATORS**

The series of books on Electronic Valves includes:

- Book I** **Fundamentals of Radio Valve Technique**
547 pages, 6" × 9", 384 illustrations.
- Book II** **Data and Circuits of Radio Receiver and Amplifier Valves**
424 pages, 6" × 9", 531 illustrations (1933/39).
- Book III** **Idem, 220 pages, 6" × 9", 267 illustrations (1940/41).**
- Book IIIA** **Idem, 487 pages, 505 illustrations (1945/50).**
- Book IIIB** **Idem, 1951/52 (in preparation).**
- Book IIIC** **Idem, on Television Valves (in preparation).**
- Book IV** **Application of the Electronic Valve in Radio Receivers and Amplifiers (Part I).**
(1) R.F. and I.F. amplification. (2) Frequency changing. (3) Determination of the tracking curve. (4) Interference and distortion due to curvature in characteristics of the receiver valves. (5) Detection.
440 pages, 6" × 9", 256 illustrations.
- Book V** **Application of the Electronic Valve in Radio Receivers and Amplifiers (Part 2)**
(6) A.F. amplification. (7) Output stage. (8) Power supply.
434 pages, 6" × 9", 343 illustrations.
- Book VI** **Application of the Electronic Valve in Radio Receivers and Amplifiers (Part 3) (in preparation).**
(9) Inverse feedback. (10) Control devices. (11) Stability and instability of circuits. (12) Parasitic feedback. (13) Interference phenomena (hum, noise and microphony). (14) Calculation of receivers and amplifiers.
- Book VII** **Transmitting Valves, 284 pages, 6" × 9", 256 illustrations.**
- Book VIIIA** **Television Receiver Design - monograph 1.**
I.F. Stages. 180 pages, 123 illustrations.
- Book VIIIB** **Television Receiver Design - monograph 2.**
Flywheel Synchronization of Saw-Tooth Generators.
165 pages, 118 illustrations.

BOOK VIII B
TELEVISION RECEIVER DESIGN
FLYWHEEL SYNCHRONIZATION

Distributors for United Kingdom:

CLEAVER HUME PRESS LTD.
42a South Audley Street — London W 1

U.S.A. and Canada:

ELSEVIER PRESS INC.
402 Lovett Boulevard — Houston 6 (Texas)
155 East 82 Street — New York 28

TELEVISION RECEIVER DESIGN

Monograph 2

FLYWHEEL SYNCHRONIZATION OF SAW-TOOTH GENERATORS

U.D.C. 621.397.62

by

P. A. NEETESON

Bibliotheek
Centraal Laboratorium PTT
St. Paulusstraat 4
Leidschendam

1953

PHILIPS' TECHNICAL LIBRARY

ATGEVOERD

All rights reserved by N.V. Philips' Gloeilampenfabrieken
Eindhoven (Holland)

All data in this book are given without prejudice
to patent rights of the above Company

C.L.



P 440,86

FOREWORD

*Parts IV, V and VI *) of this series of books deal with all those problems which relate to the applications of the electronic valve in radio receivers and amplifiers. As explained in their prefaces, the material has been based mainly on Philips' publications, but the articles have been arranged in a logical sequence and, where necessary, revised and supplemented so as to bring the subject matter up to date.*

In this manner a work has been compiled which, as a guide and source of information, is indispensable to set-makers and at the same time is greatly valued as material for practical study in secondary and higher technical training institutions.

It was, therefore, not surprising that suggestions have been received from various quarters that a similar work on the problems encountered in the design and construction of television receivers should be published. Although the technique of television reception is still in its infancy and has by no means reached a stabilized state, it has been decided to publish such a work under the title of Television Receiver Design, but in a slightly different format. In the work on radio receivers, chapters dealing with the many different aspects of the subject are printed in three bound volumes, but Television Receiver Design will comprise a series of 6 to 8 parts, each dealing with a specific aspect of television receiver design, and the whole forming a complete and comprehensive treatise.

The first part, entitled "I. F. Stages", deals with the application of the pentode in the intermediate frequency section of a superheterodyne receiver and the high frequency stages of a T.R.F. receiver. The present volume is the second part and treats of flywheel circuits and synchronization. Other parts will cover such subjects as deflection circuits, problems related to the high frequency stages etc.

It is hoped that this work will prove to be just as valuable in its particular sphere as are the series of books on the construction of radio receivers.

J. HAANTJES
PHILIPS ELECTRONIC TUBE DIVISION

*) Part VI is in course of preparation.

PREFACE

The "flywheel" system of synchronizing the scanning currents in television receivers is being adopted on a rapidly increasing scale. It possesses many advantages over the conventional direct triggering system, not the least of which is that it greatly reduces the effects of noise and man-made interference, so that, particularly in fringe areas, the quality of the received picture is considerably improved.

Although a number of technical papers dealing with flywheel synchronizing circuits have already been published, there is, so far as the author is aware, no comprehensive treatment of the principles governing their action. It is in filling this gap that this book finds its justification.

While providing a fundamental discussion of these principles, it was considered advisable to include also an elementary treatment which serves as an introduction to the subject for those not fully acquainted with the basic principles of generating saw-tooth voltages and currents. A number of practical applications are given, and also a survey of a number of electronic valves which have been specially developed for use in these circuits.

The author wishes to make grateful acknowledgment to the scientific and engineering staffs of the various laboratories of the N.V. Philips' Gloeilampenfabrieken, Eindhoven.

In particular, thanks are due to Dr. E. Oosterhuis, Dr. J. Haantjes and Ir. J. Valeton of the Physical Laboratory whose continuous interest in the development of both the theory and the practical applications of the flywheel system, and whose constructive criticism and advice have greatly widened the author's insight into the subject. We are also grateful to Ir. W. Werner and his associates in the Television Apparatus Laboratory for valuable discussions.

A number of flywheel synchronizing circuits developed by Dr. B. Dammers, Ir. P. van der Knaap and their associates in the Electron Valve Application Laboratory have been included. Finally, thanks are due to Mr. F. Garratt, Eindhoven and Mr. Harley-Carter, A.M.I.E.E., London, for reading the English text.

The Author

CONTENTS

1. Introduction	
2. Principles of saw-tooth generators	
2.1. The capacitive saw-tooth generator	4
2.2. The inductive saw-tooth generator	10
2.2.1. Complications arising with an inductive saw-tooth generator	13
3. Some practical saw-tooth generating circuits	22
3.1. Capacitive saw-tooth generating circuits	22
3.2. Inductive saw-tooth generating circuits	29
3.2.1. Saw-tooth current generator for frame deflection	30
3.2.2. Saw-tooth current generators for line deflection	30
4. Electronic valves specially developed for saw-tooth generators	34
5. Synchronization	38
5.1. Introduction	38
5.2. Methods of synchronization	39
6. Flywheel synchronization	42
6.1. Introduction	42
6.2. Principle of flywheel synchronization	43
6.3. Flywheel action of resonant circuits	44
6.3.1. Reaction of a parallel resonant circuit to a pulse of short duration	44
6.3.2. Reaction of a parallel resonant circuit to a series of periodical pulses of short duration	48
6.3.2.1. The resonant frequency of the circuit is a whole multiple of the pulse frequency	49
6.3.2.2. Pulse frequency differing by a small amount from the resonant frequency of the circuit	51
6.3.2.3. The ratio of the pulse cycle to the cycle of the resonant circuit is $m + \frac{1}{2}$	60
6.3.3. Application of flywheel resonant circuits	63

6.4. Automatic phase control	66
6.4.1. Basic principle	66
6.4.1.1. Some theoretical and practical considerations about the multivibrator and the blocking oscillator	69
6.4.1.1.1. Introduction	69
6.4.1.1.2. Symmetrical multivibrator ,	72
6.4.1.1.3. Symmetrical multivibrator with variable positive grid bias	76
6.4.1.1.4. The asymmetrical multivibrator	83
6.4.1.1.5. Asymmetrical multivibrator with variable positive grid bias	88
6.4.1.1.6. Influence of the internal resistance of the H.T. supply source	91
6.4.1.1.7. Some experimental results	93
6.4.1.1.8. The blocking oscillator	103
6.4.1.1.9. Comparison of the multivibrator and the blocking oscillator	104
6.4.2. Static conditions of the automatic phase control	108
6.4.3. Transient conditions of the automatic phase control	114
6.4.3.1. Influence of disturbances	118
6.4.3.2. Use of a special smoothing filter	123
6.4.3.3. Damped oscillatory transient condition versus overcritically damped transient condition	126
6.4.4. Application of automatic phase control	131
6.4.4.1. Deviations from the fundamental circuit	131
6.4.4.2. Practical circuits	133
Appendix I	143
Appendix II	146
Additional literature list	147
List of symbols	148

1. INTRODUCTION

Television engineering has demanded something more than the application of the experience already acquired in the technique of radio reception. Modern television receivers embody a number of interesting new developments in circuit design and the use of electronic valves, and each of these developments has brought its own peculiar difficulties and possibilities. For instance there are the problems of high-frequency, intermediate-frequency and video wide-band amplification, construction and circuit design of picture tubes, the generation of high direct voltages, electron-optical problems in the focusing and deflection of the electron beam in the picture tube, lens and mirror optics for projection television, production of saw-tooth currents and voltages required for vertical and horizontal deflection of the electron beam (scanning).

This book deals particularly with the principles involved in the generation of saw-tooth currents and voltages, synchronization by means of the additional signals specially sent out by the transmitter, so that the scanning at the receiver can be accurately synchronized with that in the transmitter, the effect of interferences on synchronization, and new circuits for minimizing this effect (flywheel synchronization). The important part played by the electronic valve in all these circuits will be self-evident.

It is presumed that the reader will be familiar with the principles of electronic scanning of a picture in the camera tube in the studio and the manner in which the transmitted picture is reproduced by similar scanning on the fluorescent screen of the picture tube (cathode-ray tube) in the receiver.

It is always the aim to make this scanning as linear as possible both in the transmitter and in the receiver, so that the speed with which the electron beam traces the succession of straight lines across the picture screen is as constant as possible. In principle, the scan need not necessarily be linear, but a constant scanning speed has the advantage that the width of the frequency band required for transmission is then reduced to the minimum for a given number of frames per second and a given number of lines per frame. The fact is that the highest frequency needed for good picture transmission depends upon the greatest speed at which two adjacent picture elements having the maximum difference in contrast — i.e. black and white — are scanned. If the scan is not linear, then some parts of the picture will be scanned at a faster rate than the average

speed required for scanning a complete picture in the same time when the scan is linear, resulting in a locally poorer picture definition or a broader frequency band to be transmitted to get the same definition as with linear scan.

At the end of each line scan the electron beam must be returned to the start of the next line as quickly as possible, while also at the end of each picture (or frame, in the case of interlaced scanning) the beam must be returned as quickly as possible to the start of the next picture (or frame) to be scanned. The manner of scanning now generally adopted therefore consists of rapid horizontal movements of the electron beam across the picture (line scan), with flybacks between lines at a much higher speed, and superimposed upon these, a much slower vertical movement (frame scan) with again a more rapid flyback at the end of each frame.

Unfortunately the number of completely scanned frames per second and the number of lines per frame have not yet been universally standardized. The systems at present employed are the following:

Country	Frames per sec	Lines per frame
U.S.A.	30	525
Gr. Britain	25	405
France	25	819 and 441
Rest of Europe	25	625

Fig. 1 graphically represents the ideal movement of the electron beam across the screen of the picture tube as a function of time, both for the horizontal and the vertical direction. The time scale and possibly also the scale for the path traversed will, however, differ for both directions.

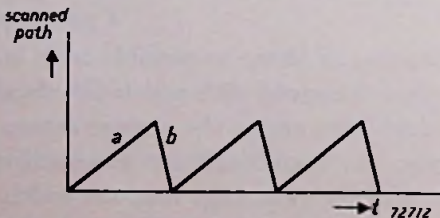


Fig. 1.

General graphical representation of the movement of the electron beam across the screen of the picture tube as a function of time, both for vertical and horizontal scanning, assuming suitable scales for horizontal and vertical coordinates.

a = forward stroke, b = flyback.

This function represented in fig. 1 has the typical form known as saw-tooth. The part a is called the forward stroke, which should be made as linear as possible, and the part b , the flyback, which should be as steep as possible but need not necessarily be linear.

There are two ways of making the electron beam follow the horizontal and vertical movements de-

scribed above, viz. by causing the electrons to pass through either an electric or a magnetic field varying in strength in a like manner to that represented in fig. 1. The first method is called **electrostatic deflection** and the other **magnetic deflection**. An electrostatic field can be formed with the aid of two plane electrodes having a potential difference varying in saw-tooth fashion as a function of time according to fig. 1; the deflection of the beam is proportional to the field strength and the latter is in turn proportional to the voltage between the electrodes. A magnetic field can be generated with the aid of two coil-halves at each side of the neck of the picture tube through which an electric current flows, and since in this case the deflection of the beam is proportional to the magnetic field strength, which is proportional to the current intensity, the current passing through the coils must likewise have a saw-tooth waveform similar to that in fig. 1.

The principles underlying the circuits employed for generating these saw-tooth voltages and currents in television receivers will now be described. Such circuits are classified under the name of **saw-tooth generators**, and as such they come under the wider heading of relaxation generators or oscillators.

2. PRINCIPLES OF SAW-TOOTH GENERATORS

The best known and most commonly employed type is the capacitive saw-tooth generator, the working of which is based, in principle, on the slow charging and rapid discharging of a capacitor. Since this type yields saw-tooth voltages it could be directly applied for electrostatic deflection. For magnetic deflection, however, it is a saw-tooth current that is needed, so that, when the capacitive saw-tooth generator is used for this purpose, its output voltage has to be converted into a current of sufficient amplitude with the aid of a suitable circuit; this circuit may consist, for instance, of an electronic valve of large output in combination with a transformer, similar to the method now commonly employed in low-frequency amplifying technique for converting audio-frequency voltages — via an output valve with matching transformer — into an audio-frequency current of sufficient strength to drive a loudspeaker coil. This is at present the usual method of generating saw-tooth currents for producing the magnetic field required in the horizontal deflection coils.

It is, however, also possible to generate a saw-tooth current direct, with the aid of an inductive saw-tooth generator. The principles of an inductive saw-tooth generator can easily be described and understood from those of a capacitive saw-tooth generator by drawing a parallel between current and voltage, self-induction and capacitance, parallel and series connection.

2.1. THE CAPACITIVE SAW-TOOTH GENERATOR

As already mentioned, the principle of the capacitive saw-tooth generator is based on the (relatively) slow charging and more rapid discharging of a capacitor. The charging can be done by connecting the capacitor (C in fig. 2) to a direct-voltage source (V_b) via a resistor (R) of a relatively high value. If the direct-voltage source has any appreciable internal resistance it may be considered to be included in the resistor R . When, at the instant $t = 0$, the voltage V across the capacitor has a value V_0 and the voltage source V_b is switched on at that same moment, a charging current i begins to flow through the circuit, and the variation of the capacitor voltage V from

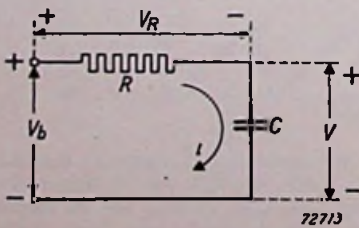


Fig. 2.

Fundamental circuit for generation of the forward stroke of a saw-tooth voltage V .

the instant $t = 0$ can be determined by applying Kirchhoff's law:

$$V + V_R = V_b, \quad \dots \dots \dots (1)$$

where V_R is the voltage across the resistor.

Now

$$V_R = iR \quad \dots \dots \dots (2)$$

and

$$V = \frac{q}{C} = \frac{\int i dt}{C} \quad \dots \dots \dots (3)$$

where q is the electric charge on the capacitor.

Differentiation of (3) gives

$$i = C \frac{dV}{dt} \quad \dots \dots \dots (3a)$$

and the combination of (2) and (3a) gives

$$V_R = RC \frac{dV}{dt} \quad \dots \dots \dots (4)$$

From (1) and (4) it follows that

$$V + RC \frac{dV}{dt} = V_b \quad \dots \dots \dots (5)$$

A possible solution is

$$V = Ae^{at} + V_b \quad \dots \dots \dots (6)$$

where A and a are constants still to be determined.

Substitution of (6) in (5) yields

$$Ae^{at} + V_b + RCaAe^{at} = V_b$$

$$\text{or} \quad 1 + RCa = 0 \quad \dots \dots \dots (7)$$

from which it follows that

$$a = -\frac{1}{RC} \quad \dots \dots \dots (8)$$

Thus one of the constants has been determined, and the solution (6) becomes

$$V = Ae^{-t/RC} + V_b \quad \dots \dots \dots (6a)$$

The other constant, A , is governed by the initial condition, viz. that for $t = 0$ the capacitor voltage must be $V = V_o$. This condition, introduced in (6a) gives

$$V_o = A + V_b$$

$$\text{or} \quad A = V_o - V_b \quad \dots \dots \dots (9)$$

Thus the final solution for the capacitor voltage V is

$$V = (V_o - V_b) e^{-t/RC} + V_b \quad \dots \dots \dots (10)$$

In fig. 3 the variation of V with time from the instant $t = 0$ is graphically represented according to the equation (10) for different values of V_0 .

Assuming that the capacitor C is shunted by a switch S with internal resistance r and that this switch, previously open, is suddenly closed at the instant $t = t_1$, then from that instant onwards the situation is as represented in fig. 4, with S closed.

With the aid of Thévenin's theorem this diagram may be transformed into that of fig. 5, where the voltage source V_b with series resistance R is converted into the current source $\frac{V_b}{R}$ with parallel resistance R .

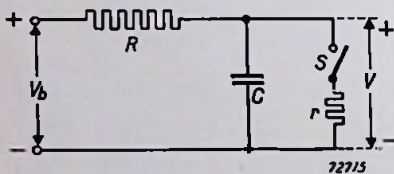


Fig. 4.

Complete fundamental circuit of a saw-tooth voltage generator, derived from fig. 2 by shunting the capacitor by a switch S .

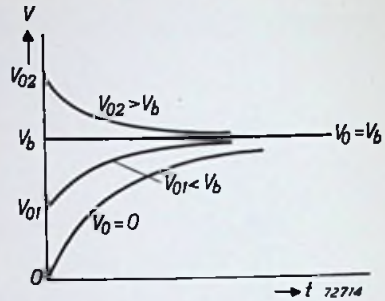


Fig. 3.

Representation of the capacitor voltage V from fig. 2 as a function of time with the initial voltage V_0 as parameter.

With the aid of Thévenin's theorem this diagram may be transformed into that of fig. 5, where the voltage source V_b with series resistance R is converted into the current source $\frac{V_b}{R}$ with parallel resistance R .

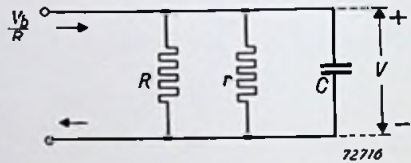


Fig. 5.

Circuit, derived from fig. 4 by replacing the voltage source V_b with the internal resistance R in series, with the aid of Thévenin's theorem, by a current source V_b/R with the internal resistance R in parallel.

This, in turn, can be replaced by the diagram of fig. 6, where the current source $\frac{V_b}{R}$, shunted by R and r , is replaced by the voltage source.

$$\frac{V_b}{R} \cdot \frac{Rr}{R+r} = V_b \frac{r}{R+r}$$

with the equivalent resistance of the parallel connection of R and r in series.

This arrangement is similar to that of fig. 2, but with different values for the external voltage and the resistance. Taking the instant $t = t_1$ as the zero point of the new time scale, then, in analogy with the expression (10) applying for the circuit of fig. 2, the solution for the variation of the capacitor voltage V with time is

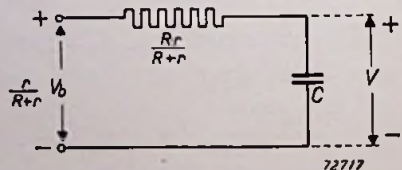


Fig. 6.

Circuit, derived from that of fig. 5 with the aid of Thévenin's theorem.

$$V = (V_1 - V_b \frac{r}{R+r})e^{-t/\frac{rRC}{R+r}} + V_b \frac{r}{R+r} \dots \dots \dots (11)$$

Here V_1 is the value of V for $t = 0$ and can be determined from (10) by substituting in that expression $t = t_1$.

Hence: $V_1 = (V_o - V_b) e^{-t_1/RC} + V_b \dots \dots \dots (12)$

Assuming that r is so small, compared with R , that V_1 is always greater than $V_b \frac{r}{R+r}$, then the variation of the capacitor voltage according to

(11) is as graphically represented in fig. 7.

Applying the simplest assumptions, namely that $V_o = 0$ and $r = 0$, equations (10) and (11) become respectively

$$V = V_b (1 - e^{-t/RC}) \dots \dots (13)$$

and $V = 0$ for $t \geq t_1 \dots \dots \dots (14)$

i.e. when the switch S with resistance $r = 0$ is closed at $t = t_1$. If it is opened at $t = t_1 + t_2$, closed again at $t = 2t_1 + t_2$, reopened at $2t_1 + 2t_2$, and so on, then the variation of V will be as indicated by the heavy line in fig. 8.

If the resistance r of the switch S is not zero but still very small compared with R , then the discharge of the capacitor takes place according to the dotted lines. Thus the voltage across the capacitor resulting from

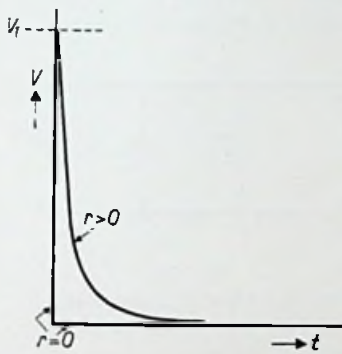


Fig. 7. 72710

Representation of the capacitor voltage V of fig. 4 as a function of time, after closing the switch (flyback), for a switch resistance $r = 0$ and for a small value of r . $V_1 =$ capacitor voltage at the moment of closing the switch.

the slow charging and rapid discharging approximates the saw-tooth function of fig. 1, but in practice, as well as in theory, an absolutely linear saw-tooth voltage is never attained in this way. The non-linearity, however, can be kept within small limits by using only a small portion of the beginning of the exponential charging curve¹⁾, but then the amplitude of the saw-tooth voltage is limited to a fraction of the total charging voltage available, so that it may be necessary

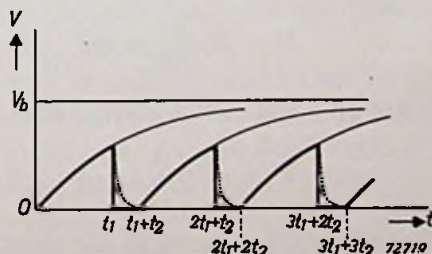


Fig. 8.

Shape of the capacitor voltage V of fig. 4 for periodically opening and closing the switch; heavily drawn line for zero switch resistance, dotted lines for small switch resistance.

¹⁾ See, e.g., Kerkhof and Werner: "Television", p. 137. Philips' Technical Library (1951).

to add an amplifying stage to make the saw-tooth voltage suitable for deflection of the electron beam. When amplification is applied, however, the non-linearity of the anode current-grid voltage characteristic of the amplifying valve can be used to advantage for compensating the non-linearity of the saw-tooth voltage²).

But there are other possibilities for linearizing the saw-tooth voltage. One of these is derived by converting the diagram of the capacitive saw-tooth generator — given once more in fig. 9 for easy reference — with the aid of Thévenin's theorem into the diagram of fig. 10, where the capacitor C is charged by a current source I_b with a resistance R in parallel.

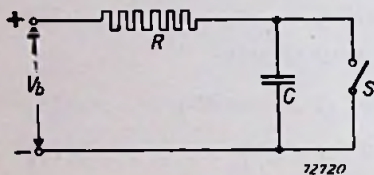


Fig. 9.

Fundamental circuit of a capacitive saw-tooth generator.

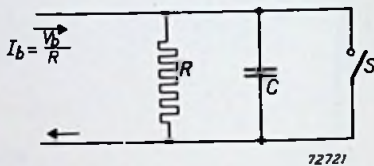


Fig. 10.

Circuit, derived from that of fig. 9 by application of Thévenin's theorem.

The value of the current is

$$I_b = \frac{V_b}{R} \dots \dots \dots (15)$$

Assuming an initial voltage of $V_o = 0$, the variation of the capacitor voltage V for both circuits is given by (13), viz. $V = V_b (1 - e^{-t/RC})$, which, when series expansion is applied for the e-power, yields:

$$V = V_b \left\{ \frac{t}{RC} - \frac{1}{2} \left(\frac{t}{RC} \right)^2 + \frac{1}{6} \left(\frac{t}{RC} \right)^3 - \dots \dots \dots \right\} \dots (16)$$

From (15) and (16) it follows that

$$V = \frac{I_b}{C} t \left\{ 1 - \frac{1}{2} \left(\frac{t}{RC} \right) + \frac{1}{6} \left(\frac{t}{RC} \right)^2 - \dots \dots \dots \right\} \dots (17)$$

The larger the value of R, the closer the capacitor voltage approaches the expression

$$V = \frac{I_b}{C} t \dots \dots \dots (18)$$

but the smaller I_b would become if the original voltage source had a constant value V_b . If, however, V_b increases proportionately with R, then

²) See, e.g., Electronic Application Bulletin 10, No. 1 (Dec. 1948), p. 22.

I_b remains constant. In the extreme case, for infinite R , i.e. with no parallel resistance across the capacitor, V_b must also be taken as being infinitely large, but such that the ratio $I_b = \frac{V_b}{R}$ remains constant at the same finite value.

If it were possible to apply in practice a current of constant strength, then it could be taken as the equivalent — derived in the foregoing manner — of a hypothetical voltage source of infinitely large value, but at the same time with an infinitely large series resistance R .

Within certain limits a pentode may serve as a current source of constant strength, and with such a valve it has indeed proved possible to obtain saw-tooth voltages of good linearity. Fig. 11 represents a circuit formed in this way; it is in fact a well-known circuit, which has been applied in the past on a fairly wide scale.

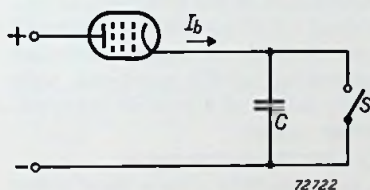


Fig. 11.

Capacitive saw-tooth generator with a pentode as constant current source for linearization of the forward stroke of the saw-tooth voltage.

It is now necessary to consider the form to be given to the switch. There are various possibilities. In the first place gas-filled diodes or triodes can be used, connected in parallel across the capacitor. While the capacitor is being charged (the forward stroke) its voltage rises until at a given moment the ignition voltage of the gas-filled valve is reached, when the capacitor discharges via the internal resistance of the valve, and the valve voltage then rapidly drops until the extinguishing voltage of the gas discharge is reached. The gas discharge then ceases and the internal resistance of the valve again becomes practically infinitely large, i.e. the “switch” is opened again, and the charging process begins anew.

High-vacuum valves can also be used as switches, and in the present stage of development of television receiving equipment these valves are almost invariably employed for this purpose. In the following pages, therefore, only this type of switch will be dealt with, though it will not be gone into too deeply because much has already been written about switches of various kinds (gas-filled as well as high-vacuum valves), such as in the articles quoted in footnotes ¹⁾ and ²⁾ and in the book quoted in footnote ³⁾.

A very simple switch in the shape of the high-vacuum type is that formed by a triode so adjusted that in the absence of an external signal on the grid, it does not pass anode current (the valve is “cut-off”). When a

³⁾ O. S. Puckle: “Time bases” (2nd edition, 1951).

series of periodic positive voltage pulses of short duration are applied to the grid, such that the triode becomes conductive only for the duration of the pulse, then, assuming that the internal resistance of the triode in the conducting state is sufficiently low, the capacitor is charged between the pulses and discharged while the pulses are present at the grid. The circuit is represented in fig. 12.

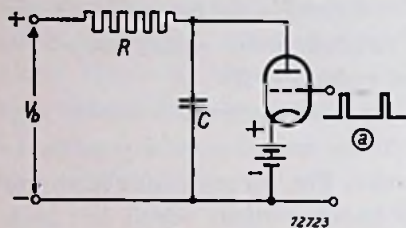


Fig. 12.

Capacitive saw-tooth generator with a vacuum valve as a switch. *a* = switching input pulses.

The manner in which the grid pulses are generated will be explained later on.

When linearization of the saw-tooth voltage, as indicated in fig. 11, is also applied to this circuit, it assumes the form represented in fig. 13.

2.2. THE INDUCTIVE SAW-TOOTH GENERATOR

Although in the present stage of television receiver design the capacitive saw-tooth generator is most commonly employed, for the sake of completeness the other possibility — the inductive saw-tooth generator — must also be discussed.

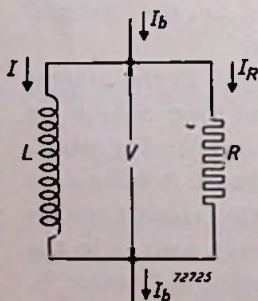


Fig. 14.

Fundamental circuit for generation of the forward stroke of a saw-tooth current *I*.

The circuit for this type of generator and the formulae applying in this case can easily be derived by replacing the voltage source by a current source acting upon a self-inductance *L* and a resistance *R* in parallel in the place of the capacitance *C* and resistance *R* in series. This gives a circuit as represented in fig. 14. Any internal resistance of the current source may be imagined as being included in *R*.

What is of importance here is the variation of the current *I* passing through the coil *L* after the current *I_b* has been switched on at the instant $t = 0$. The problem is simplified by at once assuming that for $t \leq 0$ no current flows through *L* or *R*, so that the initial condition reads: for $t = 0$, $I = 0$.

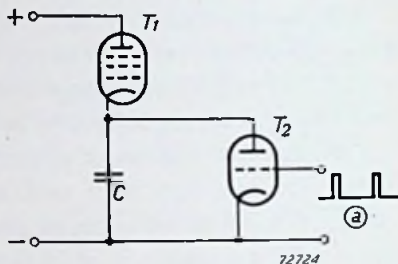


Fig. 13.

Combination of the principles of figs. 11 and 12: capacitive saw-tooth generator with electronic switch and linearization of the saw-tooth voltage by means of a pentode constant-current source.

T_1 = current-source valve

T_2 = switch tube *a* = input pulses

From the equations $I + I_R = I_b, \dots \dots \dots (19)$

$$V = L \frac{dI}{dt} \dots \dots \dots (20)$$

and $I_R = \frac{V}{R} \dots \dots \dots (21)$

it follows that $I + \frac{L}{R} \frac{dI}{dt} = I_b \dots \dots \dots (22)$

This differential equation is entirely analogous to (5) and, for the initial condition mentioned, resolves into an expression of the form (13), viz.

$$I = I_b \left(1 - e^{-\frac{R}{L} t} \right) \dots \dots \dots (23)$$

Thus the current flowing through the coil increases exponentially with a time constant $\frac{L}{R}$, whereas in the case of the capacitive saw-tooth generator the voltage across the capacitor increases exponentially with a time constant RC . Again using the commencement of the exponential current function as the forward stroke of a saw-tooth current, then, at a certain instant

t_1 , the current through the coil has to drop suddenly to zero in order to get the steepest possible flyback. This is achieved by connecting in series with the coil a switch which remains closed up to the instant t_1 and then opens.

Whereas for the discharge of the capacitor the switch was required to have the smallest possible internal resistance, here in this case the internal resistance of the switch has to be as high as possible during the flyback. Denoting the internal resistance of the switch by R_s , the situation as from the instant $t = t_1$ is as shown in fig. 15.

For determining the variation of current passing

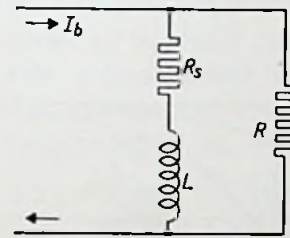


Fig. 15. 72726

Circuit, derived from that of fig. 14 by opening a switch in series with the self-inductance L . The internal resistance of the opened switch is R_s .

through the coil, this diagram may again be replaced, according to Thévenin's theorem, by an equivalent diagram with a voltage source $V_b = I_b R$ and a series resistance R acting upon R_s and L , as represented in fig. 16, the latter diagram then being again converted into that of fig. 17.

This circuit is analogous to that of fig. 14, except that here the initial condition is that the current through L is not zero but governed by the expression (23) for $t = t_1$, i.e.:

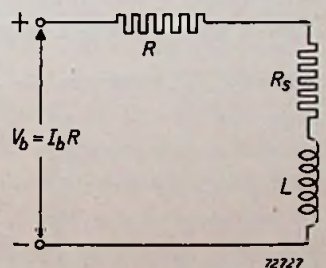


Fig. 16. 72727

Replacement circuit for that of fig. 15 after application of Thévenin's theorem.

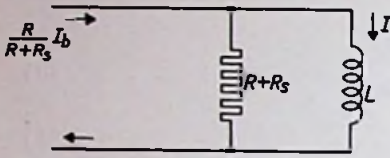


Fig. 17.

Circuit, derived from that of fig. 16 by means of Thévenin's theorem.

$$I_0 = I_b \left(1 - e^{-\frac{R}{L}t_1} \right) \dots (24)$$

The time function of the coil current I as from the instant t_1 — the zero point in the new time scale — now corresponds to the expression (10) and becomes:

$$I = \left(I_0 - I_b \frac{R}{R+R_s} \right) e^{-\frac{R+R_s}{L}t} + I_b \frac{R}{R+R_s} \dots (25)$$

Thus, if $R_s \gg R$, the current decreases exponentially from the initial value I_0 to the very low final value $I_b \frac{R}{R+R_s}$ with a time constant $\frac{L}{R+R_s}$, which is much smaller than that applying for the forward stroke. For an infinitely large R_s the coil current reaches a final value of zero in an infinitely short time.

If the switch is closed again at the moment $t = t_2$ in the time scale of (25) ($t_2 \ll t_1$), reopened at $t = t_2 + t_1$, and so on, then the variation of the coil current follows the heavy line in fig. 18.

If R_s is not infinitely large but, however, much larger than R , then the fly-back is as indicated by the dotted lines. This saw-tooth current is identical with the saw-tooth voltage of fig. 8 for the capacitive saw-tooth generator.

To arrive at a practical circuit for the inductive saw-tooth generator, the diagram of fig. 14 with current source I_b and parallel resistance R has to be transformed by the known process to a circuit with voltage source $V_b = I_b R$ and a resistance R in series, according to fig. 19.

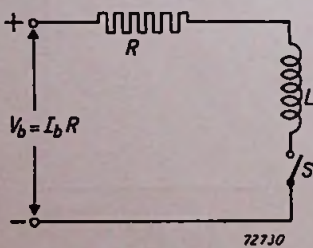


Fig. 19. See fig. 16.

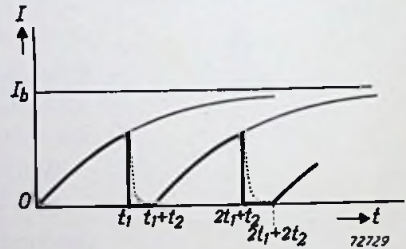


Fig. 18.

Variation of the coil current I with time when the switch, in series with the coil L in figs. 15 and 16, is periodically closed and opened; heavy line for infinitely high open-switch resistance R_s , dotted line for finite values of R_s , but R_s always $\gg R$.

circuit with voltage source $V_b = I_b R$ and a resistance R in series, according to fig. 19.

When the switch S is closed, the forward stroke of the saw-tooth current through L occurs and the flyback begins when S is opened.

Expressed in V_b instead of I_b , the expression (23) for the forward stroke becomes

$$I = \frac{V_b}{R} \left(1 - e^{-\frac{R}{L}t} \right) \dots (26)$$

or, in series expansion

$$I = \frac{V_b}{L} t \left\{ 1 - \frac{1}{2} \frac{R}{L} t + \frac{1}{6} \left(\frac{R}{L} \right)^2 t^2 - \dots \right\} \dots (27)$$

The smaller R becomes, the closer this function approaches a linear relation between I and t . For $R = 0$ the saw-tooth forward stroke is perfectly linearized. This resistance R consists of the internal resistance of the voltage source, the resistance of the coil and that of the closed switch S . Therefore, in order to obtain a saw-tooth current as linear as possible, a voltage source with low internal resistance has to be chosen, e.g. a stabilized high-tension unit; the coil has to have low losses; and the switch, e.g. an electronic valve, must have a low internal resistance in the conducting state. If an electronic valve, say a triode, is chosen for the switch, then it has to be conducting during the forward stroke and cut off during the flyback, the latter being brought about by applying short, periodic, negative voltage pulses to the control grid. The arrangement of the circuit is then as represented in fig. 20.

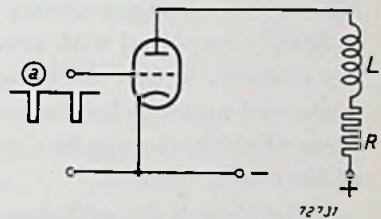


Fig. 20.

Circuit of an inductive saw-tooth generator, in which an electronic vacuum valve functions as a switch. a = switching input pulses.

2.2.1.1. COMPLICATIONS ARISING WITH AN INDUCTIVE SAW-TOOTH GENERATOR

Having thus dealt with the principles of generating saw-tooth voltages (with a capacitive saw-tooth generator) and saw-tooth currents (with an inductive generator), it might be thought that the moment has now come to deal with the materialization of these principles in practical circuits. This could indeed be done as far as the capacitive saw-tooth generators are concerned, since, apart from the manner in which the positive input pulses are obtained on the control grid of the switch valve (this will be dealt with in detail farther on), in most variants of this kind of generator employed in practice the principles of the diagram in fig. 12 are easily recognized. With saw-tooth current generators, however, it is a different matter. Especially in the circuits employed in present-day television technique, and particularly for the line scanning, it is difficult to recognize the principles of fig. 20. The fact is that with inductive saw-tooth generators complications arise which make it necessary to devise special circuit features in order to eliminate the disturbing effects of these complications. Some of these measures will now be fundamentally dealt with in order to

give some idea of the design of modern saw-tooth current generator circuits.

In the first place it will seldom be found that the self-inductance L in fig. 20 is used directly as a pair of deflection coils supplying the magnetic deflecting field in the cathode-ray tube. This is because the number of ampere-turns required, which with the present trend towards larger deflection angles of the cathode-ray beam (wide-angle deflection) is increasing more and more, is so high that with an electronic valve of reasonable power output, the number of turns needed make the dimensions of a directly connected coil impracticable. Apart from the high cost and the difficulties in manufacture, this type of coil has a relatively large self-capacitance. To overcome all these difficulties, a matching transformer is usually employed with fewer windings on the secondary side than on the primary, so that the current flowing in the anode circuit of the valve is stepped up to such a value that deflection coils having relatively few turns of thick wire can be connected to the secondary of the transformer.

But although the self-capacitance of the deflection coils can be considerably reduced in this way, further measures are still necessary to counteract the consequences of the oscillations inevitably arising with inductive saw-tooth generators as a result of this stray capacitance. The following will give some idea of what is involved.

Fig. 21 represents an ideal saw-tooth current generator, it being assumed that the voltage source V_b

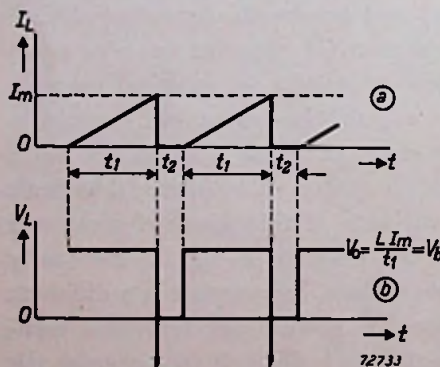


Fig. 22.

Current I_L through and voltage V_L on the coil L as a function of time for the ideal inductive saw-tooth generator of fig. 21.

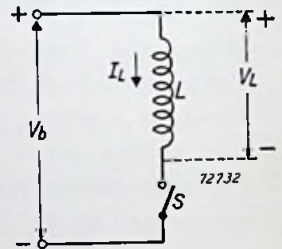


Fig. 21.

Ideal saw-tooth current generator; no internal resistances of voltage source V_b and switch S , loss-free self-inductance L .

the self-inductance L is loss-free and that the resistance of the switch S is zero in the closed position and infinite in the open state. The self-inductance may consist of the transformed inductance of the deflection coils connected to the secondary side of an ideal transformer (a loss-free transformer without stray inductance). When, under these conditions, the switch is periodically opened and closed, so that it is

kept closed for an interval of time t_1 and opened for a much shorter interval t_2 , then the characteristics of the current I_L through and the voltage V_L on the coil will be as represented respectively in figs. 22a and 22b.

In fig. 22b the arrows pointing downward represent a voltage pulse of infinitely high negative value and zero duration. Now the influence of stray capacitances, such as the self-capacitances of coils and transformer windings, wiring capacitances and the like, all of which are imagined as being concentrated in the capacitor C_p in fig. 23, is such that at the beginning of the flyback (upon the switch S being opened) the magnetic energy accumulated in the self-inductance to an amount of $\frac{1}{2} LI_m^2$ is converted into an electrostatic energy of $\frac{1}{2} C_p V_c^2$; here V_c is the capacitor voltage at the instant when all the magnetic energy has just disappeared, i.e. when the coil current is zero ($V_c = I_m \sqrt{\frac{L}{C_p}}$).

The capacitor then discharges and a current flows through the self-inductance in the opposite direction, a maximum being reached as soon as all the electrostatic energy has disappeared, i.e. when $V_c = 0$. In the assumed absence of damping resistances this alternation between the magnetic and the electrostatic state of the energy continues indefinitely. Thus we have here the known phenomenon of excitation of a parallel

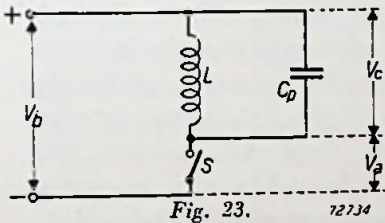


Fig. 23. Ideal inductive saw-tooth generator, taking into account stray capacitances, concentrated in C_p .

resonant circuit, in this case consisting of the self-inductance L and the capacitance C_p .

The coil current I_L and coil voltage V_L (equal to V_c) are sine functions with a mutual phase difference of 90° and a frequency equal to the resonant frequency of the LC_p circuit. Hence, this frequency is defined by

$$\omega_p = 2\pi f_p = \frac{1}{\sqrt{LC_p}}$$

The variation of these quantities I_L and V_L as a function of time, as also that of the switch voltage V_a (and also, possibly, the anode voltage of an electronic valve functioning as a switch), are represented in fig. 24 for a forward stroke and the following flyback.

Obviously such oscillations in the flyback are undesirable. In practice the internal resistance of the voltage source and of the switch in the closed position will not be zero, so that upon the switch being closed again, the oscillations will not immediately stop, with the result that at the beginning of the next forward stroke, damped oscillations will be superimposed on the linearly rising saw-tooth current. In practice damping will also occur during the flyback, since there will always be

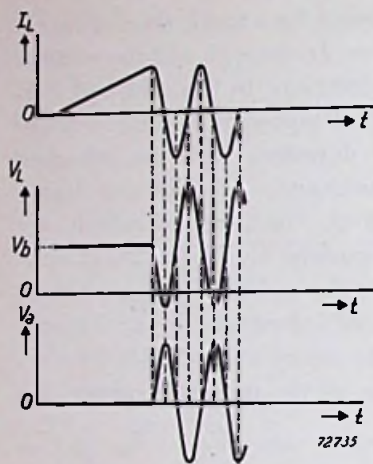


Fig. 24.

Coil current I_L , coil voltage V_L and switch voltage V_a of the circuit of fig. 23 as a function of time.

losses in the coils and the transformer. It depends upon the ratio of the time constant of the resonant circuit LC_p to the duration of the flyback to what extent the oscillations will have been reduced in amplitude at the beginning of the next forward stroke. If the losses in L could be represented by a single series resistance r , then the time constant would amount to $\frac{2L}{r}$ seconds. In television receiving technique, as far as the frame time-base generator is concerned, the duration of the flyback is usually so long compared with the time constant of the deflection circuit, that the oscillations have practically disappeared by the beginning of the forward stroke. In the case of the line time-base

generator, however, the position is somewhat different and additional measures must be taken to eliminate the disturbing effects of these oscillations. An obvious method is to apply extra damping, for instance by shunting the self-inductance L with a suitable resistance, preferably such as to convert the oscillatory reaction of the LC_p circuit into an aperiodic damped reaction (critical damping). As a rule, however, this makes the flyback too slow, so recourse must be had to other measures. An elegant solution has been found by employing an additional electronic valve, viz. a diode. Not only is the influence of the stray oscillations thereby greatly reduced, but at the same time the magnetic energy accumulated in the self-inductance at the end of the forward stroke — which in the case of a simple damping resistor is converted into heat and thus lost — is recovered. In the ideal case of loss-free coils and transformers, the whole of this energy is recovered, and in practical circuits in which some losses are inevitable, quite a large proportion of the energy is required.

One form this solution can take is that in which a diode is shunted across the switch S . In that case this diode is termed an efficiency

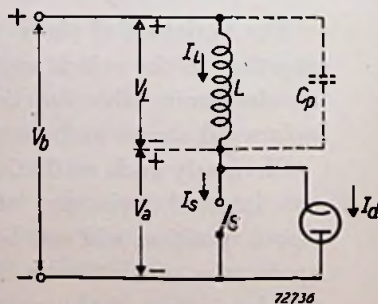


Fig. 25.

Inductive saw-tooth generator with efficiency diode.

diode. For the ideal, loss-free, case the circuit is then as represented in fig. 25.

Starting at the instant t_1 when the switch S is closed, the current and voltage characteristics are as indicated in fig. 26.

From the instant t_1 a linearly increasing current begins to flow through the self-inductance and the switch (figs. 26a and b). At the instant t_2 , when S is opened, I_s immediately drops to zero, while I_L tends to oscillate sinusoidally in the manner shown in fig. 24. The coil voltage V_L , which from t_1 to t_2 was equal to the supply voltage V_b , and also the voltage V_a , then likewise begin to oscillate according to a sine function (see fig. 24), but after a half cycle of this resonant oscillation, V_a tends to become negative and thus the diode begins to conduct.

Still considering the ideal case, the internal resistance of this diode in the conducting state is assumed to be zero, so that from the instant t_3 the self-inductance L again is connected between the positive and negative poles of the voltage source V_b , i.e. a constant voltage.

Since $V_L = L \frac{di}{dt}$, it ensues that the current must then follow a linear time function with the same slope V_b/L as during the interval t_1 to t_2 . This means that I_L , and thus also I_d , must have the forms as shown in fig. 26a and c. During the interval t_3 to t_4 the voltage source need not, therefore, supply any current, but on the contrary energy is returned to it from the accumulation of magnetic energy in the self-inductance. The energy regained in this way is equal to that which was present in

the self-inductance at the end of the forward stroke, because we are considering here the ideal case in which there are no losses. In this theoretical case, where on the average there is no energy drain on the supply source, the saving to be obtained by applying the diode is quite evident. In practice, energy has to be supplied only for making good the energy lost in the form of heat in the resistors. At the instant t_4 , when the diode current has fallen to zero, the switch S has to be closed again and the process is then repeated as represented from the instant t_1 .

The following points must be borne in mind. In practice switch S is an

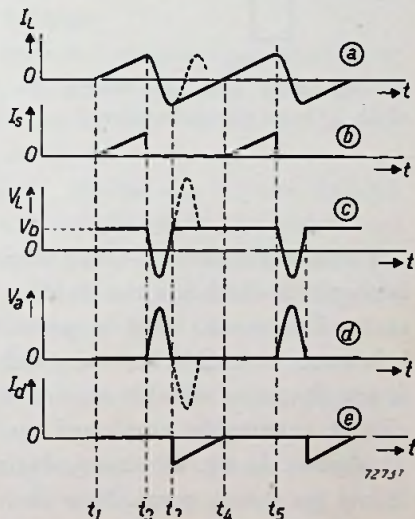


Fig. 26.

Currents and voltages, indicated in fig. 25, as functions of time.

electronic valve, which from t_1 to t_2 and from t_4 to t_5 has to be conducting and from t_2 to t_4 blocked, the latter condition being brought about by negative voltage pulses on the control grid. Between t_2 and t_3 (the flyback time) high anode voltage peaks may arise, as appears from fig. 26d, so that at least during that interval the negative grid voltage has to be quite high in order to completely suppress the anode current. Consequently, this grid voltage V_g has to be given the shape represented in fig. 27.

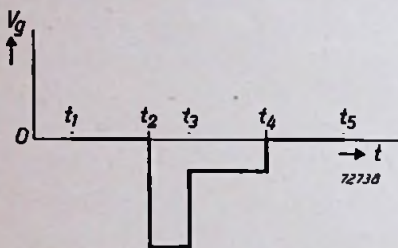


Fig. 27.

Driving pulse when the switch S of fig. 25 is an electronic valve.

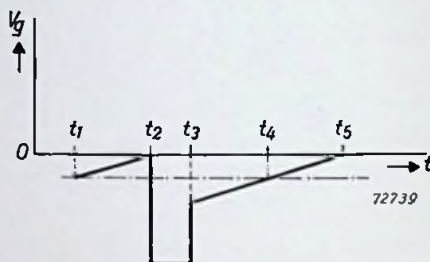


Fig. 28.

Modification of the driving pulse of fig. 27 for economical operation of the switch valve.

Dot-dash line represents the cut-off level of the valve.

Further, for the saw-tooth current to be as linear as possible, a switch S is required which has the smallest possible internal resistance in the closed state. This means that a pentode working at low anode voltages, thus below the "knee" in the anode current-anode voltage characteristic, is usually more suitable than a triode. In practice, a pentode is in fact almost invariably employed as output valve for a saw-tooth current generator. As fig. 26 shows, during the forward stroke the anode voltage is low (in theory zero). Now there are two means of avoiding an excessive screen-grid load at the beginning of the conducting part of the forward stroke (instants $t_1, t_4 \dots$ in fig. 26), where the rise in the anode current is restricted to a linear time function and the valve undergoes a sudden

transition from the blocked state to zero control-grid voltage. In the first place the trigger signals on the control grid of the pentode as shown in fig. 27 can be modified so as to give

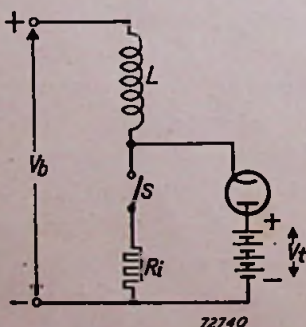


Fig. 29.

Modification of the inductive saw-tooth generator circuit of fig. 25. An auxiliary voltage V_1 is applied to the anode of the efficiency diode, to prevent the anode voltage of the switch valve dropping below a certain value.

them the shape indicated in fig. 28, so that at the instant t_4 the screen grid no longer has to take up the full amount of the sudden surge of cathode-emission current. In the second place, current distribution between screen grid and anode can be more favourably spread over the whole of the conducting period by taking steps to prevent the anode voltage dropping below a certain minimum value. This can be done, for example, by applying an inverse voltage V_t in series with the efficiency diode in the manner shown in fig. 29. In that case the internal resistance R_i of the switch must essentially be taken into account, as otherwise in the closed state the switch S would short-circuit the auxiliary voltage source. In practice the same result is reached in a simple manner, without an additional auxiliary voltage source, by extending the windings of the self-inductance (the transformer) in the manner shown in fig. 30. The shape of V_a is then as represented in fig. 31.

Another method of damping out stray oscillations in the flyback by means of a diode, and at the same time obtaining an economical circuit, is to connect the voltage source V_b to the self-inductance via a booster diode. The basic circuit of this is represented in fig. 32.

When the switch S is closed at the moment t_1 , a linearly increasing current again begins to flow through the self-inductance L , while the voltage V_L across the self-inductance is constant and equal to V_b . The self-inductance L with n_1 windings is extended with a number of windings n_2 , making in all $n_1 + n_2$ windings, so that the voltage V_B across them is $\frac{n_1+n_2}{n_1}$ times V_L ,

which means that during this part of the forward stroke $V_B = \frac{n_1+n_2}{n_1} V_b$.

At the instant t_2 , when the switch is opened, V_L and I_L assume the familiar oscillatory shape. The capacitance C is presumed to be sufficiently large to prevent any perceptible variation in the voltage across this capacitor during the flyback, so that the potential at point A in the diagram of fig. 32 with respect to the negative pole of the voltage source retains the value $V_B = \frac{n_1+n_2}{n_1} V_b$. The voltage V_K

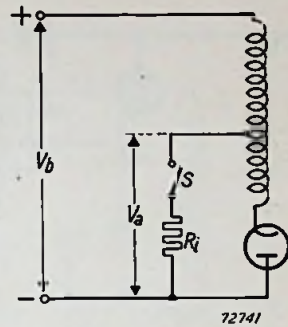


Fig. 30.

The auxiliary voltage in the circuit of fig. 29 is obtained by extending the windings of the self-inductance with a certain amount.

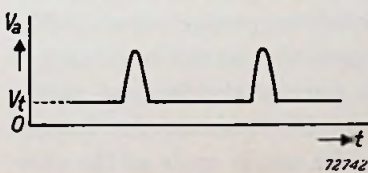


Fig. 31.

Anode voltage of the switch valve of the circuits figs. 29 and 30 during forward stroke (scan) and flyback.

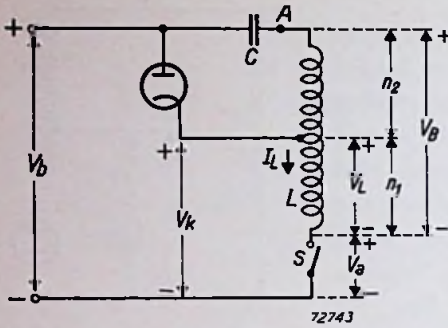


Fig. 32.

Fundamental circuit of an inductive saw-tooth generator with application of a booster diode.

n_1 and n_2 number of windings of the two halves of the self-inductance L as indicated. C booster condenser.

the diode becomes conducting once more, and, assuming the internal resistance of the diode to be zero, this means that the cathode potential then remains constant at the value $+V_b$. From that moment, therefore, on the windings n_2 there is a constant voltage, i.e. the difference in potential between point A , which amounts to $\frac{n_1+n_2}{n_1} V_b$, and the cathode of the diode, where it

is equal to V_b . Thus this potential difference is $\frac{n_1+n_2}{n_1} V_b - V_b = \frac{n_2}{n_1} V_b$,

which amounts to the same as that occurring during the interval t_1 to t_2 . This is possible only if the current flowing through the self-inductance retains the same constant slope with time. This condition arises at the instant t_3 , which follows about half an oscillation period after t_2 . The current is then equal, but in opposite direction to that at the beginning of the flyback, at the instant t_2 . Thus the first part of the forward stroke begins, and is continued until the current reaches zero at the instant t_4 , when the switch has again to be closed and a whole cycle of the saw-tooth current has been completed (t_1 to t_4).

What has been said in the foregoing about diode circuits does not, however, dispose of all the complications arising with a saw-tooth current generator. Often good use is made of the high-voltage peaks occurring on the switch (i.e. the anode of the switch valve), viz. V_a in fig. 26d and V_a in fig. 32, which latter has a shape as represented for V_K in fig. 33, but with larger peak values. The peak values of V_a may amount to some thousands of volts.

In the cathode-ray tube a direct voltage of several thousands of volts (in modern direct-view tubes 10 to 16 kilovolts) is needed for acceler-

on the cathode of the diode with respect to the negative pole is then $\frac{n_1+n_2}{n_1} V_b - \frac{n_2}{n_1} V_L$. From fig. 33 it is seen that during a half cycle of the oscillation this voltage V_K is greater than V_b , the voltage on the anode of the diode with respect to the negative pole. Consequently, during that interval of time the diode is not conducting. At the end of that half cycle, however, the cathode potential is again equal to the anode potential, with a tendency to drop lower, but then the

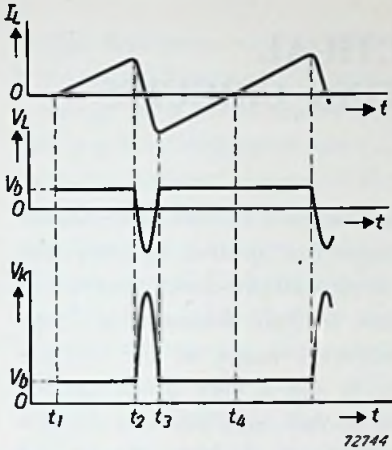


Fig. 33.

Representation of coil current I_L , voltage V_a , cathode voltage V of the booster diode from fig. 32, as functions of time.

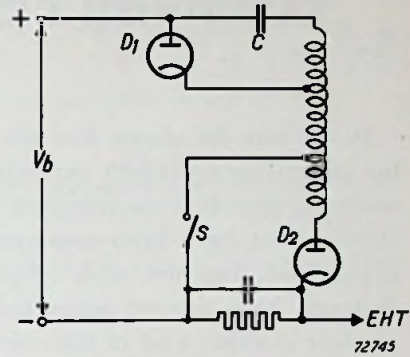


Fig. 34.

Circuit of an inductive saw-tooth generator with application of booster diode D_1 and EHT rectification by means of a diode D_2 .

ating the electrons so as to cause them to impinge on the fluorescent screen at a sufficiently high velocity to produce a reasonable brilliancy. It was therefore only logical to make use of the high voltage peaks V_a by rectifying them, for which purpose special rectifier diodes have been developed. When these voltage peaks V_a have not sufficient amplitude to yield the high direct voltage required, voltage-doubling and even voltage-trebbling circuits are employed, thus involving the use of two or three rectifying diodes. Alternatively the self-inductance L (the primary of the output transformer) is extended at the switch end with such a number of windings that the voltage peaks at the free end of these windings are of sufficient amplitude to yield the high direct voltage required. The basic circuit of such a system is represented by the diagram in fig. 34.

3. SOME PRACTICAL SAW-TOOTH GENERATING CIRCUITS

It will now be shown how the principles described in the last chapter for generating saw-tooth currents and voltages are applied in television receiving sets. It is not intended to pass in review all saw-tooth generating circuits that have been employed from time to time, because the scope of this book does not allow of that, and moreover many of the circuits designed have proved impracticable. There is not a very great variety of these circuits used in television receivers to-day, and since it is particularly this field of application with which this book deals, there is no need to enter into an exhaustive account of all saw-tooth generating circuits employed in other branches of electronics.

As already stated in the introduction, the electron beam in the cathode-ray tube can be deflected in two ways, either by means of an electrostatic field with the aid of saw-tooth voltages or by means of a magnetic field, for which saw-tooth currents have to be employed.

In television receivers employing electrostatic deflection, obviously capacitive saw-tooth generators are exclusively used, since these yield saw-tooth voltages. Following the same reasoning, one might expect that exclusively inductive saw-tooth generators would be used in receivers employing magnetic deflection, because in that case saw-tooth currents are needed. But that is not so, because, in addition to the saw-tooth current generator used in the output stage for magnetic deflection, the majority of present-day television receivers have also a capacitive saw-tooth voltage generator, supplying the voltage signals for opening and closing the switch of the inductive generator (the output valve). Therefore, although in modern television receivers magnetic deflection is practically the only system employed for deflecting the beam, this by no means implies that the capacitive saw-tooth generator is no longer of considerable importance, and consequently, in the following pages consideration will be given to both forms of saw-tooth generators.

3.1. CAPACITIVE SAW-TOOTH GENERATING CIRCUITS

Taking as starting point the system represented in fig. 12, this can be simplified by applying the input voltage pulses to the grid via a capacitor C_g , so that no additional voltage source is required for the negative grid bias. The grid is then connected to the cathode via a leak resistor R_g ; see fig. 35.

The first pulse sets up a momentary grid current giving C_g a charge such as to render the grid negative with respect to the cathode. Between the pulses the charge of C_g leaks away via R_g and the pulse voltage source. The product $R_g C_g$ is assumed to be of such a value that in the interval T between the pulses the voltage on C_g drops only slightly (according to the well-

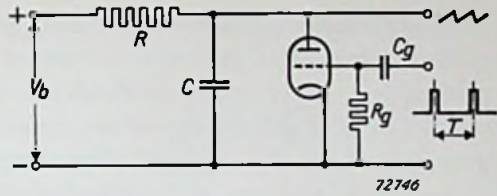


Fig. 35.

Capacitive saw-tooth generator with an electronic switch according to fig. 12, in which the necessary negative grid bias for the switch valve is obtained automatically (automatic grid biasing).

known exponential law with time constant $R_g C_g$). The second pulse causes grid current to flow again and C_g is made more negative. This process is repeated at each pulse until a stable state is reached where between two pulses just as much charge leaks away from C_g as is supplied to it by the grid current. If $R_g C_g \gg T$, then the negative grid bias is practically equal to the peak value of the pulses, and the grid is momentarily at cathode potential only while a pulse occurs; the valve is then conducting and an anode current corresponding to $v_{g1} = 0$ flows. When the peak voltage of the pulses is greater than the cut-off voltage of the valve, then between the pulses the anode current is blocked (the "switch" is open).

The question now is how the switching pulses are obtained. An obvious solution is to employ the synchronizing pulses sent out by the transmitter together with the video signal and separated therefrom in the receiver⁴). Though this was done in the early days of television technique, it was soon discarded, for the following very good reasons. In the first place, if, through some cause or other, the synchronizing pulses should fail to come through, there would be no saw-tooth output voltage and the electron beam would no longer be deflected, with the result that in all probability the stationary beam would burn a spot in the fluorescent screen of the cathode-ray tube. Another reason is that this method of generating the saw-tooth is highly susceptible to interferences, since any interfering positive signal of sufficient amplitude occurring between two synchronizing pulses makes the switch valve conducting and thus initiates a flyback of the saw-tooth at an undesired moment.

⁴) For the manner in which the line and frame synchronizing pulses can be separated from each other and from the video signal, see e.g., C. L. Richards, A Television Receiver, Philips Techn. Rev. 2, 33, 1937 (No. 2), Television Receivers, Philips Techn. Rev. 4, 342, 1939 (No. 12) and J. Haantjes and F. Kerkhof, Projection-Television Receiver, Philips Techn. Rev. 10, 364, 1949 (No. 12).

In order to avoid any risk of damage to the fluorescent screen of the cathode-ray tube in the event of failure of the synchronizing pulses, it is preferable to have a saw-tooth generator which still yields a saw-tooth voltage even in the absence of synchronizing pulses. This implies that the generator has to be self-oscillating or "self-switching". A large number of such self-switching generators have become known under the general name of relaxation oscillators. The function of the synchronizing pulses sent out by the transmitter is then confined to synchronizing the saw-tooth oscillator; they no longer serve as switching pulses, since these are automatically generated by the oscillator itself. The manner in which this synchronization is brought about will be fully dealt with later.

Just as a sinusoidal signal can be obtained without an input signal by applying in a suitable manner positive feedback between the anode and grid of an electronic valve, so a relaxation oscillator can be produced by applying a very strong positive feedback between anode and grid of the valve. This is illustrated in fig. 36, where K represents the feedback circuit. In the case of a sinusoidal oscillator, however, with certain R_g and C_g values, excessive feedback is apt to cause what is known as squegging: the sinusoidal oscillations grow so rapidly that, instead of a stable adjustment being reached automatically, a sudden flow of heavy grid current makes the grid potential with respect to the cathode so highly negative as to cause the oscillations to cease abruptly. But if the resonant circuit forming part of the circuit

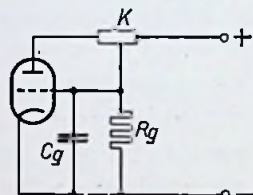


Fig. 36. 72747

General principle of a self-oscillating (or "self-switching") electronic switch, by application of a positive feedback circuit K .

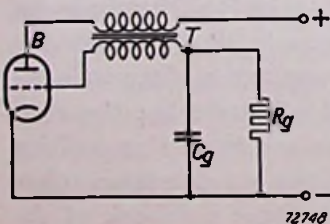


Fig. 37.

Special form of the principle of fig. 36 in which the positive feedback is obtained by means of a transformer T (blocking oscillator).

the oscillation is limited to a short grid voltage pulse and at the same time a corresponding anode-current pulse. One then has what is generally known as a blocking oscillator, which is very frequently used in television receivers, and the basic circuit of which is given in fig. 37.

Here the feedback circuit K in fig. 36 consists of the transformer T . Usually there is no need of additional damping resistors, either in the anode or the grid circuit of T , if the transformer core is made of normal l.f. laminations, the losses in the core then providing the necessary damping.

The whole circuit of the blocking oscillator should be regarded as a switch which is periodically closed for a short time (valve B conducting). When this "switch" is connected (in the same way as in fig. 9) in parallel to a capacitor C connected to the positive pole of a voltage source V via a series resistor R , then the system is as represented in fig. 38, and the desired saw-tooth voltage is produced across the capacitor C .

The polarity of the transformer connections is such that a drop in the anode voltage causes the grid voltage to rise. As soon as anode current begins to flow, the anode voltage falls and thus the grid voltage rises, as a result of which the anode current increases, the anode voltage drops still further and the grid voltage is again increased, and so on. Finally there is a strong surge of grid current which charges the capacitor C_g and thereby makes the grid negative with respect to the cathode, so that the valve is automatically blocked. This is followed by the discharge of C_g across R_g , according to the known exponential law with a time constant $C_g R_g$. At the

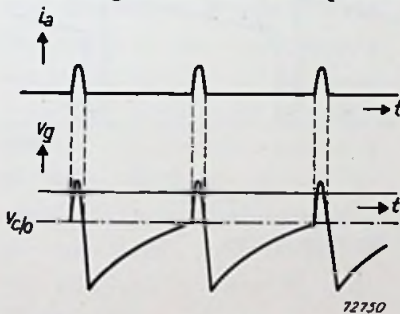


Fig. 39.

Anode current and grid voltage of the blocking oscillator valve as a function of time.

instant when the grid voltage passes through the cut-off point $V_{c/o}$ of the valve B , anode current begins to flow and the whole process is repeated. The variation of the grid voltage v_g and the anode current i_a as a function of time are given in fig. 39.

From this it is seen that a saw-tooth signal is obtained also in the grid circuit, and in practice this is often used instead of the saw-tooth voltage across the capacitor C , thereby dispensing with C and R .

Self-oscillating capacitive saw-tooth generators will be dealt with further in section 5 under the heading of "Synchronization", so that for the present what has been said above about the blocking oscillator will suffice.

Another form of generator frequently used recently in television receivers is the multivibrator, in which the positive feedback circuit K of fig. 36 consists of a complete amplifying valve with some circuit components.

The basic circuit of the multivibrator is given in fig. 40. Here B_2 represents

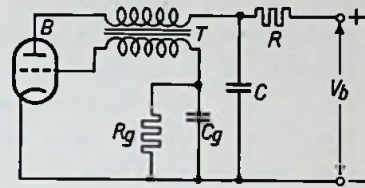


Fig. 38.

Representation of a capacitive saw-tooth generator in which the blocking oscillator acts as an automatic periodic switching device.

72749

72750

the extra amplifying valve mentioned, which acts as a phase inverter, inverting the phase of the voltage variation on the anode of B_1 before it reaches the grid of B_1 . The operation of the multivibrator is such that, while B_1 is blocked, B_2 is conducting, and vice versa, and the duration of these conditions depends upon the time constants determining the discharge of the coupling capacitors C_1 and C_2 ; the time during which B_1 is blocked is determined mainly by the time constant $R_{g1}C_1$, and the corresponding duration for B_2 by $R_{g2}C_2$. When these two time constants are equal, the multivibrator is symmetrical, the two valves being alternately conducting and blocked for the same length of time. If, however, $R_{g1}C_1 \gg$

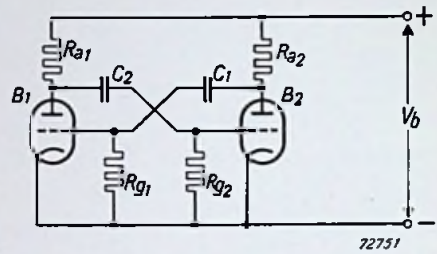


Fig. 40.

Another form of self-oscillating electronic switch, the multivibrator.

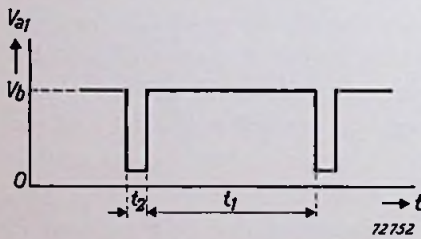


Fig. 41.

Anode voltage of valve B_1 of fig. 40, as a function of time, for a strongly asymmetric multivibrator ($R_{g1}C_1 \gg R_{g2}C_2$; see fig. 40).

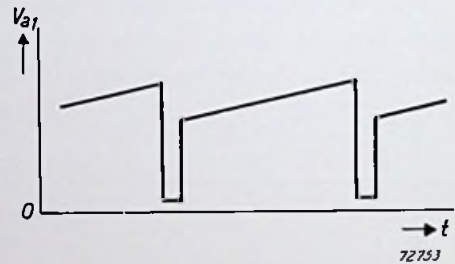


Fig. 42.

Anode voltage of valve B_1 in figs. 43a and b, as a function of time.

$R_{g2}C_2$, then B_1 is blocked for a much longer time than B_2 , thus drawing anode current during only a small part of the whole cycle, so that it can be used as a switch valve shunted across a capacitor.

In the case where $R_{g1}C_1 \gg R_{g2}C_2$, the anode voltage of B_1 in the circuit of fig. 40 will appear as shown in fig. 41, where t_1 is proportional to $R_{g1}C_1$ and t_2 proportional to $R_{g2}C_2$.

If B_1 were shunted by a capacitor C alone, this would interfere with the working of the multivibrator, since it is necessary always to have a short negative pulse of sufficient amplitude left on the anode of B_1 . Consequently a peaking resistance R_p has to be connected in series with C . Another possibility is to connect C in parallel to a part of the anode resistance R_{a1}

of B_1 . In both cases the anode voltage of B_1 takes the shape indicated in fig. 42.

If this voltage is to be used for driving the switch valve of a saw-tooth current generator, then it is an advantage to employ the peaking resistance, as will be understood from a comparison with fig. 28, which gives the shape of the signal that is then required. If it is desired to take from the multivibrator the purest possible saw-tooth voltage, then the capacitor voltage alone can be used, and not the combination of capacitor and peaking resistance voltage, in which case it will usually be necessary to earth one side of the capacitor or to connect it to the positive pole of the supply-voltage source. These two circuits with their output saw-tooth voltages are represented in figs 43a and b.

The forward stroke and the flyback of the saw-tooth — the times t_1 and t_2 respectively in fig. 41 — depend upon the time constants $R_{g1}C_1$ and $R_{g2}C_2$, as already remarked, so that by varying these constants it is possible to regulate the frequency and the duration of the pulses. This offers a simple means of varying the frequency of the saw-tooth voltage — in television receivers this has to be equal to the frequency of the synchronizing signals received — by choosing a variable resistor for R_{g1} (figs. 40 and 43). In the case of a blocking oscillator it will be obvious that the frequency can be regulated by means of the grid-leak resistor R_g (figs 37 and 38).

Apart from the time constant in the grid circuit of the switch valve (B in figs 37, 38; B_1 in figs 40, 43), the frequency of the relaxation oscillation depends also upon the direct voltage applied to the grid of that valve, which voltage has so far been assumed to be zero (grid-leak resistor connected to cathode). These two governing factors will be dealt with more fully in section 6.4 under "Automatic Phase Control", so that it may suffice to give here an explicit expression for the frequency of the two forms of relaxation oscillators described.

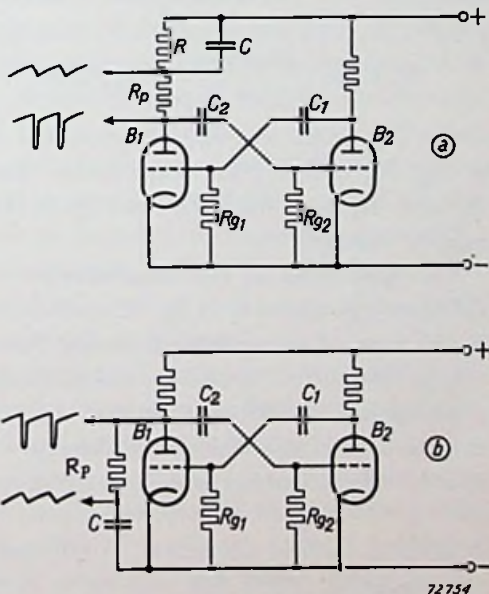


Fig. 43.

Two possible versions of the multivibrator as a capacitive saw-tooth generator.

This expression applies under the following assumed conditions: 1) at a grid-to-cathode potential zero, the internal anode- and grid resistances of the valves employed must be small compared with the anode and grid resistances in the external circuits; 2) the influence of stray- and inter-electrode capacitances must be negligible at the frequencies concerned;

$$3) \frac{R_{g1} C_1}{R_{g2} C_2} \gg 1 \quad (\text{asymmetric multivibrator})$$

$$\frac{R_{g2}}{R_{a1}} \geq 1$$

$$\frac{R_{g2} C_3}{R_{a2} C_1} \gg 1 \quad (\text{see fig. 40}).$$

Under these conditions the explicit expression that can be given for the frequency of the multivibrator is:

$$f = \frac{1}{R_{g1} C_1 \ln \frac{V_b + V_{r1}}{V'_{c/o} + V_{r1}} + R_{g2} C_2 \ln \frac{V_b + V_{r2}}{V'_{c/o} + V_{r2}}}, \dots \dots \dots (28)$$

where $V'_{c/o}$ is the cut-off voltage of the valve B_1 , $V'_{c/o}$ the cut-off voltage of B_2 , V_{r1} and V_{r2} are respectively the control voltages on the grids of B_1 and B_2 (see fig. 44), and V_b is the supply voltage.

The first term in the denominator of (28) corresponds to t_1 in fig. 41 and thus, in the case of an asymmetric multivibrator, predominates over the second term representing the time t_2 in fig. 41, so that to a good approximation the expression for the frequency may be written as:

$$f \approx \frac{1}{R_{g1} C_1 \ln \frac{V_b + V_{r1}}{V'_{c/o} + V_{r1}}}, \dots \dots \dots (29)$$

from which it appears that the frequency is inversely proportional to the time constant $R_{g1} C_1$ of the grid circuit, whilst as a rule the dependency upon the control voltage V_{r1} is fairly linear over a wide range.

For the blocking oscillator (fig. 45) a similar expression holds, viz.

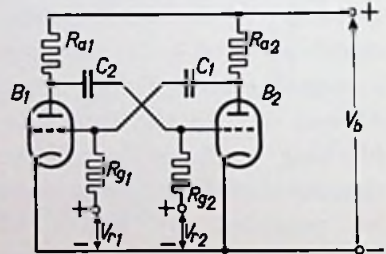


Fig. 44.

Circuit of a multivibrator with control voltages V_{r1} and V_{r2} applied to the grids of the valves B_1 and B_2 .

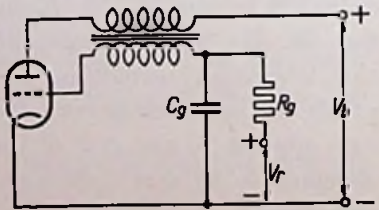


Fig. 45.

Circuit of a blocking oscillator with a control voltage V_r applied to the grid of the valve.

$$f = \frac{1}{R_g C_g \ln \frac{aV_b + V_r}{V_{c/o} + V_r}} \dots \dots \dots (30)$$

where $V_{c/o}$ is the cut-off voltage of the valve employed, V_r the control voltage on the grid and a represents a factor dependent upon the properties of the blocking transformer.

3.2. INDUCTIVE SAW-TOOTH GENERATING CIRCUITS

In television reception, magnetic deflection is nowadays almost exclusively employed, for various reasons. In the first place, for electrostatic deflection, especially with the increasing use of wide-angle deflection and high accelerating voltages now being applied more and more, the high saw-tooth voltages required would be rather difficult to produce without excessive non-linearity. Furthermore, the construction of the cathode-ray tube would be more complicated and thus more expensive, because the two pairs of deflecting electrodes at right angles to each other would have to be provided in the tube. Moreover there is the objection that a built-in electrostatic deflection system is less flexible than an external magnetic deflection system: it is easier to obtain a practically distortion-free deflection with a magnetic than with an electrostatic system (stray fields), whilst, if the deflection should become inadequate or distorted, it cannot be remedied by changing anything in the electrostatic system, so that the cathode-ray tube would have to be replaced in its entirety, whereas in the case of magnetic deflection only the coils need be adjusted or replaced.

Although, however, the present situation in television reception technique is such that magnetic deflection is almost exclusively employed, and it would therefore be expected to find only inductive saw-tooth generators in the receivers, such is not by any means the case. The most common method of generating the saw-tooth currents for the deflecting coils is in fact a combination of a self-oscillating saw-tooth voltage generator and an aperiodic saw-tooth current generator, the latter being in the form of a non-self-oscillating circuit of an inductive current generator driven by the saw-tooth output voltage of the capacitive saw-tooth generator. The following will explain how this situation has arisen.

The capacitive saw-tooth oscillator was the first to be developed. It was required, for instance, in the cathode-ray oscilloscope, where electrostatic deflection is usually applied (low electron velocities, small deflection angles). Further, capacitive saw-tooth oscillators are more easily synchronized than inductive oscillators (large negative pulses are needed on the grid of the oscillator valve; see 2.2.1 and fig. 27). In analogy with the situation in

I.f. output circuits, where, by means of an output valve of sufficient current output and a transformer, audio-frequency voltages are converted into audio-frequency currents of sufficient strength to give the coil in a loud-speaker the necessary oscillation amplitudes, in the television receiver the saw-tooth currents required for magnetic deflection are likewise generated from saw-tooth voltages of relatively small amplitude by means of an output valve and a transformer.

However, in 2.2.1 it has already been explained that the problem is much more complicated than a simple voltage amplification followed by transformation into a current. This holds for line saw-tooth generators in all cases. For frame saw-tooth generators the above analogy with the audio output stage still holds more or less. On account of the much lower frequency of the frame saw-tooth signals, the resistance of the deflection coils predominates over the reactive impedance, so that the frame saw-tooth output valve has mainly an ohmic load impedance in the anode circuit, whereas in the line saw-tooth output valve the impedance is preponderantly reactive. For the frame saw-tooth output valve, however, the input signal is in most cases not of a purely saw-tooth shape, but purposely distorted ⁵⁾ — in a certain manner in a special preceding circuit — so as to compensate the distortions in the output stage. Moreover, in this way it is possible to reduce the average current drain of the output valve.

3.2.1. SAW-TOOTH CURRENT GENERATOR FOR FRAME DEFLECTION

A circuit for vertical deflection on the cathode-ray tube MW 36-24 is given in fig. 46. This circuit is intended to operate in conjunction with a line-output circuit that contains a booster diode giving a boosted H.T. voltage of 485 V. This voltage is also used to feed the anode of the frame output pentode. The potentiometer R_5 is the vertical hold control.

The amplitude control is incorporated in potentiometer R_{12} . The linearity at the beginning of the scan is adjusted with the potentiometer R_7 in the cathode circuit of the ECL 80 valve.

3.2.2. SAW-TOOTH CURRENT GENERATORS FOR LINE DEFLECTION

In the case of the inductive saw-tooth generator for line deflection a diode is almost always used for economic operation. With an efficiency-diode circuit, the magnetic energy accumulated in the self-inductance at the end of the scan is recovered in such a way as to make the circuit very

⁵⁾ See: Electronic Application Bulletin Vol. 11, Nr. 2 (Febr. 1950), p. 23.

economical in power consumption. With a booster-diode circuit the magnetic energy is utilized for generating an additional high voltage to feed the valves in the television receiver needing a higher supply voltage; in most cases this voltage is used for the anodes of the frame blocking oscillator and the frame output valve (see fig. 46, where the voltage

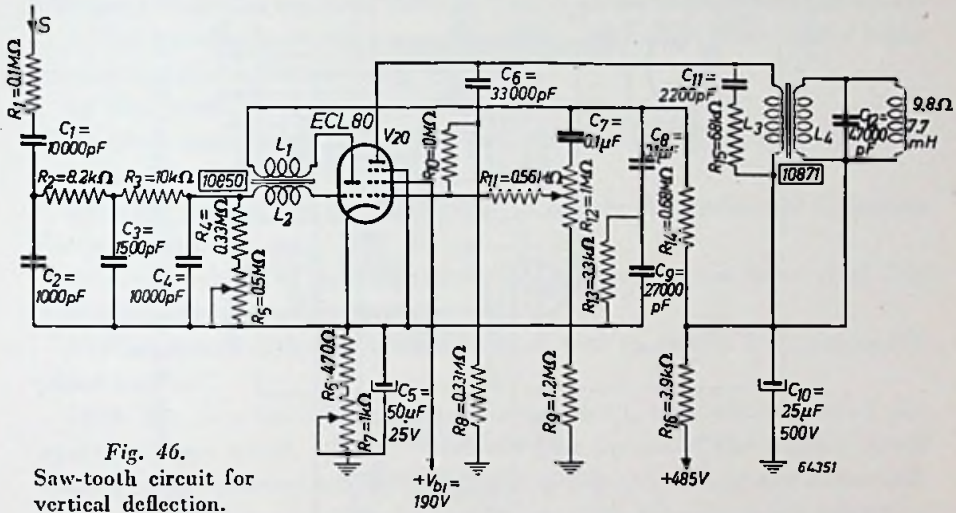


Fig. 46. Saw-tooth circuit for vertical deflection.

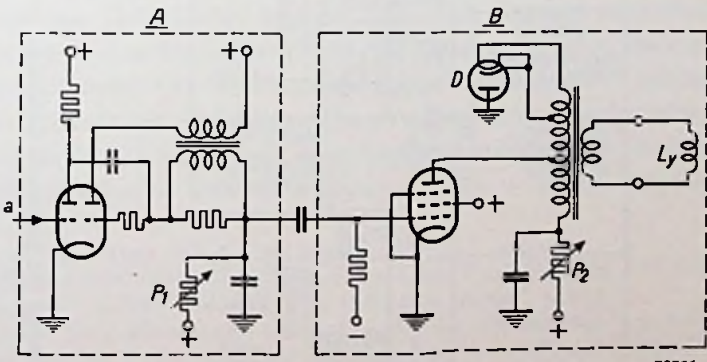


Fig. 47.

Saw-tooth current generator for horizontal deflection incorporating an efficiency diode *D*. The dotted block *A* comprises a capacitive saw-tooth oscillator (blocking oscillator) and synchronization amplifier valve, to which synchronizing pulses are fed at *a*. Block *B* contains an aperiodic inductive saw-tooth current generator, triggered by the saw-tooth output voltage of the blocking oscillator. *P*₁ = frequency control potentiometer. *P*₂ = amplitude control potentiometer. *L*_y = line deflection coils.

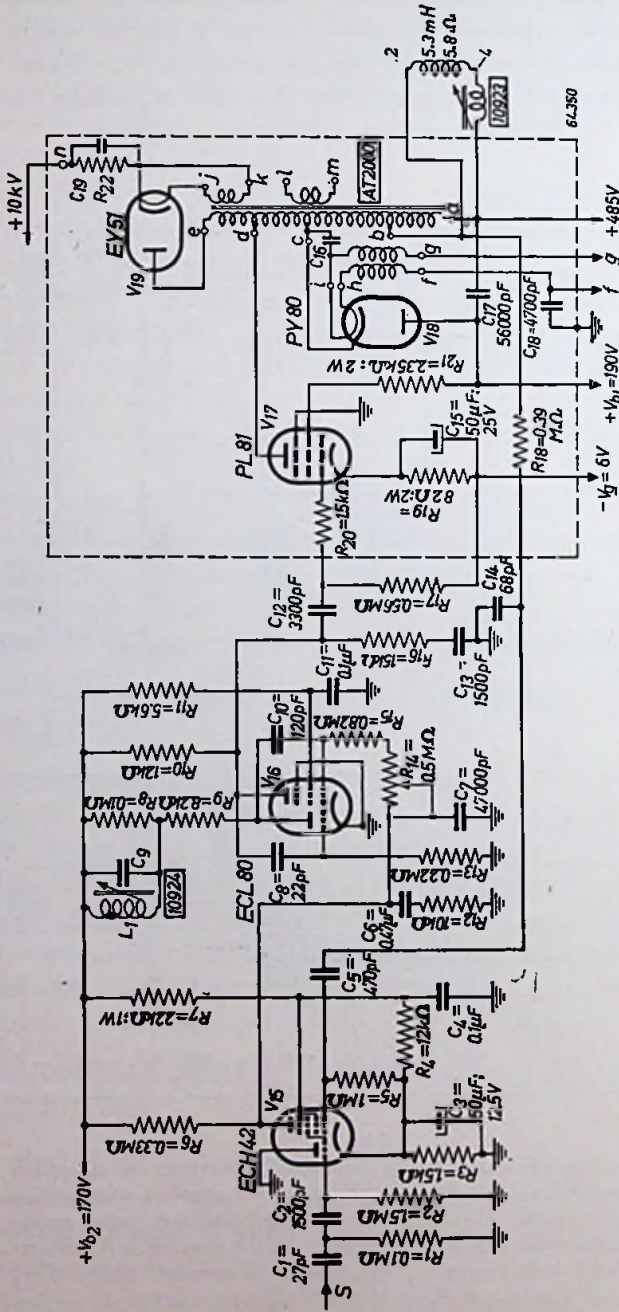


Fig. 48. Circuit for horizontal deflection, with booster diode PY 80 and EHT rectifier EY 51.

+485 V is derived from the booster circuit). This is a great advantage particularly in television receivers built for low mains voltages and in sets operating without mains transformer, and since the latter type is now being used more and more, it is not surprising that the efficiency diode has been almost entirely replaced by the booster diode. However, for the sake of completeness, a circuit for a line saw-tooth current generator with efficiency diode has not been omitted. Such a circuit is reproduced in fig. 47.

A line saw-tooth current generator with a booster diode and a high-tension rectifier is shown in fig. 48.

In this circuit the functions of the valves are as follows:

ECH 42 synchronizer; ECL 80 line multivibrator; PL 81 line output; PY 80 booster; EY 51 E.H.T. rectifier.

This line-output circuit is intended to supply the horizontal deflection for a cathode-ray tube MW 36-24.

A circuit which is very insensitive to interference has been used for synchronizing the multivibrator.

Further details of this circuit will be dealt with in section 6-4 "Automatic phase control".

Both line saw-tooth current generators dealt with above are of the aperiodic type which can be "switched" by means of the output signal from a self-oscillating saw-tooth voltage generator. As already remarked, this is the form met with in by far the majority of present-day television receivers. Recently, however, self-oscillating current generators have also come into use, though only for line deflection. Readers interested in this type are referred to the literature on the subject quoted in the footnote ⁶⁾. In section 6.4 under "Automatic phase control" a circuit of a self-oscillating line saw-tooth current generator will be given in which the difficulties involved by synchronization have been overcome and with which the latest form of synchronization — flywheel synchronization — can be applied.

⁶⁾ O. S. Puckle: "Time Bases" (2nd edition, 1951).

Bulletin der Schweizerischen Elektrotechnischen Verein 40, No. 17 (1949).

J. Haantjes: "A Self-Oscillating Line Deflection Circuit", p. 633.

R. Urtel: "Neue selbsterregte Generatoren für die Ablenkströme", p. 641.

J. Haantjes and F. Kerkhof, Proc. I.R.E. 36 (1948), p. 407, and Philips Techn. Rev. 10, No. 10 (1949), p. 307.

F. Kerkhof and W. Werner: Television (1951), p. 163, Philips Technical Library; German version "Fernsehen".

4. ELECTRONIC VALVES SPECIALLY DEVELOPED FOR SAW-TOOTH GENERATORS

From what has been said in section 2 it will be understood that the electronic valves employed in saw-tooth generator circuits will have to comply with very special requirements, according to the functions they have to fulfil. For instance, those functioning as a switch must have the lowest possible internal resistance in the conducting (closed) state, no matter whether they are self-switching (self-oscillating) or triggered by external impulses. By way of illustration the line output valve PL 81 may be compared with other output pentodes.

Of particular importance is the internal resistance of the valve at low anode voltages, i.e. below the "knee" in the Ia-Va characteristic. At $V_{g2} = 170 \text{ V}$, $V_{g3} = 0$, $V_{g1} = 0$, the internal resistance of the PL 81 is 125Ω , while that of the PL 82 is 312Ω and that of the PL 83 (video output valve) 670Ω .

Further, during the line flyback, high voltage peaks occur particularly on the anode of the line output valve, and therefore the anode connection of the PL 81 is mounted on the top of the valve in order to minimize the risk of flashover.

The requirements that have to be met by the booster diode are quite different from those of the E.H.T. rectifier. The booster anode has to withstand rather high negative voltage peaks with respect to the cathode, but these are lower than the positive peaks on the anode of the PL 81, so that there is no need of a top connection for the booster diode PY 80. The E.H.T. rectifier, on the other hand, has to withstand much higher voltages between anode and cathode, and for that reason the anode and cathode connections of the EY 51 are spaced as far as possible apart. The booster diode has also to cope with large currents, whereas those occurring in the E.H.T. rectifier are much smaller, so that the heating energy required for the PY 80 (5.7 W) is much greater than that for the EY 51 (0.57 W), and thus there is also a great difference in volume of the glass envelope.

Since only a low heating energy is needed for the EY 51, this can be taken from the line output transformer, which has a small extra winding for that purpose, as shown in fig. 48. For the filament supply of the booster diode, however, the conditions are more difficult. In the circuit of fig. 48 (a so-called primary booster circuit), the cathode of the PY 80

is subjected to voltage peaks of some thousands of volts, and if its filament were included in the normal way in the chain of filaments fed from the mains, then these voltage peaks would be applied at practically their full strength between cathode and filament. The insulation between cathode and filament, however, is not calculated to withstand such high voltages, and there is therefore a great risk of its breaking down. To avoid this danger, heater current is fed via an extra bifilar winding laid on the transformer, so that, at least with respect to the peak voltages, cathode and filament are at the same potential. There are circuits, however, where no extra windings are needed on the transformer, such as in the case of the secondary booster circuit (see fig. 49), or where a separate heating-current transformer is used with adequate insulation between the primary and secondary windings.⁷⁾

Each of these methods has its drawbacks. Both the bifilar windings and the secondary booster circuit give additional stray inductance, capacitance and losses in the transformer, which have an adverse effect upon the flyback time, the H.T. potential attainable, the suppression of stray oscillations and the efficiency of the output circuit. (In this connection it may be noted that the introduction of *Ferroxcube* as core material has proved to be of the utmost importance in giving the output transformer the most favourable properties).

The application of a separate, well-insulated heater-current transformer naturally involves additional expense, and of course the same is the case with extra bifilar windings on the transformer, so that it would, obviously, offer considerable advantages — not only as regards cost, but also from a technical point of view — if the booster diode could be so constructed that the high voltage peaks occurring during the saw-tooth flyback could safely be permitted between cathode and filament.

Such diodes have in fact been recently constructed both in the U.S.A. and in Europe. Broadly these are all based on the same principle: the

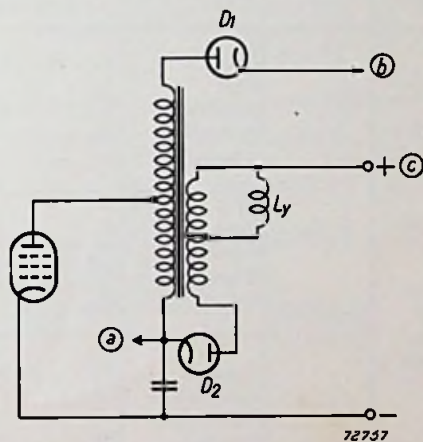




Fig. 49.

Aperiodic inductive saw-tooth generator with secondary booster circuit. D_1 = E.H.T. rectifier diode; D_2 = booster diode. a = boosted H.T.; b = E.H.T.; c = H.T. supply; L_y = line deflection coils.

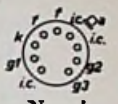
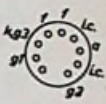
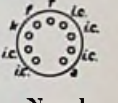
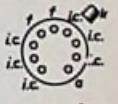
⁷⁾ See: Electronic Application Bulletin, Vol. 12, No. 8 (Aug. 1951), p. 137-139.

cathode is no longer mainly heated through direct contact with the heater insulation, but exclusively by radiation; in most of these constructions the cathode and heater are completely insulated with respect to each other. The minimum distance permitted between these two electrodes depends upon the form given to the heater construction. In the new PY 81 type of booster diode made by Philips, it has been possible to keep this distance very small, so that the energy required for the heater is about equal to that needed for the PY 80 diode (not heated by radiation).

In the following table some technical data are given for the Philips valves at present employed in saw-tooth generator circuits.

Type	Filament data	Application	Voltages Resistors	Current (mA)	Characteristic data	Base connections
ECL 80 Triode output pentode	$V_f = 6.3 \text{ V}$ $I_f = 0.3 \text{ A}$	Class A final amplifier (pentode system)	$V_a = V_b = 170 \text{ V}$ $V_{g3} = 0 \text{ V}$ $V_{g2} = 170 \text{ V}$ $V_{g1} = -6.7 \text{ V}$	$I_a = 15$ $I_{g2} = 2.8$	$S = 3.2 \text{ mA/V}$ $R_i = 0.15 \text{ M}\Omega$ $R_a = 11 \text{ k}\Omega$ $W_o = 1.0 \text{ W}$ $W'_a = 3.5 \text{ W}$	 Noval
		Sync separator (pentode system)	$V_a = 20 \text{ V}$ $V_{g3} = 0 \text{ V}$ $V_{g2} = 12 \text{ V}$ $V_{g1} = 0 \text{ V}$	$I_a = 2$		
		Typical characteristics (triode system)	$V_a = 100 \text{ V}$ $R_k = 575 \Omega$	$I_a = 4$	$S = 1.35 \text{ mA/V}$ $\mu = 18$	
		A.F. amplifier (triode system)	$V_b = 170 \text{ V}$ $R_a = 0.22 \text{ M}\Omega$ $V_{g1} = -3.5 \text{ V}$ $R_{g1} = 0.68 \text{ M}\Omega^b$	$I_a = 0.5$	$g = 11$	
EY 51 E.H.T. rectifying valve	$V_f = 6.3 \text{ V}$ $I_f = 90 \text{ m}$	Rectifier 50 c/s	$V_{tr} = \text{max. } 5 \text{ kV}$	$I_o = \text{max. } 3$	$C_{fil} = \text{max. } 0.1 \mu\text{F}$ $R_i = \text{min. } 0.1 \text{ M}\Omega$	
		Rectifier 10-500 kc/s	$V = \text{max. } 17 \text{ kV}$ <i>a inuc. p</i>	$I_o = \text{max. } 3$	$C_{fil} \text{ max. } 0.01 \eta\text{F}$ $R_i = \text{min. } 0.1 \text{ M}\Omega$	
		Pulse rectifier	$V_{a \text{ invp}} = \text{max. } 17 \text{ kV}$	$I_o = \text{max. } 0.35$ $I_{ap} = \text{max. } 80 \text{ a}$	$C_{fil} = \text{max. } 5000 \mu\text{F}$	

a) Max. pulse time $\frac{1}{2}\%$ of one cycle with a maximum of $5 \mu\text{sec}$.
 b) $R_{g1}^1 =$ grid leak of following valve.

Type	Filament data	Application	Voltages Resistors	Currents (mA)	Characteristic data	Base connections
PL 81 Line output pentode	$V_f = 21.5V$ $I_f = 0.3 A$	Typical characteristics	$V_a = 170 V$ $V_{g3} = 0 V$ $V_{g2} = 170 V$ $V_{g1} = -22 V$	$I_a = 45$ $I_{g2} = 3.0$	$S = 6.2 \text{ mA/V}$ $W_a = 8 \text{ W}$ $V_{ap}^b) = \text{max. } 7 \text{ kV}$	 Noval
PL 82 Frame or sound output pentode	$V_f = 16.5V$ $I_f = 0.3 A$	Typical characteristics	$V_a = 170 V$ $V_{g2} = 170 V$ $V_{g1} = 10.4V$	$I_a = 53$ $I_{g2} = -10$	$S = 9.0 \text{ mA/V}$ $R_i = 20 \text{ k}\Omega$ $W_a = 9 \text{ W}$ $V_{ap}^a) = \text{max. } 2.5 \text{ kV}$	 Noval
PY 80 Booster diode	$V_f = 19 V$ $I_f = 0.3 A$	Booster	$V_{a \text{ in } p}^b) = \text{max. } 4 \text{ kV}$	$I_a = \text{max. } 180$ $I_{ap} = \text{max. } 400$	$V_{kfp} = \text{max. } 650 \text{ V}^c)$ $C_a = 5.5 \text{ pF}$ $C_{filt} = \text{max } 4 \mu F$	 Noval
PY 81 Booster diode	$V_f = 17 V$ $I_f = 0.3 A$	Booster	$V_{a \text{ in } p}^b) = \text{max. } 4.5 \text{ kV}$	$I_a = \text{max. } 150$ $I_{ap} = \text{max. } 450$	$V_{kfp}^d)e) = \text{max. } 800 \text{ V}$ $V_{kfp}^e)b) = \text{max. } 4500 \text{ V}$ $C_a = 6.4 \text{ pF}$ $C_{filt} = \text{max. } 4 \mu F$	 Noval

- a) Max. pulse time 10% of one cycle with a maximum of 2 msec.
b) Max. pulse time 18% of one cycle with a maximum of 18 μ sec.
c) Max. 100 V (r.m.s.) A.C. + 500 V D.C. Cathode positive with respect to heater.
d) Max. 220 V (r.m.s.) mains voltage + 600 V D.C.
e) Cathode positive with respect to heater.

5. SYNCHRONIZATION

5.1. INTRODUCTION

For the sake of completeness and ready reference, some principles which have already been dealt with in detail in the preceding sections are briefly recapitulated here.

Most time-base generators used in television are based on the principle of a capacitor being charged to a high potential via a resistor, so that the voltage across the capacitor increases with time according to an exponential law and asymptotically approaches the value of the voltage applied ⁸). Long before the voltage across the capacitor reaches this final value, the capacitor is rapidly discharged by means of a switching device which, for the sake of simplicity, will be termed "the switch". A condition which must obviously be imposed on this switch is that its internal resistance should be as small as possible. After the switch has as far as possible discharged the capacitor, it is reopened, thus completing the cycle, and the capacitor is then charged again.

There are thus two distinct phases in the operation of the time-base generator — the first phase during which the capacitor is gradually charged (the stroke or scan) and the second phase at which it is suddenly discharged (the flyback). It is not the purpose of this chapter to deal with such matters as means for improving the linearity of the scan or for preventing unwanted oscillations (ringing) during the flyback ⁹). For the time being only the synchronization of the saw-tooth signals will be considered and, more particularly, the different methods of achieving this synchronization.

The purpose of synchronization is to ensure that the luminous representation of a picture element picked up and broadcast by the transmitter, is reproduced at a position on the image plane in the receiver which coincides with that of the original picture element at the transmitter. When a new frame is to be scanned in the transmitter, starting at the left-hand top corner of the image plane, the deflection of the electron beam of the picture tube in the receiver must be such that the electrons also impinge on the left-hand top corner of the tube screen. This means that both the saw-tooth signal of comparatively low frequency (50 or 60 c/s in the case of interlaced

⁸) See J. Jager, Comments on Circuits for Generation of Time-base Voltages, *Electr. Appl. Bull.* X, p. 15, 1948/49 (No. 1).

⁹) See, for example, *Television Receivers*, *Philips Techn. Rev.* 4, p. 342, 1939 (No. 12) and J. Haantjes and F. Kerkhof, *Projection-Television Receiver*, *Philips Techn. Rev.* 10, p. 307, 1949 (No. 10) and the article quoted in footnote ¹).

scanning), which provides for the vertical deflection of the electron beam (the frame time-base signal), and the saw-tooth signal of higher frequency (625 per complete image for the continental television standard), for the horizontal deflection of the electron beam (the line time-base signal), must be at the commencement of their stroke.

The frame time-base generator and the line time-base generator receive the "intelligence" from the transmitter to denote the instant when the stroke must end and the flyback must take place. This information is given by means of synchronizing pulses which are transmitted at the end of each frame and at the end of each line. It is beyond the scope of this book to discuss the methods for combining these pulses with the video signal in the transmitter and for separating them from this signal in the receiver¹⁰).

5.2. METHODS OF SYNCHRONIZATION

The synchronizing pulses may control the switch in the time-base generator in different ways. It is, for example, possible to use a switch which is always open unless a synchronizing signal is present, and which reacts immediately to a synchronizing pulse by remaining closed so long as the pulse continues. Such a switch might consist of a gasfilled or high-vacuum electron valve which is so adjusted that the anode current is just cut off during normal operation, but which becomes conductive and discharges the capacitor of the time-base generator by means of its anode current as soon as a positive voltage pulse is applied to its control grid.

One drawback of this type of switch is that no saw-tooth signal will be supplied if the synchronizing pulses happen to be missing for some reason. The electron beam will then no longer sweep over the screen of the picture tube and the spot will remain steady at a single point, which may lead to serious damage of the luminescent material. Another drawback is that such a switch is very sensitive to interferences. In fact, any interfering impulse of sufficient amplitude may operate the switch, i.e. render the tube conductive, so that the capacitor will be discharged.

A different method of synchronization, in which the first of these drawbacks has been eliminated and at the same time the high sensitivity to interferences has been diminished, consists in the use of a time-base generator which is self-blocking, or, as it might also be called, self-switching. Even when no synchronizing signal is present, such a circuit continues to supply a saw-tooth signal the frequency of which is mainly determined by an adjustable time constant, i.e. an RC network.

¹⁰) See, for example, C. L. Richards, *A Television Receiver*, Philips Techn. Rev. 2, p. 33, 1937 (No. 2), the first article quoted in footnote ²), and J. Haantjes and F. Kerkhof, *Projection-Television Receiver*, *ibid.* 10, p. 364, 1949 (No. 12).

The two principal types of self-blocking oscillator are the multivibrator and the blocking oscillator.

Both consist in essence of an oscillator with very heavy positive feedback; at the beginning of an oscillation the grid current of one of the electron valves employed in the circuit suddenly assumes such a high value that a capacitor is rapidly charged in such a way that the control grid becomes highly negative with respect to the cathode. In this way both the grid- and anode currents of the valve concerned consist merely of short pulses. The charged grid capacitor C is discharged via a grid leak R , as a result of which the grid becomes less negative with respect to the cathode, the voltage decreasing according to an exponential law with a time constant RC . As soon as the negative grid voltage becomes less than the cut-off voltage of the valve, anode current again starts to flow and suddenly increases to a high value, together with the grid voltage and the grid current, as a result of the heavy feedback. The capacitor C is then charged once again and the valve is again cut off, thus completing the cycle.

The variations of the anode current i_a and the grid-to-cathode voltage v_g as functions of time have been plotted in fig. 50. The frequency of this relaxation-oscillator signal may be synchronized by applying positive pulses to the control grid. These should be so limited that their maximum amplitude does not exceed the value h (see fig. 50). Interfering signals are then also limited to this value.

The broken line drawn at a height h above the exponential part of the v_g curve in fig. 50 shows that a pulse of amplitude h applied between the instants t_2 and t_3 will advance the flyback of the saw-tooth signal.

If only the synchronizing pulses are considered, it will be clear that synchronization will be possible so long as the cycle of the synchronizing signals lies between $t_3 - t_1$ (i.e. the cycle of the free-running oscillator) and $t_2 - t_1$. This illustrates the well-known fact that for adequate synchronization the frequency of the generator should be adjusted to a value slightly below that of the synchronizing pulses.

The oscillogram of fig. 50 moreover shows the reduced sensitivity to

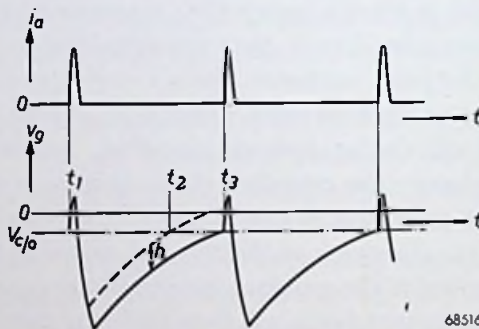


Fig. 50.
Anode current i_a and grid-to-cathode voltage v_g of a self-blocking oscillator valve, as a function of the time t . $V_{c/o}$ denotes the grid voltage at which the tube is cut off.

interfering signals, since these can initiate the flyback only during the interval from t_2 to t_3 and not during the interval from t_1 to t_2 .

The two systems mentioned above have one important feature in common, namely that each individual synchronizing pulse always determines the instant of the flyback (disregarding the case of an interfering signal initiating the flyback). In other words, the generator never has a chance to oscillate at its natural frequency. In this respect the third method of synchronization to be dealt with, i.e. "flywheel" synchronization, differs essentially from the methods discussed above. With flywheel synchronization the time-base generator is allowed to operate at its natural frequency and the influence of the synchronizing pulses is restricted to readjusting this natural frequency when it deviates from the synchronizing frequency.

6. FLYWHEEL SYNCHRONIZATION

6.1. INTRODUCTION

The term "flywheel time-base circuit" applied to a comparatively recent technique, the use of which in television receivers is steadily increasing, is aptly chosen, as it clearly describes the principle on which this method of synchronization is based. The purpose of a flywheel in mechanical constructions is to maintain the speed at which a driving spindle revolves substantially constant by minimizing the influence of sudden variations of the driving torque on the speed of the driven machine. The inertia of the flywheel provides a certain measure of smoothing, i.e. disturbances of short duration are spread out over a longer period. When the value of the driving torque changes permanently to a different level, the speed of revolution will also assume a different final value after a delay which depends on the mass of the flywheel. Similarly, in time-base generators with flywheel synchronization, the influence of disturbances in the synchronizing signals on the frequency of the saw-tooth signal is reduced, smoothed or spread out. How this is achieved is discussed in detail below.

These disturbances consist of unwanted signals superimposed on the synchronizing signal. They may be produced by various local sources, such as internal combustion engines with electrical ignition (e.g. motor cars), electric motors with commutators (e.g. vacuum cleaners), diathermy sets, radar equipment and atmospherics. The inherent noise of the receiving set may also give rise to this form of disturbance.

The amount of man-made interference received is, of course, largely dependent upon the location of the aerial with respect to the source of the interference. For example, in the vicinity of a busy thoroughfare much trouble is likely to be experienced from motor-car interference. In so-called fringe areas at considerable distances from the transmitter, where the "noise" is of the same order as, or even exceeds the signal, such noise interference is of a permanent nature and renders reasonable television reception impossible, mainly because the synchronization is completely upset by the continuous noise.

In such cases a striking improvement may be obtained by means of time-base generators with flywheel synchronization. It is true that one effect of the noise remains, in the form of a whirl of light or dark spots spreading over the picture like a snow-shower, but the improvement is nevertheless quite substantial, since the coherence of the picture is maintained.

6.2. PRINCIPLE OF FLYWHEEL SYNCHRONIZATION

There is also a method intermediate between directly synchronized time-base generators in which each individual synchronizing pulse determines the instant of the flyback, and time-base generators the natural frequency of which is maintained at the correct value by comparison with the frequency of the synchronizing signal, mentioned at the end of section 5.2.

In this intermediate method the flyback is also initiated directly by pulses, but instead of using the transmitted synchronizing pulses as such for this purpose, the pulses are derived therefrom by passing them through a flywheel circuit. This introduces a certain inertia effect, as a result of which fluctuations of the synchronizing frequency are no longer followed closely by the output signal of the flywheel circuit. Since the time-base frequency is directly determined by the frequency of these output signals, some time will elapse before fluctuations of the synchronizing frequency will be manifest in the time-base frequency. The influence of unwanted interferences is also reduced by this flywheel circuit.

The resonant circuit is a well-known electrical equivalent of the mechanical flywheel. A measure of the inertia or delaying action of such a circuit is the time constant T_c , which indicates the time taken for the amplitude of the oscillations set up in the circuit by periodical pulses at its natural frequency to increase (or decay) by an amount equal to $1 - 1/e$ of the difference between its theoretical maximum value and its original value (or the difference between its original value and its theoretical minimum value), taking as the starting point the instant at which excitation commences or at which a sudden change of the amplitude or frequency takes place. The condition prior to this change will be referred to as the "static" condition, as opposed to the "dynamic" or "transient" condition which occurs when, for example, the frequency of the pulses is changed, and lasts until a new "static" condition is reached. It will be assumed here that this will be the case after a time which is a multiple of T_c .

The time constant T_c is directly proportional to the quality factor Q of the circuit and the periodic time T_0 of the natural frequency, viz.

$$T_c = \frac{Q}{\pi} \cdot T_0,$$

as will be seen later.

The time constant contains T_c/T_0 saw-tooth cycles, which, according to the above expression, is equal to Q/π , so that the effect of the inertia of the flywheel circuit may also be expressed by stating that a sudden change

of permanent nature of the synchronizing frequency is not immediately manifest in the saw-tooth frequency, and it is not until Q/π saw-tooth cycles have elapsed that this change becomes clearly noticeable. It may thus also be said that a temporary variation of the synchronizing frequency must have a duration of at least Q/π saw-tooth cycles to affect the saw-tooth frequency noticeably. Unwanted interferences superimposed on the synchronizing signal will therefore have no serious consequences unless they occur at regular intervals corresponding approximately to the natural frequency of the circuit and, moreover, continue long enough to form a regular series of at least Q/π pulses.

To ensure a good stabilizing action it is therefore desirable to make Q of the flywheel circuit as high as possible, but the phase shift between the input and output signals which results from a variation of the synchronizing frequency and increases with the value of Q , sets a limit to the maximum value of Q . In television sets this phase shift would result in displacement of the image on the screen of the picture tube.

The narrower the limits within which the fluctuations of the synchronizing frequency occur, the higher will be the permissible Q of the resonant circuit. When the transmitter is synchronized by the mains frequency, the instability of the latter limits the maximum permissible value of Q . A free-running transmitter will usually have a much higher frequency stability, which offers the possibility of applying a very efficient flywheel action for synchronizing the receiver.

It will be useful first to discuss this intermediate form of synchronization in greater detail, because in this case the flywheel action can be more clearly distinguished. In the next section the flywheel action of resonant circuits will therefore be represented by explicit expressions and also graphically. Section 6-4 will deal exclusively with those types of time-base generators in which flywheel synchronization is obtained by applying automatic phase control between the saw-tooth and synchronizing signals, (the series being concluded by descriptions of practical circuits (Section 6.4.4)).

6.3. FLYWHEEL ACTION OF RESONANT CIRCUITS

6.3.1. REACTION OF A PARALLEL RESONANT CIRCUIT TO A PULSE OF SHORT DURATION

In practice the synchronizing signals for time-base generators of television receivers always have the form of rather narrow pulses and are made as rectangular as possible. The word narrow should be taken in the relative sense here; the frame synchronizing pulses are in fact much wider than the

line synchronizing pulses, but the pulses should be compared with the cycle of the saw-tooth which they are intended to synchronize. The width of the pulses is then at the utmost 10% to 15% of the corresponding cycle. In order to separate the line-synchronizing pulses from the frame pulses, the former are, moreover, differentiated, which renders them even narrower.

Up to now flywheel synchronization has been confined to line time-base generators owing to the difficulties arising from the inconveniently large time constant in smoothing circuits for frame-synchronizing frequencies, so that it may truly be stated that resonant circuits, used as flywheel elements, are usually excited by current or voltage pulses of very short duration. As a rule the circuits are so arranged that current pulses are supplied to the circuit, and this case will now be dealt with.

The comments will be based on the parallel resonant circuit of fig. 51, which consists of a capacitance C connected in parallel with an inductance L and a resistance r . This resistance is as a rule the dissipative resistance of the coil.

The current I is assumed to consist of one ideal pulse only, occurring at the instant $t = 0$. Such an ideal pulse is understood to be of infinitely short duration and of infinitely large amplitude, the time integral (the "content") of the pulse, however, being a finite quantity q (having the dimension of a charge).

In the first instance this pulse results in a charge q being supplied suddenly to the capacitor C at the instant $t = 0$, because the inductance represents an infinitely large impedance to the current pulse. The voltage across the capacitor, which is also the voltage V across the circuit, is thus suddenly increased from zero to a value

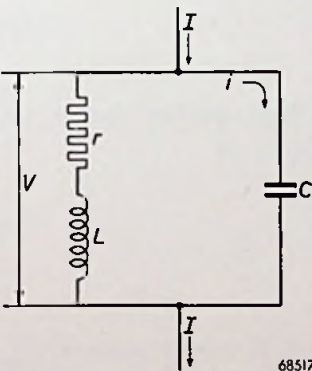


Fig. 51. Parallel resonant circuit consisting of a capacitance C and an inductance L having a resistance r .

$$V_0 = \frac{q}{C} \dots \dots \dots (31)$$

at the instant $t = 0$, assuming that no currents or voltages were present in the circuit previously, i.e. at $t < 0$.

It will now be useful to investigate what the variation of this voltage will be following the instant $t = 0$. In C , r and L a current i starts to flow, which must satisfy the following differential equation (Kirchhoff's law):

$$\frac{1}{C} \int i \, dt + L \cdot \frac{di}{dt} + ri = 0, \dots \dots \dots (32)$$

or:

$$LC \cdot \frac{d^2 i}{dt^2} + rC \cdot \frac{di}{dt} + i = 0. \quad \dots \dots \dots (32a)$$

Assume:

$$i = K \cdot e^{pt}, \quad \dots \dots \dots (33)$$

then, from eqs (32a) and (33):

$$p^2 + \frac{r}{L} \cdot p + \frac{1}{LC} = 0, \quad \dots \dots \dots (34)$$

which gives for p :

$$p = -\frac{r}{2L} \pm \sqrt{\left(\frac{r}{2L}\right)^2 - \frac{1}{LC}} \quad \dots \dots \dots (35)$$

Denoting:

$$\frac{r}{2L} = a, \quad \dots \dots \dots (36)$$

and:

$$\frac{1}{LC} = \omega_0^2, \quad \dots \dots \dots (37)$$

the following solutions are found for p :

$$\left. \begin{aligned} p_1 &= -a + \sqrt{a^2 - \omega_0^2} \\ p_2 &= -a - \sqrt{a^2 - \omega_0^2} \end{aligned} \right\} \quad \dots \dots \dots (38)$$

It is further assumed that the circuit has a high quality factor, i.e.

$$a^2 \ll \omega_0^2,$$

or:

$$\frac{r}{2L} \ll \omega_0,$$

which gives:

$$\frac{1}{2} \ll \frac{\omega_0 L}{r} = Q \quad \dots \dots \dots (39)$$

In this assumption p_1 and p_2 are imaginary, namely conjugate complex, i.e.:

$$\left. \begin{aligned} p_1 &= -a + j\omega \\ p_2 &= -a - j\omega \end{aligned} \right\}, \quad \dots \dots \dots (40)$$

in which:

$$\omega = \sqrt{\omega_0^2 - a^2} = \omega_0 \sqrt{1 - \left(\frac{1}{2Q}\right)^2} \dots \dots \dots (41)$$

The general solution of i is now:

$$i = K_1 e^{p_1 t} + K_2 e^{p_2 t} \dots \dots \dots (42)$$

K_1 and K_2 are determined by the initial conditions, namely:

- (a) $i = 0$ for $t = 0$, and
- (b) the voltage across the capacitor $V_c = V_0$ for $t = 0$.

From (a) follows that:

$$0 = K_1 + K_2, \dots \dots \dots (43)$$

whilst from (b):

$$V_c = \int_0^t \frac{i}{C} \cdot dt = \frac{1}{C} \left(\frac{K_1}{p_1} \cdot e^{p_1 t} + \frac{K_2}{p_2} \cdot e^{p_2 t} \right),$$

and for $t = 0$:

$$V_0 = \frac{1}{C} \left(\frac{K_1}{p_1} + \frac{K_2}{p_2} \right) \dots \dots \dots (44)$$

From eqs. (43) and (44):

$$K_2 = -K_1,$$

and:

$$V_0 = \frac{K_1}{C} \cdot \left(\frac{1}{p_1} - \frac{1}{p_2} \right),$$

or:

$$K_1 = V_0 C \cdot \frac{p_1 p_2}{p_2 - p_1} = - \frac{V_0 C \omega_0^2}{2 j \omega} \dots \dots \dots (45)$$

and:

$$K_2 = + \frac{V_0 C \omega_0^2}{2 j \omega} \dots \dots \dots (46)$$

With these values of the integration constants the expression for the current becomes:

$$i = - \frac{\omega_0^2}{\omega} \cdot C V_0 e^{-at} \sin \omega t, \dots \dots \dots (47)$$

while the expression for the voltage across the circuit is:

$$V = V_0 e^{-at} \left(\cos \omega t + \frac{a}{\omega} \cdot \sin \omega t \right) \dots \dots \dots (48)$$

From eqs. (39) and (41) it follows that ω is approximately equal to ω_0 , so that:

$$i \approx -\omega_0 C V_0 e^{-at} \sin \omega t, \quad \dots \dots \dots (49)$$

and

$$V \approx V_0 e^{-at} \cos \omega t. \quad \dots \dots \dots (50)$$

This is the well-known expression for the damped cosine vibration with which an excited resonant system decays.

6.3.2 REACTION OF A PARALLEL RESONANT CIRCUIT TO A SERIES OF PERIODICAL PULSES OF SHORT DURATION¹¹⁾

Assume the first (ideal) pulse to occur at the instant $t = 0$ and the following pulses at intervals $T, 2T, \dots nT$ from $t = 0$. For $0 < t < T$, eq. (50) applies for the voltage across the circuit. If this voltage is denoted by V_{01} , then:

$$V_{01} = V_0 e^{-at} \cos \omega t. \quad \dots \dots \dots (51)$$

For $T < t < 2T$ the voltage across the circuit is equal to the superposition on V_{01} of a similar voltage, but shifted over T seconds, the latter voltage resulting from the second current pulse at $t = T$. Denoting the voltage across the circuit for $T < t < 2T$ by V_{12} , then:

$$\begin{aligned} V_{12} &= V_{01} + V_0 e^{-a(t-T)} \cos \omega(t-T) = \\ &= V_0 \left\{ e^{-at} \cos \omega t + e^{-a(t-T)} \cos \omega(t-T) \right\}, \dots \dots \dots (52) \end{aligned}$$

while the voltage across the circuit for $2T < t < 3T$ is:

$$\begin{aligned} V_{23} &= V_{01} + V_{12} + V_0 e^{-a(t-2T)} \cos \omega(t-2T) = V_0 \left\{ e^{-at} \cos \omega t + \right. \\ &\quad \left. + e^{-a(t-T)} \cos \omega(t-T) + e^{-a(t-2T)} \cos \omega(t-2T) \right\}, \dots \dots \dots (53) \end{aligned}$$

which finally gives for the $(n+1)$ th and $(n+2)$ th pulse, i.e. for $nT < t < (n+1)T$:

$$\begin{aligned} V_{n,n+1} &= V_0 \left\{ e^{-at} \cos \omega t + e^{-a(t-T)} \cos \omega(t-T) + \dots \right. \\ &\quad \left. \dots + e^{-a(t-nT)} \cos \omega(t-nT) \right\}. \quad \dots \dots \dots (54) \end{aligned}$$

In this expression ω thus is the resonant angular frequency of the circuit and T is the periodic time of the pulse cycle, i.e.:

$$\omega = 2\pi f_0 = 2\pi \frac{1}{T_0},$$

¹¹⁾ For a fundamental treatise on this subject reference is made to A.H. Boerdijk, Vector Presentations of Differential Equations, their Solutions and the Derivatives thereof; thesis Delft 1951. Published after the original manuscript of this book had been written.

where f_0 is the resonant frequency of the circuit and T_0 is the natural periodic time of the circuit. It may therefore be written:

$$\omega T = 2\pi \frac{T}{T_0}.$$

The ratio $\frac{\text{periodic time of pulse cycle}}{\text{natural periodic time of the circuit}}$ or $\frac{\text{resonant frequency of the circuit}}{\text{pulse frequency}}$ will be denoted by b , hence:

$$b = \frac{T}{T_0} = \frac{f_0}{f} \dots \dots \dots (55)$$

By means of this expression eq. (54) may be written:

$$V_{n,n+1} = V_0 e^{-at} \left\{ \cos \omega t + e^{aT} \cos (\omega t - 2\pi b) + e^{2aT} \cos (\omega t - 2 \times 2\pi b) + e^{3aT} \cos (\omega t - 3 \times 2\pi b) + \dots + e^{naT} \cos (\omega t - n \times 2\pi b) \right\} \dots \dots (56)$$

The value of b has a very important bearing on the form eq. (56) assumes. A few particular cases will now be investigated in greater detail.

6.3.2.1. The resonant frequency of the circuit is a whole multiple of the pulse frequency

In this case b is a whole number, so that eq. (56) assumes a very simple form, viz.

$$V_{n,n+1} = V_0 e^{-at} \cos \omega t (1 + e^{aT} + e^{2aT} + e^{3aT} + \dots + e^{naT}) = V_0 e^{-at} \cos \omega t \cdot \frac{1 - e^{aT(n+1)}}{1 - e^{aT}} \dots \dots \dots (57)$$

As mentioned above, this expression is valid for $nT < t < (n + 1)T$. Putting $t = nT + \vartheta$, so that obviously $0 < \vartheta < T$, then:

$$V_{n,n+1} = V_0 e^{-a(nT+\vartheta)} \cos(\omega nT + \omega \vartheta) \cdot \frac{1 - e^{aT(n+1)}}{1 - e^{aT}},$$

in which:

$$\omega nT = 2\pi n \frac{T}{T_0} = 2\pi n b.$$

Since both n and b are whole numbers,

$$\cos (\omega nT + \omega \vartheta) = \cos \omega \vartheta,$$

so that:

$$\begin{aligned}
 V_{n,n+1} &= V_0 e^{aT-a\vartheta} \cos \omega \vartheta \cdot \frac{e^{-(n+1)aT} - 1}{1 - e^{aT}} = \\
 &= V_0 \cdot \frac{e^{aT}}{1 - e^{aT}} \cdot e^{-a\vartheta} \cos \omega \vartheta \left\{ e^{-(n+1)aT} - 1 \right\} = \\
 &= V_0 \cdot \frac{1}{1 - e^{-aT}} \cdot e^{-a\vartheta} \cos \omega \vartheta \left\{ 1 - e^{-(n+1)aT} \right\} . \quad (58)
 \end{aligned}$$

Eq. (58) thus represents the variation of the voltage across the circuit after the $(n + 1)^{th}$, but before the $(n + 2)^{th}$ current pulse. For $n = 0$, eq. (58) changes into eq. (50), whilst for very high values of n the voltage across the circuit approaches the static, final condition:

$$V_{n,n+1} = \frac{V_0 e^{-a\vartheta} \cos \omega \vartheta}{1 - e^{-aT}} .$$

For $\vartheta = 0$ this expression becomes:

$$V_{n,n+1} = \frac{V_0}{1 - e^{-aT}} ,$$

and for $\vartheta = T$:

$$V_{n,n+1} = \frac{V_0 e^{-aT}}{1 - e^{-aT}} ,$$

the difference of these two expressions being V_0 . This characterizes the static condition. After a pulse has

been fed to the circuit, a damped cosine oscillation is initiated which, at the end of the pulse cycle, T , has an amplitude which is an amount V_0 less than the initial amplitude. By the next current pulse the quantity V_0 is again added to the amplitude of the voltage across the circuit, which has been graphically represented in the oscillogram of fig. 52 for $b = 1$.

The mean value of the amplitude of the damped cosine function between two pulses is (in the static condition):

$$A = \frac{1}{T} \cdot \int_0^T \frac{V_0 e^{-a\vartheta}}{1 - e^{-aT}} \cdot d\vartheta = \frac{V_0}{aT(1 - e^{-aT})} \cdot \int_0^T e^{-a\vartheta} d a\vartheta = \frac{V_0}{aT} . . (59)$$

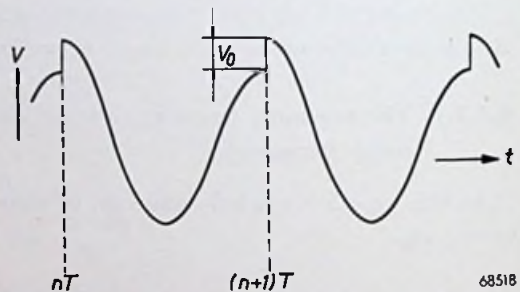


Fig. 52.

Oscillogram representing as a function of the time t the voltage V across the circuit when its resonant frequency is a whole multiple of the pulse frequency.

The static condition is that at which the voltage is thus built up to a signal which almost corresponds to a cosine law and has an angular frequency $\omega = 2\pi f_0$, whilst its amplitude is:

$$A = \frac{V_0}{aT} = \frac{V_0}{aT_0 b} = \frac{V_0 f_0}{ab} = \frac{V_0 f_0 2L}{rb} = \frac{V_0 2\pi f_0 L}{\pi r b} = V_0 \cdot \frac{Q}{\pi b} \dots \dots \dots (60)$$

The better the quality factor Q of the circuit and the smaller the value of b , the higher will be the voltage gain. When b is equal to its minimum value 1, the pulse frequency is equal to the resonant frequency of the circuit, and A is maximum. When the resonant frequency is a whole multiple of the pulse frequency, then b is a whole number larger than unity and the voltage gain decreases.

Eq. (58) not only gives information about the stationary condition (large value of n), but also about the transient.

For the general expression, eq. (58), the mean value of the amplitude of the voltage across the circuit, measured between two current pulses, becomes:

$$A_{n,n+1} = A \left\{ 1 - e^{-(n+1)aT} \right\} \dots \dots \dots (61)$$

The integers of this expression are obtained by giving n successively all whole numbers. When these integers are imagined to lie on a continuous function of time, which is obtained by substituting the time t for $(n + 1)T$, this function gives an indication of the variation of the amplitude with time and becomes:

$$A(t) = A (1 - e^{-at}) \dots \dots \dots (62)$$

This function varies exponentially with time, the time constant being:

$$\frac{1}{a} = \frac{2L}{r} = \frac{2\pi f_0 L}{\pi r} \cdot T_0 = \frac{Q}{\pi} \cdot T_0 = \frac{Q}{\pi} \cdot \frac{T}{b}$$

The time constant thus covers $Q/\pi b$ pulse cycles. In the case of a line time-base generator for a television receiver with $b = 1$, it therefore takes about Q/π lines before the amplitude of the circuit voltage has assumed a reasonable value. Conversely, this amplitude will not deviate appreciably from its original value unless at least Q/π synchronizing pulses fail in succession as a result of interferences, such as noise, etc. As in the case of a mechanical flywheel, the influence of interferences is thus reduced by the inertia of the resonant circuit, expressed in the form of the time constant Q/π .

6.3.2.2. Pulse frequency differing by a small amount from the resonant frequency of the circuit

When the pulse frequency differs by a small amount from the resonant frequency of the circuit, then:

$$T = T_0 + \tau, \dots \dots \dots (63)$$

in which T again represents the periodic time of the current pulses. T_0 is the periodic time of the resonant frequency and τ is an amount very much smaller than T_0 .

The quantity b from eq. (55) now becomes:

$$b = \frac{T}{T_0} = 1 + \frac{\tau}{T_0} \dots \dots \dots (64)$$

Denoting:

$$\frac{\tau}{T_0} = d, \dots \dots \dots (65)$$

it may be written:

$$b = 1 + d. \dots \dots \dots (66)$$

Substitution of eq. (66) in eq. (56) gives the expression for the circuit voltage between the $(n + 1)^{th}$ and the $(n + 2)^{th}$ current pulse, i.e. for $nT < t < (n + 1)T$:

$$V_{n,n+1} = V_0 e^{-at} \{ \cos \omega t + e^{aT} \cos(\omega t - 2\pi d) + e^{2aT} \cos(\omega t - 2 \times 2 \pi d) + e^{3aT} \cos(\omega t - 3 \times 2 \pi d) + \dots + e^{naT} \cos(\omega t - n \times 2 \pi d) \} \dots \dots (67)$$

The expression between braces will be denoted by S and considered as the real part of a complex expression, i.e.:

$$\begin{aligned} S &= \text{real} \left[\cos \omega t + j \sin \omega t + e^{aT} \{ \cos(\omega t - 2\pi d) + j \sin(\omega t - 2\pi d) \} + \right. \\ &\quad \left. + e^{2aT} \{ \cos(\omega t - 2 \times 2\pi d) + j \sin(\omega t - 2 \times 2\pi d) \} + \dots + \right. \\ &\quad \left. + e^{naT} \{ \cos(\omega t - n \times 2\pi d) + j \sin(\omega t - n \times 2\pi d) \} \right] = \text{real} \\ &= \text{real} \left[e^{j\omega t} + e^{aT+j(\omega t - 2\pi d)} + e^{2aT+j(\omega t - 2 \times 2\pi d)} + \dots + e^{naT+j(\omega t - n \times 2\pi d)} \right] = \\ &= \text{real} \left[e^{j\omega t} \left\{ 1 + e^{aT-j2\pi d} + e^{2(aT-j2\pi d)} + \dots + e^{n(aT-j2\pi d)} \right\} \right] = \text{real} \\ &\quad \left[e^{j\omega t} \cdot \frac{1 - e^{(n+1)(aT-j2\pi d)}}{1 - e^{aT-j2\pi d}} \right] \dots \dots \dots (68) \end{aligned}$$

Putting:

$$2\pi d = a \dots \dots \dots (69)$$

gives:

$$S = \text{real} \left[e^{j\omega t} \cdot \frac{1 - e^{(n+1)(aT-ja)}}{1 - e^{aT-ja}} \right] \dots \dots \dots (70)$$

For $\tau = 0$, i.e. $a = 0$, the combination of eqs. (70) and (67) obviously produces eq. (57).

The product aT is assumed to be so much smaller than unity that e^{aT} may be replaced by $1 + aT$. Since $T \approx T_0$, the fact that aT is very much smaller than unity amounts to $aT_0 \ll 1$ or $Q \gg \pi$, which condition can very well be satisfied in practice.

The denominator of eq. (70) will now be represented in the complex plane of fig. 53, in which X is the real and Y is the imaginary axis. With the assumption of $aT \ll 1$ it may be written that:

$$1 - e^{aT-j\alpha} = 1 - (1 + aT) e^{-j\alpha} = \bar{v} . . . (71)$$

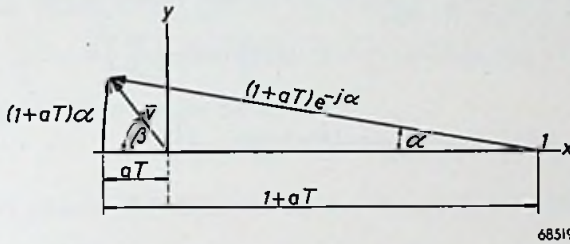


Fig. 53.

Vectorial diagram representing the denominator of eq. (70); X is the real and Y is the imaginary axis.

The angle α is small because d was assumed to be small. The amplitude of \bar{v} is then:

$$|v| \approx \sqrt{(aT)^2 + (1 + aT)^2} \alpha^2, (72)$$

while the phase angle β of \bar{v} is:

$$\beta = \arctan \frac{1 + aT}{aT} \cdot \alpha (73)$$

Since $aT \ll 1$, \bar{v} may be approximated by:

$$\bar{v} \approx aT \sqrt{1 + \left(\frac{\alpha}{aT}\right)^2} \cdot e^{j(\pi-\beta)},$$

or:

$$\bar{v} \approx -aT \sqrt{1 + \left(\frac{\alpha}{aT}\right)^2} \cdot e^{-j\beta}, (74)$$

which gives for S :

$$S = \text{real} \left[\frac{e^{j\omega t} \cdot \frac{1 - e^{(n+1)(aT - ja)}}{-aT \sqrt{1 + \left(\frac{a}{aT}\right)^2} \cdot e^{-j\beta}}}{\left[\frac{e^{j(\omega t + \beta)} \left\{ 1 - e^{(n+1)(aT - ja)} \right\}}{-aT \sqrt{1 + \left(\frac{a}{aT}\right)^2}} \right]} \right] \dots \dots \dots (75)$$

The voltage across the circuit for $nT < t < (n + 1)T$ can now be calculated from eqs. (67) and (75), giving:

$$V_{n,n+1} = V_0 e^{-at} \cdot \text{real} \left[\frac{e^{j(\omega t + \beta)} \left\{ e^{(n+1)(aT - ja)} - 1 \right\}}{aT \sqrt{1 + \left(\frac{a}{aT}\right)^2}} \right] =$$

$$\frac{V_0 e^{-at}}{aT \sqrt{1 + \left(\frac{a}{aT}\right)^2}} \cdot \text{real} \left[e^{j(\omega t + \beta)} \left\{ e^{(n+1)(aT - ja)} - 1 \right\} \right] \dots \dots \dots (76)$$

A new variable time ϑ will again be introduced, such that:

$$t = nT + \vartheta,$$

in which $0 < \vartheta < T$. The voltage across the circuit is then:

$$V_{n,n+1} = \frac{V_0 e^{-a\vartheta + aT}}{aT \sqrt{1 + \left(\frac{a}{aT}\right)^2}} \cdot \text{real} \left[e^{j(\omega t + \beta)} \left\{ e^{-j(n+1)a} - e^{-(n+1)aT} \right\} \right],$$

or, since:

$$\omega t = \omega nT + \omega \vartheta = \omega n(T_0 + \tau) + \omega \vartheta = 2\pi n + 2\pi n \frac{\tau}{T_0} +$$

$$+ \omega \vartheta = 2\pi n + n2\pi d + \omega \vartheta = 2\pi n + na + \omega \vartheta,$$

it may be written:

$$e^{j\omega t} = e^{j(na + \omega \vartheta)},$$

and

$$V_{n,n+1} = \frac{V_0 e^{-a\vartheta + aT}}{aT \sqrt{1 + \left(\frac{a}{aT}\right)^2}} \cdot \text{real} \left[e^{j(\omega \vartheta + \beta - a)} \left\{ 1 - e^{-(n+1)(aT - ja)} \right\} \right] \dots (77)$$

A representation in the complex plane of the complex quantity between braces, denoted by \bar{w} , is given in fig. 54.

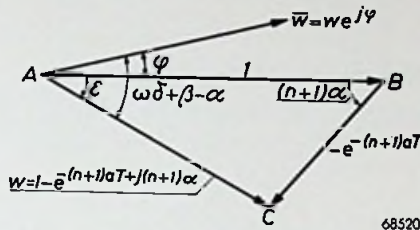


Fig. 54.

Vectorial diagram representing the form between braces of eq. (77), denoted by \bar{w} .

According to the cosine rule in the triangle ABC , the modulus of \bar{w} is:

$$|w| = \sqrt{1 + e^{-2(n+1)Ta} - 2e^{-(n+1)Ta} \cos(n+1)\alpha} \dots (78)$$

Denoting the phase angle by ϕ , then:

$$\phi = \omega\delta + \beta - \alpha - \epsilon \dots (79)$$

The value of ϵ can be determined from another property of the triangle ABC , viz.

$$\frac{\sin\{\epsilon + (n+1)\alpha\}}{\sin \epsilon} = \frac{1}{e^{-(n+1)\alpha T}},$$

which gives:

$$\tan \epsilon = \frac{\sin(n+1)\alpha}{e^{(n+1)\alpha T} - \cos(n+1)\alpha} \dots (80)$$

The form between braces of eq. (77) can now be replaced by:

$$\bar{w} = |w| e^{j\phi}, \dots (81)$$

which gives for the voltage across the circuit:

$$V_{n,n+1} = \frac{V_0 e^{-a\delta + aT}}{aT \sqrt{1 + \left(\frac{\alpha}{aT}\right)^2}} \cdot \text{real} \left[|w| e^{j\phi} \right] =$$

$$\frac{V_0 e^{-a\delta + aT}}{aT \sqrt{1 + \left(\frac{\alpha}{aT}\right)^2}} \cdot |w| \cos(\omega\delta + \beta - \alpha - \epsilon) \dots (82)$$

This is a damped cosine function of frequency ω , i.e. the resonant frequency of the circuit. Eq. (82) applies to the case of $0 < \delta < T$.

Replacement of the integers nT by a continuously time variable t , such that $(n + 1)T = t$, gives an impression of the variations of the amplitude and phase as a function of time, viz.

$$|w| = \sqrt{1 + e^{-2at} - 2e^{-at} \cos \frac{\alpha}{T} \cdot t}, \quad \dots \dots \dots (83)$$

and

$$\tan \varepsilon = \frac{\sin \frac{\alpha}{T} \cdot t}{e^{at} - \cos \frac{\alpha}{T} \cdot t} \dots \dots \dots (84)$$

The mean value of the amplitude of the voltage across the circuit measured between two current pulses now becomes:

$$A_{n,n+1} = \frac{V_0}{aT} \cdot \frac{|w|}{\sqrt{1 + \left(\frac{\alpha}{aT}\right)^2}}, \quad \dots \dots \dots (85)$$

and

$$V_{n,n+1} = A_{n,n+1} e^{-a\delta} \cos(\omega\vartheta + \beta - a - \varepsilon). \quad \dots \dots (86)$$

For a comparison of this expression with that for $V_{n,n+1}$ applying to the case of $T = T_0$, eqs. (62), (59) and (58) must be combined to:

$$V_{n,n+1} = \frac{V_0}{aT} \cdot (1 - e^{-at}) e^{-a\delta} \cos \omega\vartheta, \quad \dots \dots (87)$$

whereas, for a small detuning $T = T_0 + \tau$, from eqs. (86) and (85):

$$V_{n,n+1} = \frac{V_0}{aT} \sqrt{\frac{1 + e^{-2at} - 2e^{-at} \cos \frac{\alpha}{T} \cdot t}{1 + \left(\frac{\alpha}{aT}\right)^2}} \cdot e^{-a\delta} \cos(\omega\vartheta + \beta - a - \varepsilon), \quad \dots \dots (88)$$

in which $\alpha = 2 \pi d = 2\pi\tau/T_0$ is a measure of the detuning of the circuit with respect to the pulse frequency, and $a = \tau/2L = \pi/QT_0$ is a measure of the quality factor of the circuit.

The time t may be expressed in T_0 , so that in eq. (87) the time function in the amplitude becomes:

$$F_0(t) = 1 - e^{-at} = 1 - e^{-aT_0 \frac{t}{T_0}},$$

which, by making use of the relation $aT_0 = \pi/Q$, gives:

$$F_0(t) = 1 - e^{-\frac{\pi}{Q} \frac{t}{T_0}}, \dots \dots \dots (89)$$

whereas in eq. (88) the time function in the amplitude becomes:

$$F(t) = \sqrt{\frac{1 + e^{-2\frac{\pi}{Q} \frac{t}{T_0}} - 2e^{-\frac{\pi}{Q} \frac{t}{T_0}} \cos 2\pi \frac{d}{1+d} \frac{t}{T_0}}{1 + \left(2Q \cdot \frac{d}{1+d}\right)^2}} \dots (90)$$

In the case of a detuning the circuit voltage is moreover subject to a phase shift:

$$\varphi_0 = \beta - \alpha - \varepsilon = \arctan \frac{a}{aT} - \alpha - \arctan \frac{\sin \frac{a}{T} \cdot t}{e^{at} - \cos \frac{a}{T} \cdot t}$$

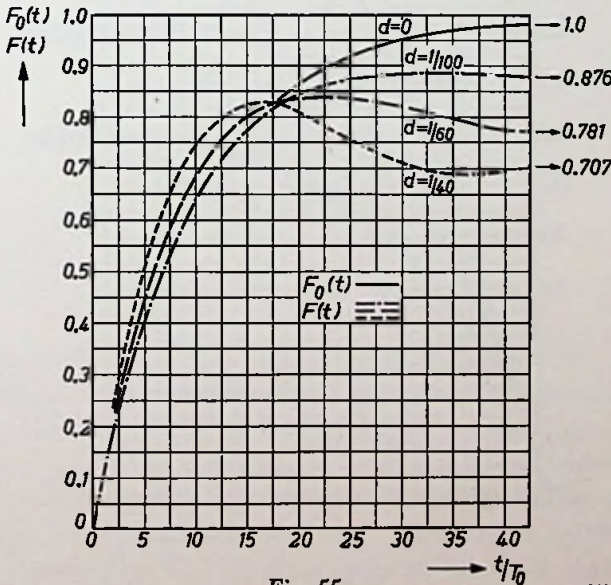


Fig. 55.

68521

$F_0(t)$ and $F(t)$ according to eqs (89) and (90) as functions of the time t/T_0 , for different values of the detuning d and a quality factor $Q = 31.4$. The arrow heads at the right indicate the final values reached by the different functions after an infinitely long time.

which gives:

$$\varphi_0 = \arctan 2Q \cdot \frac{d}{1+d} - 2\pi d - \arctan \frac{\sin 2\pi \frac{d}{1+d} \cdot \frac{t}{T_0}}{e^{\frac{\pi}{Q} \frac{t}{T_0}} - \cos 2\pi \frac{d}{1+d} \cdot \frac{t}{T_0}} \quad (91)$$

Attention is drawn to the fact that for $t = 0$ it can easily be derived from eq. (84) that:

$$\tan \varepsilon = \frac{\alpha}{aT},$$

i.e. $\varepsilon \approx \beta$ for $\alpha T \ll 1$ for $t = 0$, so that in this case:

$$\varphi_0 = -\alpha.$$

When t is very large, φ_0 approaches $\beta - \alpha$.

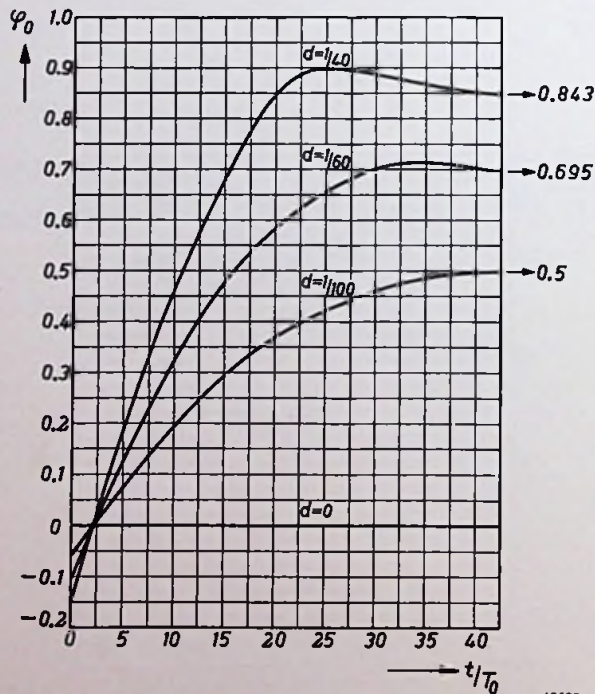


Fig. 56.

Phase angle φ_0 according to eq. (91) as a function of the time t/T_0 , for different values of the detuning d and a quality factor $Q = 31.4$. The arrow heads indicate the final values reached by the different functions after an infinitely long time.

The variations of $F_0(t)$, $F(t)$ and φ_0 as functions of time have been plotted graphically in figs. 55 and 56. Fig. 55 gives four cases, viz. $F_0(t)$ for $d = 0$, and $F(t)$ for $d = 1/100$, $d = 1/60$ and $d = 1/40$, Q/π being 10 in all cases, i.e. $Q = 31.4$.

Fig. 56 gives the phase angle φ_0 as a function of t/T_0 , also for $Q = 31.4$ and for $d = 0$, $d = 1/100$, $d = 1/60$ and $d = 1/40$.

In both figures the horizontal arrow heads indicate the levels reached by the functions concerned after an infinitely long time. It should be noted that the detuning $d = 1/60$ corresponds to the pulse frequency being situated at a point on the response curve which coincides with the points at which this curve has dropped to $1/\sqrt{2}$ of its maximum (see fig. 57).

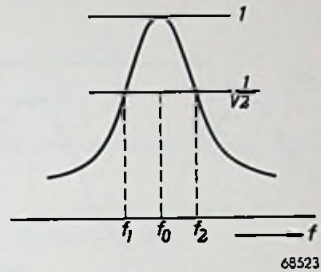


Fig. 57. Response curve of a resonant circuit.

The pulse frequency f is therefore f_1 or f_2 in that case, and since

$$2 \times 2\pi\Delta f = \frac{r}{L}, \quad \dots \dots \dots (92)$$

in which Δf is $f_2 - f_0$ or $f_0 - f_1$, it may be written:

$$d = \frac{\tau}{T_0} = f_0 (T - T_0),$$

or, since $T = 1/f$:

$$d = f_0 \left(\frac{1}{f} - \frac{1}{f_0} \right) = \frac{f_0 - f}{f} = \frac{\Delta f}{f} \dots \dots \dots (93)$$

From eqs. (92) and (93):

$$2 \times 2\pi f d = \frac{r}{L},$$

which gives:

$$2d = \frac{1}{Q}.$$

For $Q = 10\pi = 31.4$ the value of d is therefore about $1/60$.

Recapitulating, it may thus be stated that after the transient, which is always determined by the time constant $1/a$, a static, final condition is reached when, starting at the instant $t = 0$, a series of current pulses is fed to the resonant circuit with a frequency which may differ by a certain amount from that of the resonant frequency. According to eq. (88) the mean value of the amplitude of the circuit voltage at this final condition is:

$$V_\infty = \frac{V_0}{aT} \cdot \frac{1}{\sqrt{1 + \left(\frac{a}{aT}\right)^2}} = \frac{V_0}{aT} \cdot \frac{1}{\sqrt{1 + \left(2Q \cdot \frac{d}{1+d}\right)^2}}, \quad \dots \dots \dots (94)$$

while the corresponding phase angle φ_0 is:

$$\varphi_{0\infty} = \beta - a = \arctan \frac{1 + aT}{aT} a - a \approx \frac{a}{aT} = 2Q \cdot \frac{d}{1 + d} \quad (95)$$

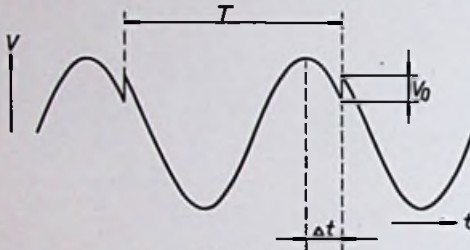


Fig. 58. 68524

Oscillogram similar to that of fig. 52, but applying to the case in which the pulse frequency differs by a small amount from the resonant frequency of the circuit.

When in analogy to fig. 52, the circuit voltage is plotted as a function of time for the case of the resonant circuit being detuned with respect to the frequency of the current pulses by which the circuit is excited, an oscillogram as shown in fig. 58 is obtained.

The phase shift $\beta - a$ corresponds to a time shift Δt of the current pulse with respect to

the maximum of the circuit voltage, i.e.:

$$\Delta t = \frac{\beta - a}{2\pi} \cdot T \quad (96)$$

6.3.2.3. The ratio of the pulse cycle to the cycle of the resonant circuit is $m + 1/2$.

When the ratio of the pulse cycle to the cycle of the resonant circuit is $m + 1/2$, m being a whole number, then b in eq. (55) becomes:

$$b = m + \frac{1}{2},$$

which gives for the voltage across the circuit (cf. eq. (56)):

$$V_{n,n+1} = V_0 e^{-at} \left[\cos \omega t + e^{aT} \cos \left\{ \omega t - (m + \frac{1}{2})2\pi \right\} + e^{2aT} \cos \left\{ \omega t - 2(m + \frac{1}{2})2\pi \right\} + e^{3aT} \cos \left\{ \omega t - 3(m + \frac{1}{2})2\pi \right\} + \dots + e^{naT} \cos \left\{ \omega t - n(m + \frac{1}{2})2\pi \right\} \right]$$

Hence:

$$\begin{aligned} V_{n,n+1} &= V_0 e^{-at} \left\{ \cos \omega t + e^{aT} \cos (\omega t - \pi) + e^{2aT} \cos \omega t + e^{3aT} \cos (\omega t - \pi) + e^{4aT} \cos \omega t + \dots + e^{naT} \cos (\omega t - n\pi) \right\} = \\ &= V_0 e^{-at} \cos \omega t \left\{ 1 - e^{aT} + e^{2aT} - e^{3aT} + e^{4aT} - \dots + (-1)^n e^{naT} \right\} = \\ &= V_0 e^{-at} \cos \omega t \cdot \frac{1 - (-e^{aT})^{n+1}}{1 + e^{aT}} \end{aligned}$$

If n is an even number, this becomes:

$$V_{n,n+1} = V_0 e^{-at} \cos \omega t \cdot \frac{1 + e^{(n+1)aT}}{1 + e^{aT}}, \quad \dots \quad (97)$$

and if n is an odd number:

$$V_{n,n+1} = V_0 e^{-at} \cos \omega t \cdot \frac{1 - e^{(n+1)aT}}{1 + e^{aT}}. \quad \dots \quad (98)$$

Introducing once again a new time variable by setting $t = nT + \vartheta$, in which $0 < \vartheta < T$, then:

$$V_{n,n+1} = V_0 e^{-a\vartheta + aT} \cos(\omega\vartheta + \omega nT) \cdot \frac{e^{-(n+1)aT} - (-1)^{n+1}}{1 + e^{aT}},$$

in which:

$$\omega nT = \omega n(m + \frac{1}{2}) T_0 = n(m + \frac{1}{2}) 2\pi.$$

Hence, for even values of n :

$$\cos(\omega\vartheta + \omega nT) = \cos(\omega\vartheta),$$

whilst for odd values of n :

$$\cos(\omega\vartheta + \omega nT) = -\cos(\omega\vartheta),$$

which gives:

$$\begin{aligned} V_{n,n+1} &= -V_0 e^{-a\vartheta + aT} (-1)^{n+1} \cos \omega\vartheta \cdot \frac{e^{-(n+1)aT} - (-1)^{n+1}}{1 + e^{aT}} = \\ &= \frac{V_0 e^{-a\vartheta + aT}}{1 + e^{aT}} \cdot \cos \omega\vartheta (-1)^{n+1} \left\{ (-1)^{n+1} - e^{-(n+1)aT} \right\} = \\ &= \frac{V_0 e^{-a\vartheta}}{1 + e^{-aT}} \cdot \cos \omega\vartheta \left\{ 1 - (-1)^{n+1} e^{-(n+1)aT} \right\}. \quad \dots \quad (99) \end{aligned}$$

The variation of the amplitude of this damped cosine function thus differs for even and odd values of n . For very high values of n both cases approach each other. The mean value of the amplitude over a pulse cycle T is:

$$A_{n,n+1} = \frac{V_0}{1 + e^{-aT}} \cdot \left\{ 1 - (-1)^{n+1} e^{-(n+1)aT} \right\}, \quad \dots \quad (100)$$

so that for even values of n , when the integers of $(n+1)T$ are again replaced by a continuous time variable:

$$A_{n,n+1} = \frac{V_0}{1 + e^{-aT}} \cdot (1 + e^{-at}), \quad \dots \quad (101)$$

and for odd values of n :

$$A_{n,n+1} = \frac{V_0}{1 + e^{-aT}} \cdot (1 - e^{-at}). \quad \dots \quad (102)$$

Eq. (101) gives the variation of the amplitude of the circuit voltage for the "even" pulse intervals as a function of time, whilst eqs. (102) gives this variation for the "odd" pulse intervals.

Since $n = 0$ for the first current pulse, the time variable t from eqs (101) and (102) becomes T , giving for eq. (101):

$$A_{\text{even}} = V_0, \dots \dots \dots (101a)$$

and for eq. (102):

$$A_{\text{odd}} = V_0 \cdot \frac{1 - e^{-aT}}{1 + e^{-aT}} \dots \dots \dots (102a)$$

The variation of the voltage across the circuit has been plotted in fig. 59 for $m = 0$. The upper dash-dot line corresponds to eq. (101), and the lower dash-dot line to eq. (102). For large values of n the amplitude of both the "even" and "odd" cycles approaches the same value:

$$A_{\infty} = \frac{V_0}{1 + e^{-aT}} \approx \frac{1}{2} V_0 \cdot (103)$$

At this ratio of the frequency of the current pulse to the resonant frequency of the circuit the amplitude is obviously not increased to a multiple of V_0 , its maximum value being at the utmost about one half of V_0 .

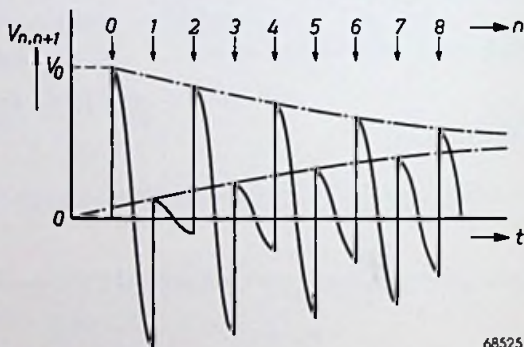


Fig. 59.

Oscillogram similar to those of figs. 52 and 58, but applying to the case in which the ratio of the pulse cycle to the cycle of the resonant circuit is $m + 1/2$. The upper dash-dot line corresponds to even values of n (eq. 101) and the lower dash-dot line to odd values of n (eq. 102). The different values of n are indicated by the arrow heads at the top.

SUMMARY OF 6.3.2

For $t > 0$ small current pulses occur having a frequency $f = 1/T$ and a content $q = \int Idt$. The first pulse is assumed to occur at the instant $t = 0$, and the pulses flow through a parallel resonant circuit according to fig. 51.

The voltage V across the circuit shows a discontinuity at each current pulse in the form of a surge $V_0 = q/C$. Between the pulses the voltage variation corresponds to a damped cosine function with a damping factor

$$a = \frac{r}{2L}$$

and an angular frequency

$$\omega = \sqrt{\omega_0^2 - a^2} = 2\pi f_0 = \frac{2\pi}{T_0},$$

in which $\omega = 2\pi$ times the resonant frequency of the circuit, and $\omega_0^2 = 1/LC$.

$Q = \omega L/r$ is the quality factor of the circuit, and the mean value of the amplitude over a pulse cycle is denoted by A . The phase shift between the fundamental of the pulse frequency and the circuit voltage (cosine function) is denoted by φ_0 .

In the case of $T = bT_0$, b being a whole number:

$$A = V_0 \cdot \frac{Q}{\pi b} (1 - e^{-at}),$$

and:

$$\varphi_0 = 0. \quad (\text{cf. fig. 52})$$

In the case of $T = T_0 + \tau$, in which $\tau \ll T_0$ and $\tau/T_0 = d$:

$$A = V_0 \cdot \frac{Q}{\pi} \sqrt{\frac{1 + e^{-2at} - 2e^{-at} \cos(\Delta\omega t)}{1 + \left(2Q \cdot \frac{d}{1+d}\right)^2}},$$

in which $\Delta\omega$ is the difference between ω and the angular frequency of the pulse, and:

$$\varphi_0 = \arctan 2Q \cdot \frac{d}{1+d} - 2\pi d - \arctan \frac{\sin(\Delta\omega t)}{e^{at} - \cos(\Delta\omega t)} \quad (\text{cf. figs 55 and 56}).$$

In the case of $T/T_0 = m + 1/2$, in which m is a whole number, the amplitude $A_{n,n+1}$ of the circuit voltage between the instants $t = nT$ and $t = (n+1)T$ is:

$$A_{n,n+1} = \frac{V_0}{1 + e^{-aT}} \cdot \left\{ 1 - (-1)^{n+1} e^{-at} \right\},$$

which shows that $A_{n,n+1}$ assumes different values for even and odd values of n (cf. fig. 59).

6.3.3. APPLICATION OF FLYWHEEL RESONANT CIRCUITS

Whatever the ratio of the pulse frequency to the frequency of the resonant circuit may be, the transients occurring during the transition from one stationary condition to another are determined by the same time constant $1/a$, which depends only on the circuit elements r and L , i.e.:

$$\frac{1}{a} = T_c = \frac{2L}{r} = \frac{Q}{\pi} \cdot T_0.$$

As pointed out above, in a line time-base generator synchronized via a flywheel circuit tuned to the line frequency, it takes about Q/π "line times" before a sudden permanent change of the synchronizing pulses noticeably affects the amplitude of the circuit voltage. The influence of disturbances of short duration on the synchronization therefore decreases as the time constant increases.

It might therefore be suggested to increase the quality factor Q of the circuit to the maximum practicable value. A lower value of Q may, however, be necessary for the following reasons. First, it is necessary to take into account the rapidity with which the saw-tooth frequency is again "caught" by the synchronization after this has been disturbed during a short interval. The higher the value of Q , the longer will it take for the synchronization to be restored. A second limit is set to the value of Q by the frequency stability of the synchronizing signals. In transmitters synchronized by the mains frequency, the relative frequency fluctuations of the synchronizing signals will be equal to those of the mains. If the mains frequency fluctuates from 49 c/s to 51 c/s, i.e. 2% to either side of the correct value, it is obvious that the detuning

$$d = \frac{\tau}{T_0} = \frac{T - T_0}{T_0} = \frac{f_0 - f}{f} = - \frac{\Delta f}{f}$$

will also fluctuate up to 2%. It is certainly possible for such variations to occur in practice. If at such detuning a phase shift φ_0 of maximum 45° is tolerated, this means that, according to eqs. (92) and (93), the quality factor of the circuit may not exceed the value of $Q = 1/2d = 25$.

In free-running transmitters (for example those equipped with a crystal-controlled master oscillator) the frequency fluctuations of the synchronization are usually very much smaller, so that the flywheel action of the circuit may be made much more effective by employing a higher value of Q .

As mentioned previously, the phase shift between the circuit voltage and the synchronizing pulses must not be allowed to become excessive, because this would be manifest as a displacement of the image on the screen of the picture tube unless counteracted by special measures.

One of the simplest practical circuits for flywheel synchronization is roughly indicated in fig. 60. The synchronizing pulses are transformed into a sinusoidal signal which serves as input signal for the circuit A . If necessary, this signal is shifted in phase in A , where it is also transformed into a new pulsatory signal which is used as trigger signal for the time-base generator G .

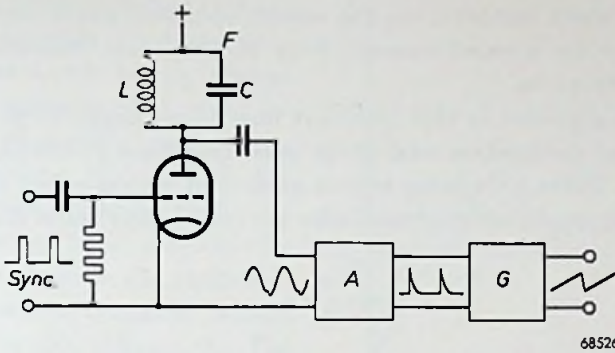


Fig. 60.

Basic circuit of a time-base generator with a flywheel circuit F . The output voltage of the valve to which the synchronizing pulses are applied is fed to a circuit A in which the phase may be shifted and the sinusoidal input voltage is transformed into pulses which serve as a trigger signal for the time-base generator G .

With interlaced scanning, a series of pulses known as “equalizing pulses”, having twice the line frequency, are transmitted before, during and after the frame synchronizing pulses proper. It is obvious that these will have a large influence on the voltage across the resonant circuit, this frequency ratio being the most unfavourable as far as the gain is concerned. It will take a time in the order of the time constant $T_c (= 1/a$ second) before the original amplitude, which was reached just before the equalizing pulses, has dropped sufficiently and a new static condition is reached at which the maximum value of the amplitude will obviously be $\frac{1}{2} V_0$ (cf. eq. 103).

If the duration of these equalizing pulses does not exceed $1/a$ second, i.e. the time constant of the circuit, the interference may still be acceptable. If not, special means must be provided to suppress these pulses of twice the synchronizing frequency.

At present the frame synchronizing pulses are accompanied by equalizing signals during 9 line times, so that the condition

$$\frac{1}{a} = \frac{Q}{\pi} \cdot T_0 > 9 T_0,$$

or

$$Q > 9\pi$$

would have to be satisfied if the interference is to be kept within reasonable limits. This condition is, however, in contradiction to the condition previously discussed, i.e. $Q = 25$, so that the interference will usually be troublesome when no special measures are taken. This has been confirmed by practice.

Finally, a short comment on the results obtained where the pulse frequency differs by a small amount from the resonant frequency of the circuit, will be given.

It is to be expected in this case that beat notes might be produced by interference of the fundamental of the pulse frequency f with the resonant frequency f_0 . These beat notes indeed occur and are expressed in eqs. (83) and (85) as an amplitude modulation by the cosine form under the root sign, i.e.

$$\cos \frac{\alpha}{T} \cdot t .$$

The argument of this cosine function may be written:

$$\begin{aligned} \frac{\alpha}{T} \cdot t &= \frac{2\pi d}{T} \cdot t = 2\pi \frac{T - T_0}{T_0 T} \cdot t = 2\pi \left(\frac{1}{T_0} - \frac{1}{T} \right) t = \\ &= 2\pi (f_0 - f) t = 2\pi |\Delta f| t = |\Delta \omega| t . \end{aligned}$$

The frequency of this modulation term is therefore equal to the frequency difference Δf , i.e. the difference between the resonant and pulse frequencies.

6.4. AUTOMATIC PHASE CONTROL

6.4.1. BASIC PRINCIPLE

In the circuits to be discussed, flywheel synchronization is obtained by deriving a control voltage from the phase shift between the synchronizing signal and the relaxation voltage, which control voltage is applied to the control grid of the valve by which the relaxation voltage is generated. The phase shift changes when one of the frequencies is subject to variation, and the resulting variation of the control voltage can be made such that the difference in frequency is eliminated.

Fig. 61 clearly shows how the frequency of a relaxation oscillator can be varied by means of a control voltage. In this figure only the exponential part of the total cycle of the relaxation voltage at the control grid of the self-blocking valve, as depicted in fig. 50 of section 5.2, has been drawn.

When the control voltage between control grid and cathode is zero, the variation of the alternating grid voltage will be as shown by curve 1, which asymptotically approaches the line $V_c = 0$. Apart from the short pulses, the duration of the cycle is then from $t = 0$ to t_1 , where the curve 1 intersects the dash-dot line representing the cut-off voltage.

When, however, a control voltage $V_c = V_2$ is applied to the grid, the exponential part of the alternating grid-voltage curve approaches the line

$V_c = V_2$ and varies according to curve 2, so that the cycle is reduced to t_2 . Similarly, at a still higher voltage $V_c = V_3$ between grid and cathode, the alternating grid voltage varies according to curve 3, the cycle now being reduced to t_3 .

Since the periodic time of the relaxation voltage is the reciprocal of its frequency, the latter is thus controlled by the voltage V_c . The frequency is, however, determined not only by the direct voltage between grid and cathode, but also by the time constant RC in the grid circuit. This may also be explained by means of fig. 61. Assume RC to be increased. The three exponential curves 1, 2 and 3 then become less steep and the points t_1, t_2 and t_3

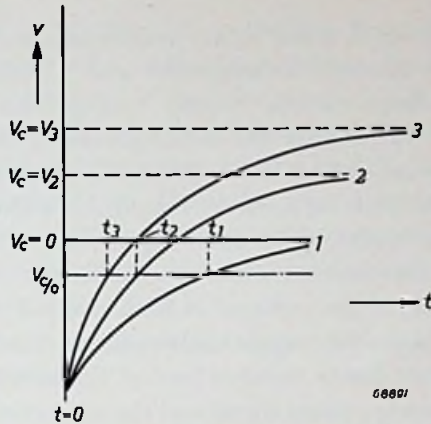


Fig. 61.

Influence of a control voltage V_c applied to the grid of an oscillator valve in a relaxation oscillator on the periodic time of the generated voltage. At $V_c = 0$ this cycle is t_1 , at $V_c = V_2$ the cycle is t_2 , and at $V_c = V_3$ the cycle is reduced to t_3 . The dash-dot line $V_{c/0}$ denotes the cut-off voltage of the oscillator valve.

are shifted to the right, which means that the frequency decreases. When, on the other hand, RC is decreased, t_1, t_2 and t_3 are shifted to the left and the frequency increases. A detailed treatment of the dependence of the frequency of a multivibrator and a blocking oscillator on time constants, control voltage, valve properties will be given in section 6.4.1.1.

By using a variable resistor for the grid leak R across the capacitor C , the relaxation frequency can be roughly adjusted to that of the synchronizing pulses. As soon as the former then comes within the collecting zone of the automatic phase control, it is maintained at the correct value by means of the control voltage V_c .

For the most familiar types of time-base generators, i.e. the blocking oscillator and the multivibrator, it can be proved theoretically and experimentally that the frequency of the relaxation signal is to a good approximation proportional to the control voltage V_c between grid and cathode and inversely proportional to the time constant

$$RC = T_d \dots \dots \dots (104)$$

in the grid circuit of the self-blocking valve, whose grid- and anode currents consist of short pulses. The frequency f can then be expressed by the formula

$$f = \frac{k}{T_d} \cdot (\gamma + \gamma_0), \dots \dots \dots (105)$$

in which k and γ_0 are constants which depend only on the cut-off voltages of the self-blocking valve and γ stands for the ratio V_c/V_b of the control voltage to the supply voltage (see section 6.4.1.1.).

To simplify the investigation of the automatic phase control, it will be assumed that both the synchronizing signal and the generated wave have the form of narrow rectangular pulses and that these are applied to the two control grids of an EQ 80 valve¹²). A basic feature of this valve is that, under correct working conditions, current will flow in the anode circuit only if the voltages at both control grids exceed simultaneously a certain value with respect to the cathode, in which case the anode current is within wide limits independent of the amplitude of the grid voltages. When the synchronizing signal and the relaxation voltage coincide partially, the anode current will thus consist of pulses the widths of which depend on the overlap of the two pulses, in other words on their phase relation.

By including a resistance R in the anode circuit, voltage pulses of varying widths are thus obtained. These may be smoothed by connecting a sufficiently large capacitance C across R , the mean value of the voltage across this RC combination then being proportional to the width and the frequency of the anode current pulses (cf. Appendix I, p. 143).

According to fig. 62, the mean value of the voltage V_c between the anode and cathode of the EQ 80 valve is:

$$V_c = V_b - IR \cdot \frac{\tau}{T}, \quad (106)$$

in which:

V_b = the anode supply voltage,

I = the amplitude of the anode-current pulses,

τ = the duration of the anode-current pulses, which is also a measure of the phase relation between the two input pulses, and

T = the periodic time of the anode-current pulses (c) which is equal to that of the synchronizing pulses (a).

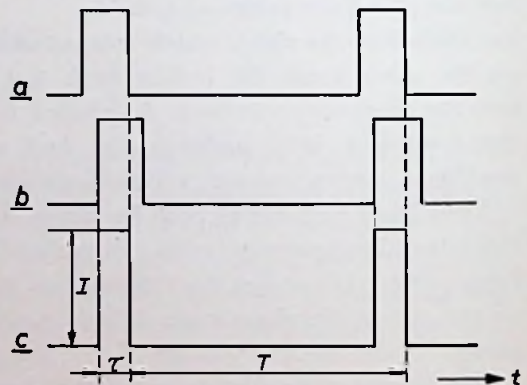


Fig. 62.

a Synchronizing pulses at one control grid of the EQ 80.

b Relaxation pulses at the other control grid of the EQ 80.

c Resulting anode-current pulses.

¹²) J. L. H. Jonker and A. J. W. M. van Overbeek, The φ -detector, A New Valve for F.M. Receivers, Electr. Appl. Bull. X, p. 109, 1949 (No. 5).

The voltage V_c given by eq. (106) is suitable for controlling the self-blocking oscillator valve. When the relaxation frequency increases, τ also increases and the control voltage V_c decreases, so that the relaxation frequency is automatically readjusted to its original value. When, on the other hand, the relaxation frequency decreases, τ becomes smaller and V_c increases, so that the frequency is also readjusted. Similarly, when the synchronizing frequency increases (or decreases), τ decreases (or increases), so that V_c , and therefore the relaxation frequency, increases (or decreases) according to the variations of the synchronization.

6.4.1.1. Some theoretical and practical considerations about the multivibrator and the blocking oscillator

6.4.1.1.1. Introduction

Multivibrator circuits as already indicated by Abraham and Bloch as far back as 1919, and several variations therefrom, have proved useful tools for generating pulse- and sawtooth-shaped signals.

An important quantity, that is often required to be known first of all, is the frequency of the relaxation signal of the multivibrator.

A very rough rule of thumb for determining this frequency is the following:

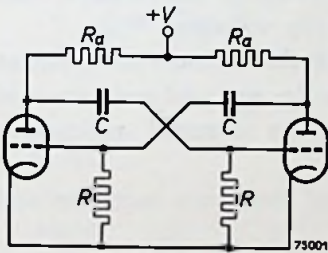


Fig. 63.

Basic symmetrical multivibrator circuit.

The frequency of a symmetrical multivibrator is equal to the reciprocal of the product of grid leak resistance and coupling capacitance between the anode of one valve and grid of the other valve. So:

$$f = 1/RC \dots \dots \dots (107)$$

This rule, however, only gives a very rough approximation. Other rules of thumb have been given¹³⁾:

The frequency of a symmetrical multivibrator with grid leaks connected between grids and cathode is

$$f = 0.3 1/RC \dots \dots \dots (108)$$

The frequency of the same, but with grid leaks connected between grids and positive H.T. supply, should be:

$$f = 1/RC \dots \dots \dots (109)$$

Obviously, it may be expected that for positive grid bias voltages between zero and H.T. supply the frequency must have a value:

$$f = a 1/RC, \dots \dots \dots (110)$$

with

$$0.3 < a < 1 \dots \dots \dots (111)$$

¹³⁾ N. W. Mather, "Multivibrator Circuits". Electronics Oct. 1946.

The fact that the frequency of a multivibrator is a function of the grid bias is well known ¹⁴).

The article, quoted in footnote ¹³) also gives an expression for the frequency of an asymmetrical multivibrator (fig. 64; $R_1 C_1 \neq R_2 C_2$)

$$f = 2 f_1 f_2 / (f_1 + f_2), \dots \dots \dots (112)$$

where f_1 = the frequency of a symmetrical multivibrator with time-constant $R_1 C_1$, and f_2 = the frequency of a symmetrical multivibrator with time constant $R_2 C_2$. Thus:

$$f_1 = a / R_1 C_1$$

$$f_2 = a / R_2 C_2,$$

which gives:

$$f = a 2 / (R_1 C_1 + R_2 C_2) \dots \dots \dots (113)$$

For a symmetrical multivibrator ($R_1 C_1 = R_2 C_2 = RC$) this expression becomes identical to (110).

Furthermore it is mentioned that the frequency of a multivibrator is almost independent of the positive H.T. supply voltage, except for extremely low supply voltages.

Later on it will be shown that the frequency is theoretically independent of the supply voltage, provided the internal anode- and grid resistances of the valves used are small compared with the external resistances in the circuit.

At low supply voltages, however, the internal resistance increases and frequency deviations can be expected.

Waveform and frequency of a multivibrator signal can, with certain simplifying assumptions, be determined ¹⁵).

Complete calculations lead to rather complicated expressions, which cannot be brought into explicit form.

To arrive at explicit expressions, simplifying assumptions have to be introduced later.

Therefore, to arrive with minimum exertion at a significant result, it is more advantageous to start with reasonable simplifying assumptions, which mostly will be met in practice.

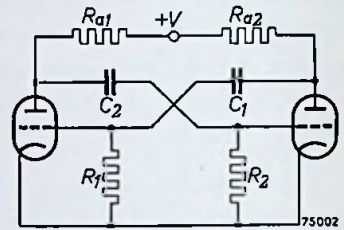


Fig. 64.
Basic asymmetrical multivibrator circuit.

¹⁴) S. Bertram, "The Degenerative Positive Bias Multivibrator" Proc. I.R.E. 36, Feb. 1948, 277.

¹⁵) F. Vecchiacchi: "Meccanismo di funzionamento e frequenza del multivibratore" Altafrequenza 9, 1940, 745.

M. V. Kiebert Jr. and A. F. Inglis, "Multivibrator circuits" Proc. I.R.E. 33, 1945, 534.

R. Feinberg, "Symmetrical Multivibrators" Wireless Engineer 26, May 1949, 153.

R. Feinberg, "Asymmetrical Multivibrators" Wireless Engineer 26, Oct. 1949, 325.

Such assumptions are the following: the internal anode resistance of the valves in the conducting state and the internal grid resistance at zero or positive grid-cathode potential are very small compared with the external resistances in the anode- and grid-circuits. Furthermore it is assumed that the influence of the stray capacitances of the valve electrodes and the wiring, which shunt the resistances and can have considerable effects on the wave shape of the relaxation signal at high frequencies, is negligible. More precisely, this means that the time constants containing these stray-capacitances, are very small compared with the frequency and rise-time of the relaxation signal.

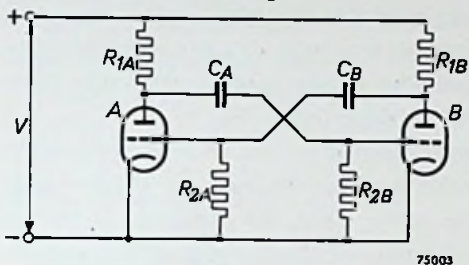


Fig. 65.

Multivibrator circuit, indicating the notation of circuit components used in the text.

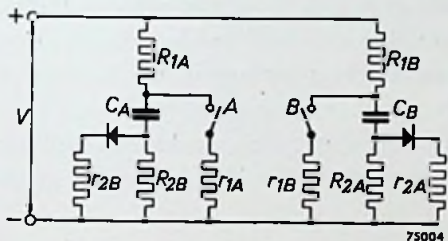


Fig. 66.

Equivalent circuit of the multivibrator of fig. 65.

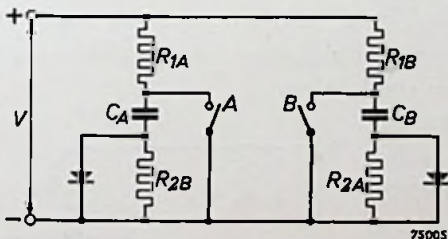


Fig. 67.

Equivalent circuit of the multivibrator, assuming anode- and grid-internal resistances to be negligibly small compared with the external circuit resistances.

A and B being conducting, i.e. having a zero or positive grid-cathode potential.

If the voltage across R_2 becomes zero or positive with respect to the negative terminal of the H.T. supply, then R_2 is shunted with r_2 in

Under these assumptions the multivibrator action may be described as a switching device that brings the two valves alternately from the conducting into the non-conducting state in a switching time that is negligibly small compared with the total period of the relaxation signal which results from this switching action.

Choosing the circuit of fig. 65 as a starting point, the multivibrator action can be explained by substituting this circuit by that of fig. 66, in which r_1 and r_2 represent the internal anode- and the internal grid resistance respectively in the case of valves

parallel. This is indicated by the insertion of two rectifier symbols in series with r_{2A} and r_{2B} .

When valve A (or B) is conducting, then switch A (or B) is closed. When the valves are in the non-conducting state, then the switches are open.

Now, assuming the internal resistances r_{1A} , r_{1B} , r_{2A} and r_{2B} negligibly small with respect to the other resistances of the circuit, the equivalent circuit of the multivibrator becomes as depicted in fig. 67.

The switching mechanism of the multivibrator is such that either valve A is non-conducting and valve B conducting, or the reverse state exists. The time periods during which these states exist, are determined by the time constants, which regulate the charging or discharging of the capacitors C_A and C_B .

Because of the charging or discharging currents of these capacitors, varying voltages are generated across the anode and grid resistances R_1 and R_2 respectively. The voltage across the grid leak R_2 of the non-conducting valve will at a given moment reach a value at which anode current starts (the cut-off voltage), and at this moment the positions of the two valves are in a very short time (negligibly small in consequence of the initial assumptions) switched over to the reverse state. This mechanism will now be considered in detail in order to determine the frequency of the multivibrator.

6.4.1.1.2. Symmetrical multivibrator

The multivibrator is symmetrical if valves A and B are of the same type, and $R_{1A} = R_{1B}$, $R_{2A} = R_{2B}$, $C_A = C_B$.

Assuming the multivibrator has just been switched from one state, in which valve B is cut off and valve A conducting, into the other state with valve B conducting and valve A non-conducting.

Then the equivalent circuit for the multivibrator indicated in fig. 68 is valid. If this condition should last infinitely, the capacitor at A would attain the voltage $+V$ of the H.T. supply with respect to the negative lead. Just before switching, the capacitor between point B (anode of valve B) and point G_A (grid of valve A) was in the same condition as the capacitor between A and G_B after switching. As this condition did not last for an infinitely long time, the voltage across C, indicated by V_{CB} , will not have risen to the value $+V$,

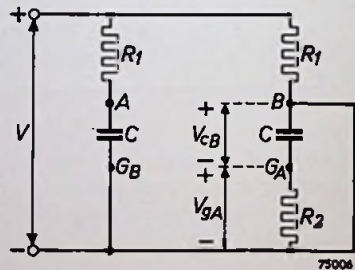


Fig. 68.

Equivalent circuit of a symmetrical multivibrator in one of the two possible quasi-stable states

but will have reached only a lower value, indicated by V_0 , at the moment of switching. So the situation of fig. 68 starts with a voltage $V_{CB} = V_0$ at the moment of switching which will be noted by $t = 0$, zero point of the time-axis.

Capacitor C_B discharges via the resistance R_2 and would after an infinitely long time have reached a value zero. The time function with which the voltage across C_B changes from the initial value V_0 to the final zero value is:

$$V_{CB} = V_0 e^{-t/T_d} \dots \dots \dots (114)$$

with a time constant:

$$T_d = R_2 C \dots \dots \dots (115)$$

The grid voltage of valve A , V_{gA} , is equal to this capacitor voltage, but with opposite sign, so:

$$V_{gA} = -V_0 e^{-t/T_d} \dots \dots \dots (116)$$

After a certain time t_1 this grid voltage attains a critical value V_{gc} at which anode current starts to flow in valve A , and at this moment the multivibrator switches over to the other state, in which valve A is conducting and valve B cut off.

This time t_1 is half the period of the multivibrator signal, for the new state after switching-over will last as long as the first state, because the multivibrator was assumed to be symmetrical. Thus, after another t_1 seconds, the second state will be suddenly reversed to the first state with valve A non-conducting, and valve B conducting.

From expression (116) t_1 can be determined, as for $t = t_1$, the grid voltage V_{gA} will be $-V_{gc}$, giving

$$V_{gc} = V_0 e^{-t_1/T_d} \dots \dots \dots (117)$$

The unknown factor V_0 , however, will have to be determined. This can be done by considering the course of V_{CB} with time in the second half of the period. It should be kept in mind that after another half period of t_1 seconds,

V_{CB} must have again reached the initial value V_0 of the first half period, assuming the multivibrator to have attained a stationary state.

During the second half of the period, the circuit of fig. 69 represents the multivibrator condition.

The initial value of V_{CB} for this half period is V_{gc} . The final value would be $+V$, if this condition lasted indefinitely. V_{CB} changes exponentially with a time constant

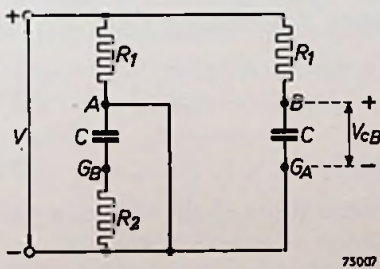


Fig. 69.

Equivalent circuit of a symmetrical multivibrator in the second quasi-stable state (compare with fig. 68).

$$T_c = R_1 C \quad \dots \dots \dots (118)$$

from the initial value V_{g_c} to the final value V , thus:

$$V_{C_B} = V - (V - V_{g_c}) e^{-t/T_c} \quad \dots \dots \dots (119)$$

For $t = t_1$ the value $V_{C_B} = V_0$ is attained, so V_0 is now defined by the expression:

$$V_0 = V - (V - V_{g_c}) e^{-t_1/T_c} \quad \dots \dots \dots (120)$$

From (117) and (120) V_0 can be eliminated and an expression is obtained, containing t_1 as the only unknown quantity.

Calling

$$e^{-t_1/T_c} = x, \quad \dots \dots \dots (121)$$

(117) and (120) can be transformed to:

$$V_0 = V_{g_c}/x \quad \dots \dots \dots (122)$$

and

$$V_0 = V - (V - V_{g_c}) x^{T_d/T_c} \quad \dots \dots \dots (123)$$

Eliminating V_0 gives:

$$V_{g_c} = [V - (V - V_{g_c}) x^{T_d/T_c}] x \quad \dots \dots \dots (124)$$

In general, it will not be easy to obtain an explicit expression for x , and at the same time for t_1 from (124). Therefore the results obtained will be changed in such a way as to be able to plot the results graphically. For this purpose the expressions (117) and (120) will be written in the following way:

$$V_0/V = V_{g_c}/Vx \quad \dots \dots \dots (125)$$

$$V_0/V = 1 - (1 - V_{g_c}/V) x^{T_d/T_c} \quad \dots \dots \dots (126)$$

The quotient V_{g_c}/V will be called D .

This is a practically constant quantity, as the cut-off voltage of a valve is nearly proportional to the H.T. supply voltage V . The constant D can be determined from the valve characteristics. Substituting $V_{g_c}/V = D$ in (125) and (126) results in:

$$V_0/V = D/x \quad \dots \dots \dots (127)$$

and:

$$V_0/V = 1 - (1 - D) x^d, \quad \dots \dots \dots (128)$$

where $d = T_d/T_c$ is the quotient of the discharging and the charging time constant of the capacitor C .

Also

$$d = R_2/R_1, \quad \dots \dots \dots (129)$$

i.e. the quotient of the grid leak resistance and the anode resistance.

Plotting graphically the quantity V_0/V as a function of x , according to

(127) and (128), gives the solution for x as the point of intersection of these two graphs.

In fig. 70 two cases have been represented, viz. for $D = 1/10$ and for $D = 1/20$. Curves II, representing expression (128), have been plotted with d as parameter. In practice, values of d smaller than 1, and of D larger than $1/10$, will seldom be met. It may be observed that one of the intersection

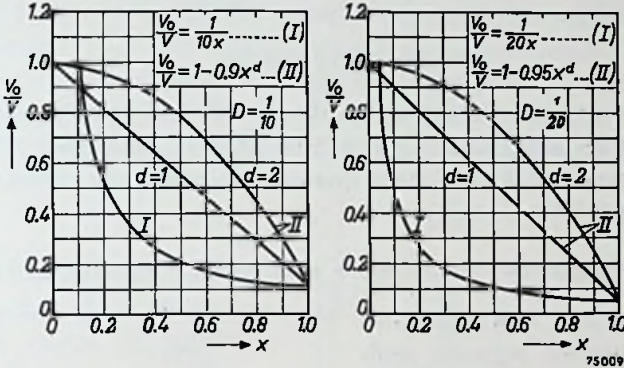


Fig. 70.

Graphs for determination of the frequency of the output signal of a symmetrical multivibrator for different values of the ratio of the discharging- to the charging time-constant of the coupling capacitors (parameter d) and for two values of the cut-off voltage of the valves (parameter D).

points of curves I and II nearly always occurs at the same value of x , viz. at about $x = D$. This means that the quotient V_0/V is nearly always equal to unity, and this in turn indicates the fact that the capacitor voltage at its maximum practically reaches the value $+V$.

It should also be pointed out that there always exists a second intersection point of curves I and II, determining the fixed value $x = 1$.

However, this has no physical significance, as for $x = 1$ or $e^{-t_1/T_d} = 1$, the value $t_1 = 0$ would result. The period of the multivibrator signal would be zero, the quotient V_0/V would be equal to D , or V_0 would be equal to V_{Gc} , in other words the grid voltage would just reach the cut-off value and at the same time be driven negative again, assuming this state of affairs could be realized physically.

Recapitulating, if it is desired to obtain an exact idea of the value of the frequency of a symmetrical multivibrator, the graphical process described above should be applied. For most cases in practice, however, it will be sufficient to apply the approximation $x = D$, or:

$$e^{-t_1/T_d} = D$$

$$\text{or } t_1/T_d = \ln 1/D \dots \dots \dots (130)$$

The *period* of the multivibrator signal is:

$$T = 2t_1 = 2 T_d \ln 1/D \dots \dots \dots (131)$$

The *frequency* is the reciprocal value

$$f = 1/(2T_d \ln 1/D) \dots \dots \dots (132)$$

So the quantity *a*, mentioned in the introduction is:

$$a = fT_d = 1/(2 \ln 1/D) \dots \dots \dots (132a)$$

As can be seen, *a* is dependent on the cut-off voltage of the valves. Most values of *D* occurring in practice will be situated between 1/10 and 1/50. For these extreme values of *D* the quantity *a* assumes the values 0.218 (*D* = 1/10) and 0.128 (*D* = 1/50).

6.4.1.1.3. Symmetrical multivibrator with variable positive grid bias

When the grid leak resistances are not connected between grids and negative H.T. lead, but between grids and a positive voltage supply +*V_r*, the equivalent circuit of the multivibrator can be represented by fig. 71 instead of fig. 67, and the influence of this control voltage *V_r* on the frequency of the multivibrator signal can be investigated by similar considerations as exposed in the preceding section.

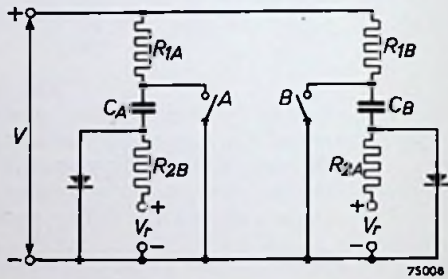


Fig. 71.

Equivalent circuit of a symmetrical multivibrator with a positive control voltage *V_r* applied to the grids, neglecting internal anode- and grid-resistances.

In the first half of the period, the condition of the multivibrator is assumed to be such that valve A is cut off, and valve B conducting. In that case the circuit of fig. 68 is changed to that of fig. 72. The initial voltage across the capacitor at B, viz. *V_{CB}*, has again an as yet unknown value *V₀* at a time *t* = 0 (immediately after the switching of the multivibrator into this state). Now, *V_{CB}* tends, according to an exponential function with a time constant:

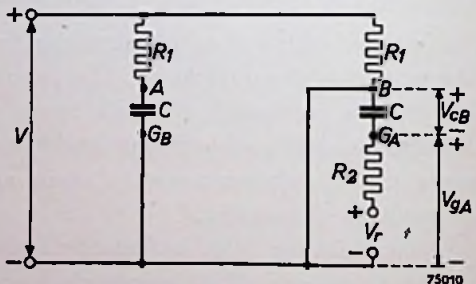


Fig. 72.

Replacement circuit of a symmetrical multivibrator with grid control voltage *V_r* in one of its quasi-stable states.

$$T_d = R_2 C \dots \dots \dots (133)$$

from this initial value V_0 to a final value $-V_r$, so that the variation of V_{CB} with time during this half period can be represented by the following expression:

$$V_{CB} = (V_0 + V_r) e^{-t/T_d} - V_r \dots \dots \dots (134)$$

The grid voltage of valve B is equal to V_{CB} , but with opposite sign, and at the instant $t = t_1$ this voltage reaches the critical value $-V_{gc}$, the cut-off voltage, at which moment the two valves change their conditions, valve A becoming conductive and valve B cut off. The time t_1 , half the period of the complete multivibrator signal, can be determined from the following condition:

$$V_{gc} = (V_0 + V_r) e^{-t_1/T_d} - V_r \dots \dots \dots (135)$$

From the instant $t = t_1$, for another period of t_1 seconds, the equivalent circuit of fig. 73 is valid.

Putting the instant $t = t_1$ as zero time for the second half period, lasting t_1 seconds, the following expression for the variation of V_{CB} with time during this period is obtained:

$$V_{CB} = V - (V - V_{gc}) e^{-t/T_c} \quad (136)$$

with $T_c = R_1 C \dots \dots (137)$

V_{CB} rises exponentially from the initial value V_{gc} to a final value $+V$ with a time constant T_c . However, after t_1 seconds the grid voltage of valve A reaches the cut-off value and again the multivibrator is switched to the condition that was assumed for the first half period. As a stationary condition is assumed to be attained, the voltage V_{CB} must be again V_0 at the end of the second half period. In other words, putting $t = t_1$ in expression (136) must make V_{CB} equal to V_0 , thus:

$$V_0 = V - (V - V_{gc}) e^{-t_1/T_c} \dots \dots \dots (138)$$

Introducing $x = e^{-t_1/T_d} \dots \dots \dots (139)$

changes expressions (135) and (138) into

$$V_0/V = (D + V_r/V) 1/x - V_r/V \dots \dots \dots (140)$$

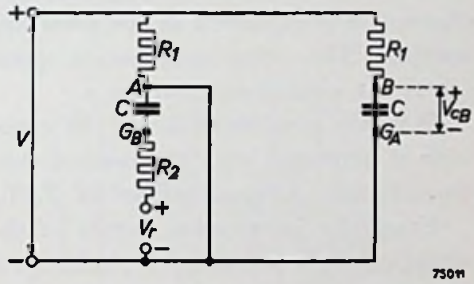


Fig. 73.

Equivalent circuit of a symmetrical multivibrator with grid control voltage V_r in the second quasi-stable state (compare with fig. 72).

and $V_0/V = 1 - (1 - D) x^{T_d/T_c}$, (141)

where $D = V_{gc}/V$.

The most convenient solution for x from these two equations is by means of a graphical method.

In fig. 74 both functions have been plotted for $D = 1/10$. Curves I represent equation (140) with V_r as parameter, whilst curves II represent equation (141) with T_d/T_c as parameter.

Both curves have always two points of intersection, one of which is the point $x=1$ which has no further physical significance, as is explained in the preceding section. The other intersection point gives the wanted solution for x .

It is now possible to derive the variation of frequency with the control voltage V_r for different values of T_d/T_c .

From the intersection points of the set of curves I with curve II, holding for the chosen value of T_d/T_c , the value of x as a function of V_r/V is found. From x the frequency is derived in the following way:

$$x = e^{-t_1/T_d}$$

$$t_1/T_d = \ln 1/x$$

$$t_1 = T_d \ln 1/x.$$

The period of the multivibrator signal is

$$T = 2t_1,$$

or $T = 2 T_d \ln 1/x$ (142)

The frequency is $f = 1/T$, or:

$$f = 1/(2T_d \ln 1/x), \dots \dots \dots (143)$$

or $a = fT_d = 1/(2 \ln 1/x)$ (144)

Here a is the same quantity as given in expression (110).

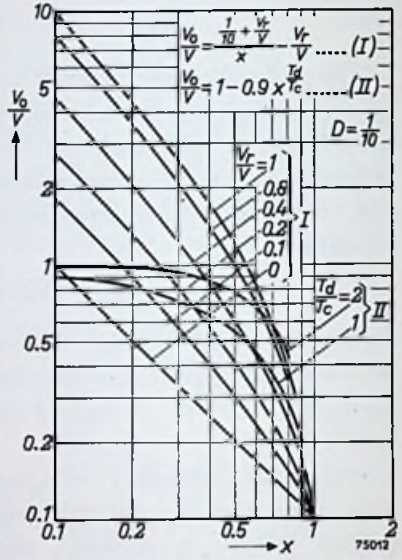


Fig. 74. Graph for determination of the frequency of a symmetrical multivibrator with grid control voltage V_r and ratio of discharging to charging time-constant T_d/T_c as parameters for a certain cut-off voltage value (for which D is a measure).

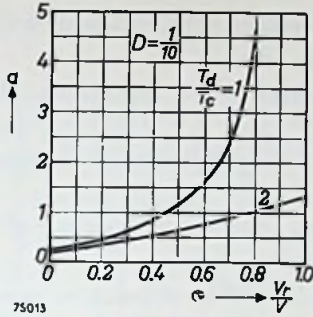


Fig. 75.

Graphs derived from fig. 74, giving an impression of the dependency of the multivibrator frequency on the grid control voltage V_r , for two values of the ratio T_d/T_c and a certain cut-off voltage, determined by D .

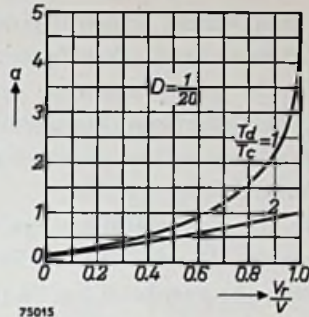


Fig. 77.

Same as fig. 75, but derived from fig. 76.

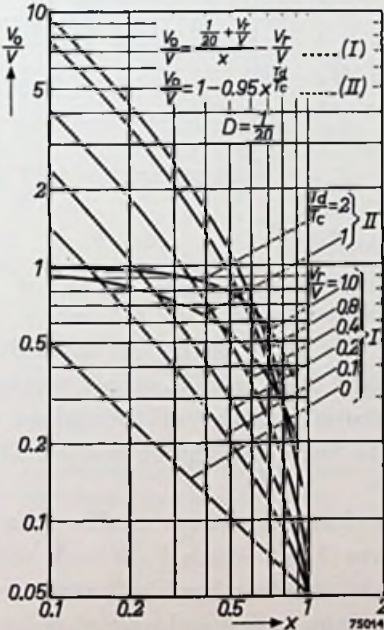


Fig. 76.

Same as fig. 74 for another value of the cut-off voltage.

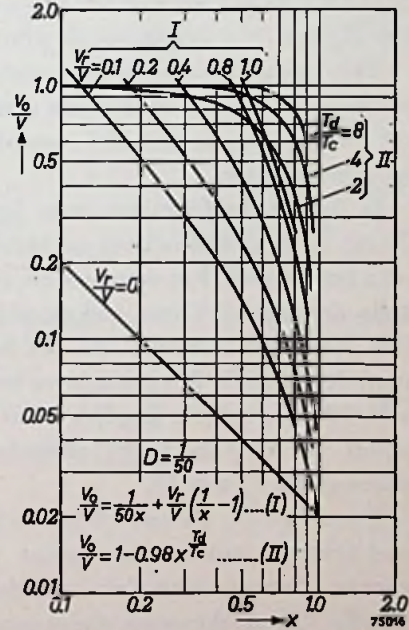


Fig. 78.

Same as figs. 74 and 76 for a third value of the cut-off voltage.

In fig. 75 the quantity a is plotted as a function of the control voltage V_r , more exactly as a function of the ratio of V_r to the H.T. supply voltage V ;

this ratio will be termed the relative control voltage. The values of a from fig. 75 have been taken from the graphs of fig. 74.

Fig. 76 gives again a graphical representation of equations (140) and (141), this time for a value of $D = 1/20$.

Fig. 77 shows the quantity a as a function of the relative control voltage, as derived from fig. 76.

Fig. 78 is identical to figs. 74 and 76 with still another value of the parameter D , viz. $D = 1/50$.

From the graphs of fig. 78 the values of a for different relative control voltages have again been derived and plotted in fig. 79. It is seen that for $D = 1/10$ and $D = 1/20$, the function $a = f(V_r/V)$ does not change much for values of $T_d/T_c \geq 2$ (see figs. 75 and 77), and in the case $D = 1/50$ the same holds for values of $T_d/T_c \geq 4$ (see fig. 79).

Thus, generally speaking, the frequency of a symmetrical multivibrator is a nearly linear function of the control voltage, applied to the control grids of the valves, for all values of D ($1/10 \geq D \geq 1/50$) and for all values of T_d/T_c (or R_2/R_1) ≥ 4 occurring in practice.

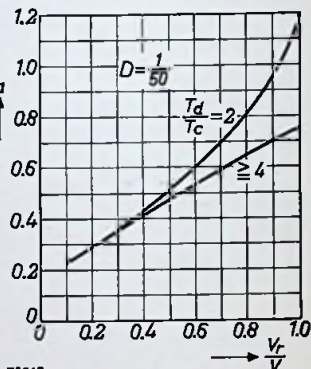
This linear function is independent of T_d/T_c ; it only contains D , that is the ratio of the cut-off voltage V_{gc} to the H.T. supply voltage V , as a parameter.

In fig. 80 the functions from figs. 75, 77 and 79 for $T_d/T_c \geq 4$ have been gathered and plotted on a larger scale. For comparison, an experimentally determined curve, indicated by the dotted line, has been included. As can be seen, the value of D for the valve used (type EFF 51) must have been about $1/20$. The H.T. supply voltage was 200 V, which implies that the cut-off voltage of the valves is about 10 V. This is in accordance with the valve characteristics. The value of T_d/T_c was 10.

From figs. 74, 76 and 78 it can be seen that x is always smaller than 1 and that the intersection point of curves I for which $V_r/V = 1$, with curves II occur with values of x that become smaller when T_d/T_c increases. For $T_d/T_c > 4$, therefore, the second term of the right-hand part of expression (141) can practically be neglected, so that:

$$V_0/V = 1 \dots \dots \dots (145)$$

This indicates that the voltages across the capacitors have at the end of a charging period attained a value equal to the H.T. supply voltage V .



75017
Fig. 79.
Same as figs. 75 and 77, but derived from fig. 78.

Substituting (145) in (140) yields:

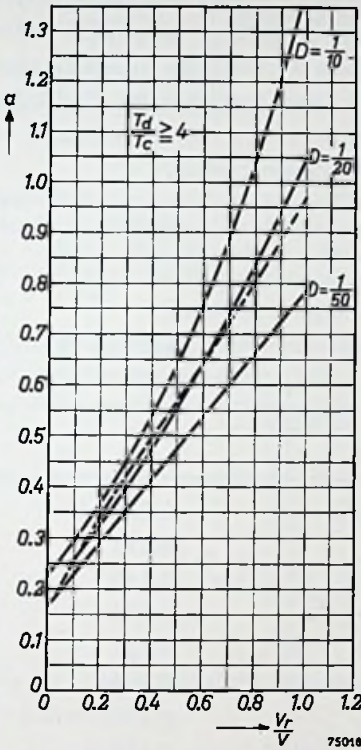


Fig. 80.

Dependency of the frequency of a symmetrical multivibrator on the grid control voltage as derived from figs. 74, 76 and 78 for a ratio of the discharging to the charging time constant of the coupling capacitors $T_d/T_c \geq 4$ (fully drawn curves). An experimentally determined curve is represented by the dotted line.

$$\left(D + V_r/V \right) \frac{1}{x} = 1 + V_r/V$$

or
$$1/x = \frac{1 + V_r/V}{D + V_r/V}$$

or
$$e^{t_1/T_d} = \frac{1 + V_r/V}{D + V_r/V}$$

or
$$t_1 = T_d \ln \frac{1 + V_r/V}{D + V_r/V} \dots (146)$$

The period of the multivibrator signal is:

$$T = 2 T_d \ln \frac{1 + V_r/V}{D + V_r/V} \dots (147)$$

and the frequency:

$$f = \frac{1}{2 T_d \ln \frac{1 + V_r/V}{D + V_r/V}} \dots (148)$$

The quantity $a = fT_d$ thus becomes:

$$a = \frac{1}{2 \ln \frac{1 + \gamma}{D + \gamma}} \dots (149)$$

where $\gamma = V_r/V; \dots (150)$

γ is the relative control voltage.

D is a measure for the "grid base" of the valves at a certain H.T. supply voltage V .

It should be noted that, for a control voltage $V_r = 0$, or $\gamma = 0$, expression (149) changes into expression (132a), as would be expected.

In the introduction it was already mentioned that the frequency of the multivibrator will not be greatly influenced by variations in the H.T.

supply voltage V . Only at rather low values of V does this influence increase. This can easily be checked experimentally by taking the control voltage V_r as a fixed fraction of V , for instance $\gamma = 0$ or $\gamma = 1$ (grid leaks to negative connection, respectively to positive connection of the H.T. supply) in order to keep γ constant with varying supply voltage V . The only quantity that may vary with V is then D . Now it is a well-known fact that the grid base of a valve is within certain limits proportional to the supply voltage, so that $D = V_{gc}/V$ will also be practically independent of V .

Experimental results are given in Tables 1 and 2.

For table 1 the conditions were:

Valve EFF 51 (double pentode)

$$R_{1A} = R_{1B} = 11 \text{ k}\Omega$$

$$C_A = C_B = 3000 \text{ pF}$$

$$R_{2A} = R_{2B} = 100 \text{ k}\Omega$$

$$V_r = 0$$

(see fig. 71)

Table 1

$+V$ (V)	Frequency measured (c/s)	a
70	786	0.236
80	709	0.213
90	652	0.196
100	614	0.184
125	557	0.167
150	538	0.161
200	519	0.156
250	500	0.150
290	500	0.150

For table 2 the same data were valid, except $V_r = V$, so $\gamma = 1$.

Table 2

$+V$ (V)	Frequency measured (c/s)	a
70	3357	1.007
80	3348	1.004
90	3321	0.996
100	3321	0.996
125	3321	0.996
150	3357	1.007
200	3430	1.029
250	3482	1.045
290	3482	1.060

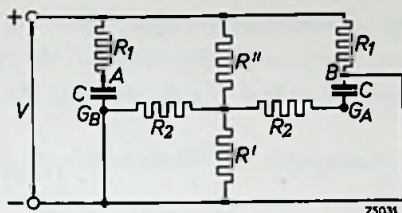


Fig. 81.

Same as fig. 72, but the control voltage source V_r with internal resistance zero is replaced by a voltage divider $R' - R''$ across the H.T. supply source V .

A practical remark must be added here. Up till now the control voltage source has been assumed to have a negligibly small internal resistance. In practice the control voltage will usually be taken from a voltage divider, shunted across the H.T. supply voltage.

In fig. 81 this voltage divider is represented by the resistances R' and R'' . Fig. 81 is to be compared with fig. 72.

The final results of the theoretical considerations of this circuit are such that expressions (140) and (141) have to be replaced by (140a) and (141a)

$$V_0/V = (D + V_1/V) 1/x - V_1/V \dots \dots \dots (140a)$$

$$V_0/V = 1 - (1 - D) x^{T_d/T_c}, \dots \dots \dots (141a)$$

where

$$D = V_{gc}/V; x = e^{-t_1/T_d}$$

$$V_1 = \frac{R'R_2}{R'R_2 + R'R'' + R_2R''} V$$

$$T_d = (R_2 + R_p) C$$

R_p = the equivalent resistance of the three resistances R', R'' and R_2 in parallel,

$$\text{and } T_c = R_1 C.$$

6.4.1.1.4. The asymmetrical multivibrator

The asymmetrical properties can be indicated in the following way: valve A and circuit elements with an index A need no longer be identical with the corresponding quantities that have an index B (see fig. 65).

In the condition with valve A cut off, valve B conducting, the circuit of the multivibrator can be schematically represented by fig. 82, where internal resistances of anode and grids of the valves have been neglected under the formerly stated conditions.

Capacitor C_A is charged with a time constant $T_{C1} = R_{1A} C_A$, starting at a voltage V_{gcB} , the cut-off value of the grid of valve B, and exponentially in-

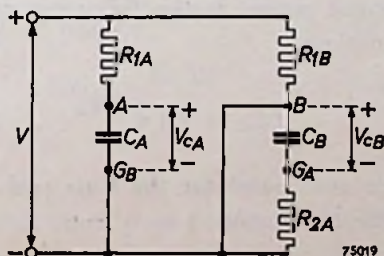


Fig. 82.

Equivalent circuit of an asymmetrical multivibrator in one of its two possible quasi-stable states.

creasing to a final voltage V , which should be reached after an infinitely long time.

Thus, the variation with time of the voltage across C_A is, putting the time of start of this condition $t = 0$:

$$V_{CA} = V - (V - V_{gcB}) e^{-t/T_{c1}} \dots \dots \dots (151)$$

In the same period capacitor C_B is being discharged with a time constant $T_{d2} = R_{2A} C_B$, starting with an initial value V_B and exponentially decreasing to zero. Thus, the variation with time of the voltage across C_B can be represented as:

$$V_{CB} = V_B e^{-t/T_{d2}} \dots \dots \dots (152)$$

After a time t_1 seconds, V_{CB} has reached the value V_{gcA} , and at that instant the grid voltage of valve A is V_{gcA} , the cut-off value. Valve A becomes conducting, the multivibrator switches over in the other state, during which valve A is conducting, valve B cut off. The time t_1 is defined by expression (152). By substituting $t = t_1$ and $V_{CB} = V_{gcA}$:

$$V_{gcA} = V_B \cdot e^{-t_1/T_{d2}} \dots \dots \dots (153)$$

At the instant $t = t_1$, the voltage across C_A is given by (151). Calling this value V_A , gives:

$$V_A = V - (V - V_{gcB}) e^{-t_1/T_{c1}} \dots \dots \dots (154)$$

This value is the initial value of V_{CA} for the second state of the multivibrator, during which its equivalent circuit is as represented in fig. 83.

Capacitor C_A is now being discharged with a time constant $T_{d1} = R_{2B} C_A$ from an initial value V_A according to (154) down to zero for infinitely long time. The variation with time of V_{CA} in this second period is the following exponential function:

$$V_{CA} = V_A e^{-t/T_{d1}} \dots \dots (155)$$

The zero point for the time scale coincides with the instant $t = t_1$ from the preceding period.

The final value of V_{CA} is not zero, for as soon as the value V_{gcB} is passed, valve B becomes conducting and the multivibrator again switches back to the state that was described for the first period.

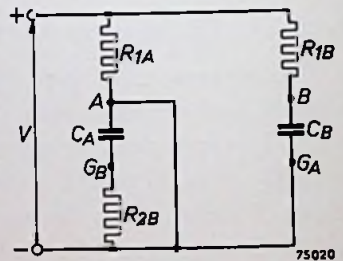


Fig. 83. Same as fig. 82 for the other quasi-stable state of an asymmetrical multivibrator.

Let this occur at a time $t = t_2$. Then, at this instant $t = t_2$, a complete cycle has been performed, and the period of this complete cycle is given by

$$T = t_1 + t_2.$$

t_2 is determined by expression (155) by substituting $t = t_2$ and $V_{C_A} = V_{g_{CB}}$:

$$V_{g_{CB}} = V_A e^{-t_2/T_{d1}} \dots \dots \dots (156)$$

The voltage across capacitor C_B during the second period can be determined by considering the charging of this capacitor with a time constant $T_{C_2} = R_{1B} \cdot C_B$ from an initial value $V_{g_{cA}}$ to a final value V for infinitely long time. This yields an exponential function:

$$V_{C_B} = V - (V - V_{g_{cA}}) e^{-t/T_{c2}} \dots \dots \dots (157)$$

However, before the final value V is reached, the multivibrator switches over and capacitor C_B becomes discharged. As a stationary multivibrator action is assumed, the voltage across C_B at the moment of switching is again at the same value at which the cycle started, viz. V_B , thus

$$V_B = V - (V - V_{g_{cA}}) e^{-t_2/T_{c2}} \dots \dots \dots (158)$$

Expressions (153), (154), (156) and (158) represent four equations with four unknown quantities, viz. t_1 , t_2 , V_A and V_B . Two of them, V_A and V_B , can easily be eliminated, leaving two equations with two unknown quantities.

Introducing for the latter

$$x = e^{-t_1/T_{d2}} \dots \dots \dots (159)$$

$$y = e^{-t_2/T_{d1}} \dots \dots \dots (160)$$

results in the following equations:

$$V_{g_{cB}}/y = V - (V - V_{g_{cB}}) x^{T_{d2}/T_{c1}} \dots \dots (161)$$

$$V_{g_{cA}}/x = V - (V - V_{g_{cA}}) y^{T_{d1}/T_{c2}} \dots \dots (162)$$

Substituting

$$V_{g_{cA}}/V = D_A \dots \dots \dots (163)$$

$$V_{g_{cB}}/V = D_B \dots \dots \dots (164)$$

changes (161) and (162) into:

$$y = \frac{D_B}{1 - (1 - D_B) x^{k_1 m}} \dots \dots \dots (165)$$

$$x = \frac{D_A}{1 - (1 - D_A)y^{k_2/m}} \dots \dots \dots (166)$$

with

$$k_1 = \frac{T_{d1}}{T_{c1}} = \frac{R_{2B}}{R_{1A}} \dots \dots \dots (167)$$

$$k_2 = \frac{T_{d2}}{T_{c2}} = \frac{R_{2A}}{R_{1B}} \dots \dots \dots (168)$$

$$m = \frac{T_{d2}}{T_{d1}} = \frac{R_{2A}}{R_{2B}} \frac{C_B}{C_A} \dots \dots \dots (169)$$

The unknown x and y now again can be solved by a graphical method. To this purpose equations (165) and (166) are plotted in a graph with D_A and D_B as parameters, and for certain values of k_1 , k_2 and m . The points of intersection give the solution for x and y , from which t_1 and t_2 can be determined in the following way:

$$x = e^{-t_1/T_{d1}}, y = e^{-t_2/T_{d2}},$$

$$t_1 = T_{d2} \ln 1/x, t_2 = T_{d1} \ln 1/y.$$

The period of the complete cycle of the multivibrator is:

$$T = t_1 + t_2 = T_{d2} \ln 1/x + T_{d1} \ln 1/y \dots \dots \dots (170)$$

and the frequency:

$$f = 1/T = \frac{1}{T_{d2} \ln 1/x + T_{d1} \ln 1/y} \dots \dots \dots (171)$$

In all cases a point of intersection is found for which $x = 1$ and $y = 1$. As in the previous cases of the symmetrical multivibrator, this solution has no physical significance.

Considering the quantities k_1 , k_2 and m more closely, it can be stated that k_1 is the ratio of the discharging time constant to the charging time constant of capacitor C_A , k_2 is the same ratio for capacitor C_B , whilst m is a measure for the asymmetry of the multivibrator.

Generally the grid leak resistors will be larger than the resistances in the anode circuits, which implies that k_1 and k_2 will usually be greater than unity.

For a strongly asymmetrical multivibrator m is very large or very small. Assume $m \ll 1$; as $k_2 \geq 1$, k_2/m will be $\gg 1$.

The value of y is always situated between zero and unity. Only in the case of y approximating to unity will the function $y^{k_2/m}$ attain a value that

is not very small with respect to unity. For all other values of y equation (166) may to a good approximation be simplified to

$$x = D_A \dots \dots \dots (172)$$

Substituting this value of x in equation (165) yields for the corresponding value of y :

$$y = \frac{D_B}{1 - (1 - D_B) D_A^{k_1/m}} \dots \dots \dots (173)$$

If $m \gg 1$, it can easily be shown in the same way that with good approximation the following simplified expressions hold:

$$y = D_B \dots \dots \dots (174)$$

$$x = \frac{D_A}{1 - (1 - D_A) D_B^{k_2/m}} \dots \dots \dots (175)$$

In the case where the asymmetry is not very pronounced, some examples are graphically plotted below.

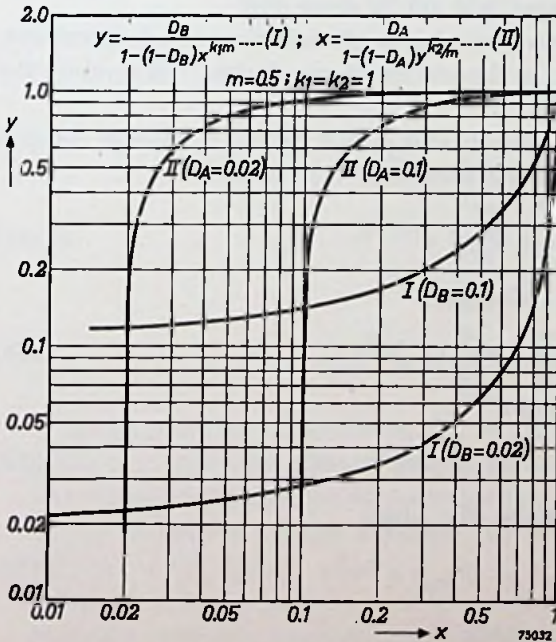


Fig. 84.

Graph for determination of the frequency of an asymmetrical multivibrator with the cut-off voltage of the valves as parameter.

For the sake of simplification k_1 is assumed to be equal to k_2 . Fig. 84 represents in curves I equation (165) with D_B as parameter; in curves II equation (166) with D_A as parameter, for $k_1 = k_2 = 1$ and $m = \frac{1}{2}$.

Even for this not very asymmetrical multivibrator circuit, it will be seen that the intersection points are found at values of x nearly equal to D_A .

In fig. 85 a much more asymmetrical case is represented, viz. $m = 0,1$, whilst k_1 en k_2 have again be chosen equal to unity. Here the approximation $x = D_A$ is to a much greater extent valid.

6.4.1.1.5. *Asymmetrical multivibrator with variable positive grid bias*

In the general multivibrator circuit, represented in fig. 65, a variable positive supply voltage V_{rA} must be supposed to be included between the negative lead of the H.T. supply and the lower end of the grid leak resistor R_{2A} . Similarly a positive variable supply voltage V_{rB} between the negative lead of the H.T.

supply and the lower end of the grid leak resistor R_{2B} must be assumed.

The complete derivation of the expressions governing the time functions that represent the grid voltages, will not be given here.

It will be clear that the same reasoning as given in the preceding sections, and following the same lines in the process of calculation, will produce the following results:

For the first part of the multivibrator period, lasting t_1 seconds, expression (153) appears in the altered version of (153 a) as:

$$V_{g_{cA}} = (V_B + V_{rA}) e^{-t_1/T_{d2}} - V_{rA} \dots \dots \dots (153a)$$

Expression (154) remains unchanged:

$$V_A = V - (V - V_{g_{cB}}) e^{-t_1/T_{c1}} \dots \dots \dots (154)$$

Expression (156) changes into:

$$V_{g_{cB}} = (V_A + V_{rB}) e^{-t_2/T_{d1}} - V_{rB} , \dots \dots \dots (156a)$$

whilst expression (158) remains the same:

$$V_B = V - (V - V_{g_{cA}}) e^{-t_2/T_{c2}} \dots \dots \dots (158)$$

Elimination of V_A and V_B yields:

$$V_{g_{cA}} = \{ V - (V - V_{g_{cA}}) e^{-t_2/T_{c2}} + V_{rA} \{ e^{-t_1/T_{d2}} V_{rA}$$

$$V_{g_{cB}} = \{ V - (V - V_{g_{cB}}) e^{-t_1/T_{c1}} + V_{rB} \{ e^{-t_2/T_{d1}} V_{rB}$$

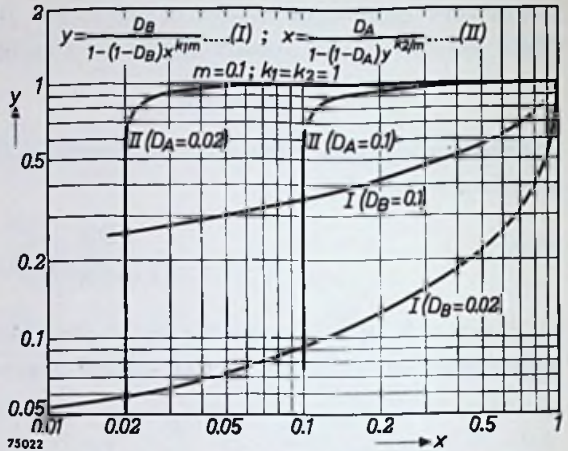


Fig. 85.

Same as fig. 84, but for a much more asymmetrical multivibrator.

Introducing again:

$$x = e^{-t_1/T_{d2}}$$

and
gives:

$$y = e^{-t_2/T_{d1}}$$

$$V_{g_{cA}} + V_{rA} = \{V - (V - V_{g_{cA}}) y^{T_{d1}/T_{c2}} + V_{rA}\} x.$$

$$V_{g_{cB}} + V_{rB} = \{V - (V - V_{g_{cB}}) x^{T_{d2}/T_{c1}} + V_{rB}\} y.$$

Dividing both parts of the equations by V :

$$\frac{D_A + \gamma_A}{x} = 1 - (1 - D_A) y^{k_2/m} + \gamma_A \quad \dots \quad (176)$$

$$\frac{D_B + \gamma_B}{y} = 1 - (1 - D_B) x^{k_1/m} + \gamma_B, \quad \dots \quad (177)$$

where:

$$D_A = \frac{V_{g_{cA}}}{V}$$

$$D_B = \frac{V_{g_{cB}}}{V}$$

$$\gamma_A = \frac{V_{rA}}{V}$$

$$\gamma_B = \frac{V_{rB}}{V}$$

$$k_2 = \frac{T_{d2}}{T_{c2}} = \frac{R_{2A}}{R_{1B}}$$

$$k_1 = \frac{T_{d1}}{T_{c1}} = \frac{R_{2B}}{R_{1A}}$$

$$\text{and } m = \frac{T_{d2}}{T_{d1}} = \frac{R_{2A} C_B}{R_{2B} C_A}.$$

Choosing certain values for k_1 , k_2 , m , D_A and D_B , expressions (176) and (177) can again be plotted graphically with γ_A and γ_B as parameters. The points of intersection of corresponding curves then give the variation of the frequency of the asymmetrical multivibrator with the control voltage on the grids.

Up till now the positive grid bias sources V_{rA} and V_{rB} were assumed to have a negligibly small internal resistance. If this were not the case, the internal resistance would have to be taken into account, the only effect being an increase of the grid leak resistance with an amount equal to the internal resistance.

As already mentioned when dealing with the symmetrical multivibrator, the positive control voltage applied to the grids of the valves will in practice very often be taken from the H.T. supply by means of a voltage divider or potentiometer. Fig. 86 gives the circuit for the case of two separate voltage dividers $R'_A - R''_A$, and $R'_B - R''_B$, which will be required when the control voltage on one grid must be different from that on the other grid.

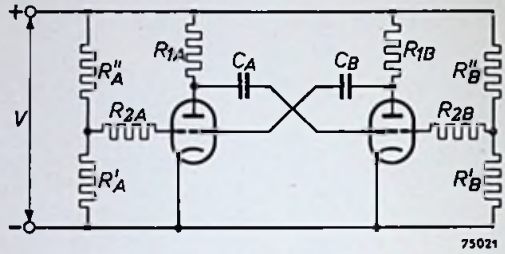


Fig. 86.

Asymmetrical multivibrator with control voltages on the grids derived from the H.T. supply via voltage dividers $R'_A - R''_A$ and $R'_B - R''_B$.

The equations from which the frequency can be graphically determined can be written in the same form as equations (176) and (177), if only γ_A be replaced by V_{1A}/V and:

$$\gamma_B \quad \text{by} \quad \frac{V_{1B}}{V}$$

$$k_1 \quad \text{by} \quad \frac{R_{2B} + R_{pB}}{R_{1A}}$$

$$k_2 \quad \text{by} \quad \frac{R_{2A} + R_{pA}}{R_{1B}}$$

$$m \quad \text{by} \quad \frac{(R_{2A} + R_{pA}) C_B}{(R_{2B} + R_{pB}) C_A}$$

where:

$$V_{1A} = \frac{R'_A}{R'_A + R''_A} \cdot V.$$

$$V_{1B} = \frac{R'_B}{R'_B + R''_B} \cdot V.$$

$$R_{pA} = \frac{R'_A R''_A}{R'_A + R''_A}$$

$$R_{pB} = \frac{R'_B \cdot R''_B}{R'_B + R''_B}$$

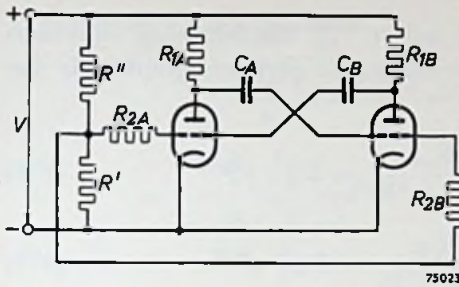


Fig. 87.

Same as fig. 86, but with grid control voltages derived from a common voltage divider $R'-R''$.

When both grids must have the same positive bias voltage, this can be taken from a single potentiometer, as represented in the circuit of fig. 87. Now equations (176) and (177) still hold, but with the following substitutions and modifications:

$$V_{1A}/V \text{ for } \gamma_A,$$

$$V_{1B}/V \text{ for } \gamma_B,$$

$$T_{d2} = (R_{2A} + R_{pA}) C_B$$

$$T_{d1} = (R_{2B} + R_{pB}) C_A$$

T_{c1} and T_{c2} remain unchanged.

$$V_{1A} = \frac{R' R_{2B}}{R' R_{2B} + R' R'' + R_{2B} R''} \cdot V.$$

$$V_{1B} = \frac{R' R_{2A}}{R' R_{2A} + R' R'' + R_{2A} R''} \cdot V.$$

R_{pA} = the equivalent resistance of R' , R'' and R_{2B} , all three in parallel.

R_{pB} = the same for R' , R'' and R_{2A} in parallel.

6.4.1.1.6. Influence of the internal resistance of the H.T. supply source

In all preceding considerations and calculations the internal resistance of the H.T. supply source has been neglected. The influence of this internal resistance can however be determined. The equivalent circuit of the multivibrator will now be as depicted in fig. 88 (see for comparison fig. 71).

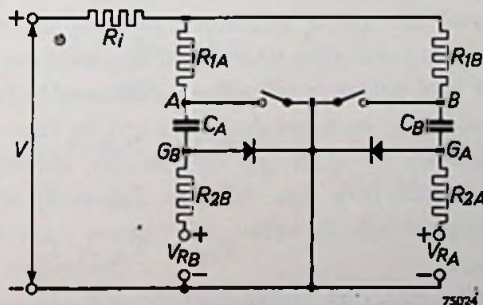


Fig. 88.

Asymmetrical multivibrator with grid control voltages and a common anode resistance R_i of both valves.

The resistance R_i represents the internal resistance of the H.T. supply eventually increased with an externally applied common anode resistance of both valves.

Now, instead of equations (176) and (177), the following equations (178) and (179) are the basic expressions for deriving graphically the frequency of the multivibrator:

$$\frac{D_A + \gamma_A}{x} = \frac{R_{1A}}{R_{1A} + R_i} + \gamma_A - \left(\frac{R_{1A}}{R_{1A} + R_i} - D_A \right) y^{k_2/m} \dots (178)$$

$$\frac{D_B + \gamma_B}{y} = \frac{R_{1B}}{R_{1B} + R_i} + \gamma_B - \left(\frac{R_{1B}}{R_{1B} + R_i} - D_B \right) x^{k_1/m} \dots (179)$$

$$D_A = \frac{V_{g_cA}}{V} \qquad D_B = \frac{V_{g_cB}}{V}$$

$$\gamma_A = \frac{V_{r_A}}{V} \qquad \gamma_B = \frac{V_{r_B}}{V}$$

$$x = e^{-t_1/T_{d_2}} \qquad y = e^{-t_2/T_{d_1}}$$

$$k_1 = \frac{T_{d_1}}{T_{c_1}} \qquad k_2 = \frac{T_{d_2}}{T_{c_2}} \qquad m = \frac{T_{d_2}}{T_{d_1}}$$

$$T_{d_1} = R_{2B} C_A \qquad T_{d_2} = R_{2A} C_B$$

$$T_{c_1} = \left(R_{1A} + \frac{R_i R_{1B}}{R_i + R_{1B}} \right) C_A$$

$$T_{c_2} = \left(R_{1B} + \frac{R_i R_{1A}}{R_i + R_{1A}} \right) C_B$$

For a symmetrical multivibrator:

$$\gamma_A = \gamma_B = \gamma$$

$$D_A = D_B = D$$

$$R_{1A} = R_{1B} = R_1$$

$$T_{d_1} = T_{d_2} = T_d$$

$$T_{c_1} = T_{c_2} = T_c$$

The equations (178) and (179) become:

$$\frac{D + \gamma}{x} = \frac{R_1}{R_1 + R_i} + \gamma - \left(\frac{R_1}{R_1 + R_i} - D \right) y^{T_d/T_c} \dots (180)$$

$$\frac{D + \gamma}{y} = \frac{R_1}{R_1 + R_i} + \gamma - \left(\frac{R_1}{R_1 + R_i} - D \right) x^{T_d/T_c} \dots (181)$$

If moreover $T_d \gg T_c$, then:

$$\frac{D + \gamma}{x} = \frac{D + \gamma}{y} = \frac{R_1}{R_1 + R_i} + \gamma,$$

or $\frac{1}{x} = \frac{1}{y} = e^{t_1/T_d} = \left(\frac{R_1}{R_1 + R_i} + \gamma \right) \frac{1}{D + \gamma},$

or $t_1 = T_d \ln \frac{\frac{R_1}{R_1 + R_i} + \gamma}{D + \gamma}.$

The frequency of the multivibrator signal will be:

$$f = \frac{1}{2 T_d \ln \frac{\frac{R_1}{R_1 + R_i} + \gamma}{D + \gamma}}, \dots \dots \dots (182)$$

and the factor $a = f T_d = \frac{1}{2 \ln \frac{\frac{R_1}{R_i + R_1} + \gamma}{D + \gamma}} \dots \dots \dots (183)$

For $R_i = 0$ this expression becomes equal to (149).

6.4.1.1.7. *Some experimental results*

Several symmetrical multivibrator circuits according to fig. 63 have been made, including a variable positive grid bias source with low internal resistance (stabilized H.T. supply) connected between the negative lead of the H.T. supply V and the lower end of the grid leak resistors R_{2A} and R_{2B} and using two types of double valves, viz. an ECC 40 (double triode) and an EFF 50 (double pentode). Anode- and grid resistors have always been chosen so large as to permit the value of the internal anode- and grid resistances to be neglected.

The variation of frequency with grid bias was measured and compared with the values derived theoretically with the aid of expression (148). In this expression three quantities are of importance, viz. T_d , D and γ . Exact determination of the values of these quantities is necessary. This is not always as easy as it might appear at a first sight. Consider, for instance, $T_d = R_2 C$.

It is not sufficiently accurate to take the nominal values of R_2 and C , because fairly large tolerances may occur with respect to their nominal value. It is of course possible to measure in some way or another their real value as accurately as may be desired, but this is not a very practical or quick method. To avoid this, relative frequency values have been introduced, by comparing all frequencies with the frequency corresponding to a grid control voltage $V_r = 0$, or $\gamma = V_r/V = 0$. The control voltage $V_r = 0$ is exactly defined and does not depend on measurement, for all that is necessary is to connect the lower end of the grid leak resistors to the negative H.T. supply lead. Calling the frequency for $\gamma = 0$, f_0 , it follows from expression (148):

$$f_0 = \frac{1}{2 T_d \ln 1/D} \dots \dots \dots (184)$$

The relative frequency for an arbitrary value of γ between zero and unity then can be expressed as follows:

$$F = \frac{f}{f_0} = \frac{\ln 1/D}{\ln \frac{1 + \gamma}{D + \gamma}} \dots \dots \dots (185)$$

Still greater difficulties are met when the exact value of D , or the cut-off voltage V_{gc} of the valves, is required. Even if the anode current of a valve could be entirely suppressed, so that even with the most sensitive microampere meter no current would be indicated, then V_{gc} would certainly not be equal to the value of the negative grid voltage at which anode current first starts to flow, for it will always take a finite amount of increase of the anode current before the multivibrator switches over into the other condition. To avoid the uncertainty in the determination of D , the following procedure has been applied.

As already mentioned, the value $\gamma = 0$ is easily obtained. The same holds for $\gamma = 1$, or $V_r = V$, as this is attained by connecting the lower ends of the grid leak resistors to the positive H.T. supply lead. No voltmeter reading is necessary. Calling the multivibrator signal frequency f_1 for $\gamma = 1$, then the following relation between f_0 and f_1 is derived from expression (148):

$$\frac{f_1}{f_0} = \frac{\ln 1/D}{\ln \frac{2}{D + 1}} \dots \dots \dots (186)$$

The frequencies f_0 and f_1 can easily be determined when a good signal generator is available, for instance by producing Lissajous figures on the screen of an oscilloscope.

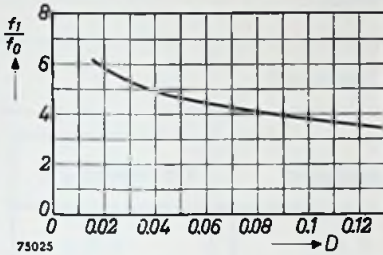


Fig. 89.

Maximum possible frequency variation of a symmetrical multivibrator, when using the H.T. supply voltage as grid control voltage, as a function of the cut-off voltage of the valves.

From the ratio of f_1 and f_0 and expression (186) a certain value for D can be determined. With this experimentally derived value of D the intermediate values of the relative frequency for $0 < \gamma < 1$ can be calculated with the aid of expression (185).

For easy reference expression (186) has been plotted graphically in fig. 89.

In the following tables some experimental results are given. Measured and calculated values of the relative frequency are given, together with the percentage variation between the calculated

and measured values. In both columns representing the relative frequency F , this quantity will be the same for $\gamma = 0$ ($F = 1$) and for $\gamma = 1$.

Table 3

Valve: ECC 40
 Supply voltage: $V = 225$ V
 Anode resistances: $R_{1A} = R_{1B} = 111$ k Ω
 Grid leak resistances: $R_{2A} = R_{2B} = 500$ k Ω
 Coupling capacitors: $C_A = C_B = 340$ pF
 Measured: $f_1/f_0 = 4.70$
 From fig. 89: $D = 0.049$

F

γ	Measured	Calculated	Deviation %
0	1	1	—
0.0889	1.36	1.46	7
0.1956	1.77	1.90	7
0.378	2.41	2.57	6.5
0.578	3.12	3.27	4.7
0.778	3.81	3.95	3.6
1	4.70	4.70	—

Table 4

Only difference from table 3: grid leaks have been doubled.

$$R_{2A} = R_{2B} = 1 M\Omega.$$

Measured: $f_1/f_0 = 4.60$.

From fig. 89: $D = 0.0525$.

F

γ	Measured	Calculated	Deviation %
0	1	1	—
0.0889	1.422	1.44	1.2
0.1956	1.81	1.873	3.4
0.378	2.43	2.53	4.0
0.578	3.14	3.215	2.1
0.778	3.815	3.85	1.0
1	4.60	4.60	—

Table 5

Only difference from table 4: grid leaks $R_{2A} = R_{2B} = 2 M\Omega$.

Measured: $f_1/f_0 = 4.63$

From fig. 89: $D = 0.051$

F

γ	Measured	Calculated	Deviation %
0	1	1	—
0.0899	1.418	1.45	2.2
0.1956	1.83	1.886	3.0
0.378	2.545	2.56	0.6
0.578	3.20	3.23	0.9
0.778	3.825	3.90	0.2
1	4.63	4.63	—

Table 6

Valve: EFF50
 Supply voltage: $V = 225$ V
 Anode resistances: $R_{1A} = R_{1B} = 11 k\Omega$
 Grid leak resistances: $R_{2A} = R_{2B} = 1 M\Omega$

Coupling capacitors: $C_A = C_B = 3300 \text{ pF}$

Measured: $f_1/f_0 = 5.48$

From fig. 89: $D = 0.0265$

F

γ	Measured	Calculated	Deviation %
0	1	1	—
0.0445	1.296	1.35	4
0.133	1.775	1.85	4
0.342	2.75	2.81	2
0.445	3.18	3.12	-1.8
0.667	4.12	4.14	0.5
0.889	5.00	5.01	0.2
1	5.48	5.48	—

Table 7

Only difference from table 6: grid leaks: $R_{2A} = R_{2B} = 100 \text{ k}\Omega$

Measured: $f_1/f_0 = 5.94$

From fig. 89: $D = 0.0185$

F

	Measured	Calculated	Deviation %
0	1	1	—
0.0889	1.667	1.72	3
0.1956	2.215	2.32	5
0.378	3.102	3.20	3
0.511	3.69	3.80	3
0.667	4.48	4.49	0.2
0.778	5.04	4.97	-1.2
0.889	5.63	5.45	-3
1	5.94	5.94	—

Table 8

Differences from table 6: grid leaks: $R_{2A} = R_{2B} = 100 \text{ k}\Omega$

Coupling capacitors: $C_A = C_B = 340 \text{ pF}$

Measured: $f_1/f_0 = 6.09$

From fig. 89: $D = 0.0165$

F

γ	Measured	Calculated	Deviation %
0	1	1	—
0.0889	1.66	1.757	5.8
0.1956	2.095	2.37	13
0.378	2.97	3.28	10
0.511	3.625	3.89	7
0.711	4.615	4.79	6
0.889	5.52	5.59	1.2
1	6.09	6.09	—

Table 9

Only difference from table 6:

Coupling capacitors: $C_A = C_B = 340 \mu\text{F}$

Measured: $f_1/f_0 = 5.9$

From fig. 89: $D = 0.019$

γ	Measured	Calculated	Deviation %
0	1	1	—
0.0899	1.69	1.71	1.1
0.1956	2.24	2.308	3.0
0.378	3.08	3.185	3.3
0.578	4.00	4.08	2.0
0.778	4.87	4.93	1.1
1	5.9	5.9	—

The mean deviation of all tables is 3.63%.

The asymmetrical multivibrator can be treated in the same way, if it is allowed to apply the simplest expression for its frequency, viz.

$$f = \frac{1}{(T_{d1} + T_{d2}) \ln \frac{1 + \gamma}{D + \gamma}} \dots \dots \dots (187)$$

This expression originates from expressions (176) and (177), if k_2/m and k_1/m both are $\gg 1$, and if $\gamma_A = \gamma_B = \gamma$, $D_A = D_B = D$.

Experiments with an asymmetrical multivibrator gave the following results:

- Valve used: EFF 50
- Supply voltage: $V = 225 \text{ V}$
- $R_{1A} = R_{1B} = 10 \text{ k}\Omega$
- $R_{2A} = R_{2B} = 1 \text{ M}\Omega$
- $C_A = 180 \text{ pF}$
- $C_B = 1000 \text{ pF}$
- So: $m = 5.5, k_1 = k_2 = 100$

Results of measured and calculated relative frequencies are given in table 10.

Table 10 F

γ	Measured	Calculated	Deviation %
0	1	1	—
0.089	1.62	1.68	4.0
0.189	2.31	2.22	-4.0
0.356	3.08	3.00	-2.5
0.533	3.85	3.78	-1.8
0.778	5.00	4.80	-4.0
1	5.77	5.77	—

General Survey

Assuming that the internal anode- and grid resistances of the valves used in multivibrator circuits are negligibly small compared with the externally applied resistances, and that the influence of stray capacitances in the valves and the circuit is not yet appreciable, the frequency of the multivibrator signal can be determined in the following way:

A. Graphical method

With a *symmetrical multivibrator* the quantity V_0/V is plotted graphically first according to the equation:

$$\frac{V_0}{V} = \frac{D + \gamma}{x} - \gamma \dots \dots \dots (140)$$

and secondly according to

$$\frac{V_0}{V} = 1 - (1 - D)x^{T_d/T_c} \dots \dots \dots (141)$$

The two curves found in this way always have a point of intersection for $x = 1$, which has no physical significance; but there is another intersection point giving a certain value of x . From this value the frequency can be determined from the following relations:

$$x = e^{-t_1/T_d}$$

$$t_1 = T_d \ln 1/x.$$

The multivibrator period is:

$$T = 2 T_d \ln 1/x.$$

The frequency is:

$$f = \frac{1}{2 T_d \ln 1/x}.$$

The symbols used stand for

- D = ratio of cut-off voltage to H.T. supply voltage
- γ = ratio of grid control voltage to H.T. supply voltage
- T_d = product of grid leak resistance and coupling capacitance
- T_c = product of anode resistance and coupling capacitance
- t_1 = half period of the multivibrator signal

With an *asymmetrical multivibrator* the following graphs are plotted: first, the quantity y as a function of x according to the expression

$$y = \frac{D_B + \gamma B}{1 - (1 - D_B) x^{k_1 m} + \gamma B}, \dots \dots \dots (177)$$

and secondly the quantity x as a function of y according to the expression

$$x = \frac{D_A + \gamma A}{1 - (1 - D_A) y^{k_2/m} + \gamma A} \dots \dots \dots (176)$$

Both curves have always a common point at $x = 1, y = 1$, which has no further significance. The second common point gives certain values for x and y , from which the frequency of the multivibrator signal can be determined by the aid of the following relations:

$$t_1 = T_{d_2} \ln 1/x,$$

$$t_2 = T_{d_1} \ln 1/y.$$

The period is $T = t_1 + t_2$.

The frequency $f = \frac{1}{t_1 + t_2}$.

Significance of symbols used:

D_A = ratio of cut-off voltage of valve A to H.T. supply voltage

D_B = same for valve B

γ_A = ratio of grid control voltage of valve A to H.T. supply voltage

γ_B = same for valve B

$$k_1 = \frac{R_{2B}}{R_{1A}} \quad k_2 = \frac{R_{2A}}{R_{1B}} \quad m = \frac{R_{2A} C_B}{R_{2B} C_A}$$

$$T_{d1} = R_{2B} C_A \quad T_{d2} = R_{2A} C_B$$

B. *Explicit expressions for the frequency*

Symmetrical multivibrator

$$\text{If } \frac{1}{10} \geq D \geq \frac{1}{50} \quad \text{and } \frac{T_d}{T_c} \geq 4,$$

$$\text{then } \frac{V_0}{V} \approx 1.$$

Then expression (140) is simplified to $x = \frac{D + \gamma}{1 + \gamma}$,

from which it is derived that the frequency

$$f = \frac{1}{2T_d \ln \frac{1 + \gamma}{D + \gamma}}$$

Asymmetrical multivibrator

First approximation

$$\text{If } m \ll 1 \text{ and } k_2 \geq 1,$$

$$\text{then } x \approx \frac{D_A + \gamma_A}{1 + \gamma_A}$$

$$y = \frac{D_B + \gamma_B}{1 - (1 - D_B) x^{k_1 m} + \gamma_B}$$

A corresponding case is:

$$m \gg 1 \text{ and } k_1 \geq 1.$$

$$\text{Then: } y \approx \frac{D_B + \gamma_B}{1 + \gamma_B}$$

$$x = \frac{DA + \gamma A}{1 - (1 - DA)y^{k_2/m} + \gamma A}$$

Second approximation

$$\text{If } m \gg 1, k_2 \geq 1 \text{ and} \\ k_1 m \gg 1,$$

$$\text{then } x \approx \frac{DA + \gamma A}{1 + \gamma A}$$

$$y \approx \frac{DB + \gamma B}{1 + \gamma B}$$

Correspondingly, if $m \ll 1$, $k_1 \geq 1$ and

$$k_2/m \gg 1,$$

then again:

$$x \approx \frac{DA + \gamma A}{1 + \gamma A}$$

$$y \approx \frac{DB + \gamma B}{1 + \gamma B}.$$

In all four cases mentioned, the frequency is found from

$$f = \frac{1}{T_{d_2} \ln 1/x + T_{d_1} \ln 1/y}.$$

If, moreover, in the second approximation

$$DA = DB = D \text{ and } \gamma A = \gamma B = \gamma,$$

$$\text{then } x = y = \frac{D + \gamma}{1 + \gamma}$$

$$t_1 = T_{d_2} \ln \frac{1 + \gamma}{D + \gamma}, \quad t_2 = T_{d_1} \ln \frac{1 + \gamma}{D + \gamma};$$

thus the frequency will be:

$$f = \frac{1}{(T_{d_2} + T_{d_1}) \ln \frac{1 + \gamma}{D + \gamma}}.$$

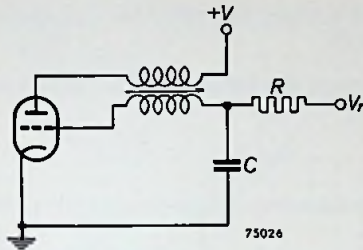


Fig. 90.
Basic circuit of a blocking oscillator.

6.4.1.1.8. The blocking oscillator

The fundamental diagram of a blocking oscillator is given in fig. 90. The frequency of the relaxation signal generated by the blocking oscillator can be expressed in the following way:

$$f = \frac{1}{T_d \ln \frac{a + \gamma}{D + \gamma}}, \quad (188)$$

in which the symbols represent the following:

$T_d = RC =$ time constant of the blocking oscillator

$D = V_{g_c}/V$

$V_{g_c} =$ cut-off grid voltage of the valve

$V =$ H.T. supply voltage

$\gamma = V_r/V$

$V_r =$ control voltage applied to the grid of the valve

$a =$ a quantity dependent on the transformer construction and properties

a is a measure for the transformation of anode voltage variations into corresponding grid voltage variations.

The quantity a can best be determined experimentally. In the same way as described for the multivibrator circuits, the frequency f_0 for $\gamma = 0$ and f_1 for $\gamma = 1$ should be measured. From these two values, with the aid of expression (188), the quantities a and D are derived.

A practical example will be given. From a pentode EF 50, the combination cathode, first and second grids was used as a triode blocking oscillator according to fig. 90. The anode was kept at a constant voltage of 100 V. The H.T. supply voltage was 160 V, the grid leak resistance $R = 100 \text{ k}\Omega$, the grid capacitor $C = 2100 \text{ pF}$. At a control voltage $V_r = 0$ ($\gamma = 0$), a frequency $f_0 = 2058 \text{ c/s}$, and at $V_r = V = 160 \text{ V}$ ($\gamma = 1$), a frequency $f_1 = 31500 \text{ c/s}$ was measured.

From these values the quantities D and a were calculated.

$D = 0.018, a = 0.182.$

Substituting these values in expression (188) gave to a good approximation the measured frequency values as a function of the control voltage (or γ). Table 11 gives the frequency variation with γ (control volt-

age V_r) in the second column as measured and in the third as calculated from (188).

The fourth column represents the percentage deviation of the calculated from the measured values of the frequency.

Table 11

γ	Frequency		Deviation %
	measured	calculated	
0	2058	—	—
0,172	7788	7640	-1.8
0,281	11160	10900	-2.2
0,406	14767	14500	-1.6
0,625	20864	20900	+0.1
0,750	24430	24600	+0.6
0,875	27570	28000	+1.5
1	31500	—	—

6.4.1.1.9. Comparison of the multivibrator and the blocking oscillator

As already pointed out earlier, the frequency of a multivibrator can under some assumptions, which are generally in agreement with practical conditions, be represented by the expression

$$f = \frac{1}{(T_{d2} + T_{d1}) \ln \frac{1 + \gamma}{D + \gamma}} \dots \dots \dots (187)$$

if the two valves A and B are identical, so that $D_A = D_B = D$, and moreover, $V_{rA} = V_{rB}$, so that $\gamma_A = \gamma_B = \gamma$. For a symmetrical multivibrator, $T_{d1} = T_{d2} = T_d$, which gives an expression for the frequency

$$f = \frac{1}{2T_d \ln \frac{1 + \gamma}{D + \gamma}} \dots \dots \dots (148)$$

The quantity γ determines the variation of the frequency as a function of the control voltage. This function can be given as:

$$f(\gamma) = \frac{1}{\ln \frac{1 + \gamma}{D + \gamma}} \dots \dots \dots (189)$$

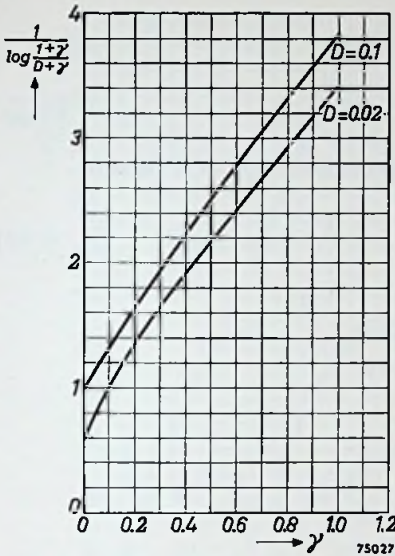


Fig. 91.

Graphical representation of the function which determines the dependency of the frequency of a symmetrical multivibrator on the grid control voltage.

f_0 for $\gamma = 0$. From (187) and (148) it follows that:

$$F = \frac{\log 1/D}{\log \frac{1+\gamma}{D+\gamma}} \dots (191)$$

This relative frequency is graphically represented in fig. 92 for two different values of D , viz. $D = 0.1$ and $D = 0.02$.

The maximum frequency variation increases with decreasing D . From both figs. 91 and 92 it can be seen that the frequency varies with the control voltage nearly as a linear function. Therefore, in many practical cases, the graphs of fig. 91 can be approximated by straight lines drawn through the lowest value

$\frac{1}{\log 1/D}$ at $\gamma = 0$ and the highest value

which now will be more closely examined. Fig. 91 represents a graph of the expression $\frac{1}{\log \frac{1+\gamma}{D+\gamma}}$, from which $f(\gamma)$ can be calculated as:

$$f(\gamma) = \frac{1}{2.303 \log \frac{1+\gamma}{D+\gamma}} \dots (190)$$

In order to obtain an idea of the maximum possible frequency variation when γ varies from zero to unity, it is advantageous to introduce again a relative frequency F , that is the ratio of the frequency f to the frequency

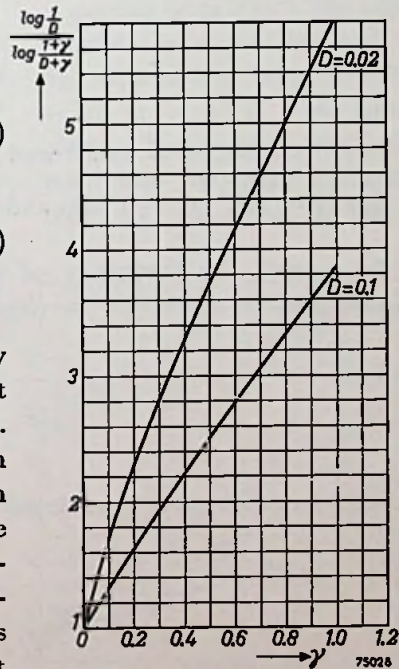


Fig. 92.

Same as fig. 91, but all values expressed relative to the value for zero abscissa.

$$\frac{1}{\log \frac{1}{1+D}} \text{ at } \gamma = 1.$$

The linear function, replacing the expression (190), will then be

$$F(\gamma) = \frac{1}{2.303} \left(\frac{1}{\log \frac{1}{1+D}} - \frac{1}{\log \frac{1}{D}} \right) (\gamma + \gamma_0), \dots (192)$$

in which the constant γ_0 is determined by:

$$F(0) = \frac{1}{2.303 \log \frac{1}{D}} = \frac{1}{2.303} \gamma_0 \left(\frac{1}{\log \frac{1}{1+D}} - \frac{1}{\log \frac{1}{D}} \right),$$

$$\text{or: } \gamma_0 = \frac{1}{\frac{\log \frac{1}{D}}{\log \frac{1}{1+D}} - 1} \dots (193)$$

For $D = 0.02$, $\gamma_0 = 1/4.83$ and $F(\gamma) = 1.225 (\gamma + 0.21)$.

For $D = 0.1$, $\gamma_0 = 1/2.85$ and $F(\gamma) = 1.237 (\gamma + 0.35)$.

In general, the frequency of an asymmetrical multivibrator varies approximately according to expressions (187) and (192) as follows:

$$f = \frac{1}{T_{d_2} + T_{d_1}} \left(\frac{1}{\ln \frac{2}{1+D}} - \frac{1}{\ln \frac{1}{D}} \right) (\gamma + \gamma_0), \dots (194)$$

and the frequency of a symmetrical multivibrator is approximately given by

$$f = \frac{1}{2T_d} \left(\frac{1}{\ln \frac{2}{1+D}} - \frac{1}{\ln \frac{1}{D}} \right) (\gamma + \gamma_0) \dots (195)$$

γ_0 is given by expression (193).

The frequency of a blocking oscillator is given by expression (188). The dependence on the control voltage is contained in the factor

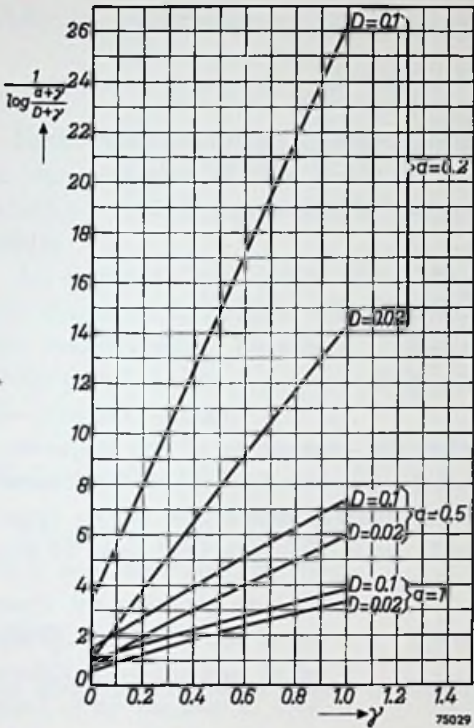


Fig. 93.

Same graphs as in fig. 91, but valid for the blocking oscillator for different blocking transformer properties (parameter a).

$$f(\gamma) = \frac{1}{\ln \frac{a + \gamma}{D + \gamma}} \quad (196)$$

Fig. 93 gives an impression of the shape of this function, as it represents the function

$$\frac{1}{\log \frac{a + \gamma}{D + \gamma}} \quad (= 2.303 f(\gamma))$$

with the quantities a and D as parameters.

For the same reason as already mentioned with the multivibrator, viz. to obtain an idea of the maximum attainable frequency variation with γ varying from 0 to 1, the same function is again depicted in fig. 94, but now relative to its value at $\gamma = 0$. This figure clearly demonstrates that the maximum frequency variation increases with both D and a

decreasing. For $a = 1$ the same function arises as was found for the multivibrator. As in practice a will generally be smaller than unity, the maximum frequency variation of the blocking oscillator will usually be greater than that of the multivibrator. Figs. 93 and 94 show that the frequency variation with control voltage is nearly linear, as was the case with the multivibrator. Therefore it can be represented in analogy with expressions

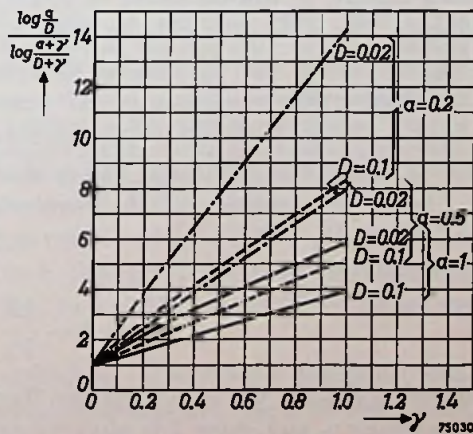


Fig. 94.

Same as fig. 93, but with relative values as in fig. 92.

(194) and (195) by the following linear function:

$$f = \frac{1}{T_d} \left(\frac{1}{\ln \frac{a+1}{D+1}} - \frac{1}{\ln \frac{a}{D}} \right) (\gamma + \gamma_0), \dots (197)$$

in which:

$$\gamma_0 = \frac{1}{\frac{\log \frac{a}{D}}{\log \frac{a+1}{D+1}} - 1} \dots (198)$$

In conclusion, it can be stated that the dependence of the frequency of the two types of relaxation oscillator, represented by the multivibrator and the blocking oscillator, on a control voltage supplied to one or more of the control grids of the valves used, can in most practical cases be expressed as a linear function:

$$f = a (\gamma + \gamma_0) \dots (199)$$

The factor a is inversely proportional to a time constant contained in the circuit.

6.4.2. STATIC CONDITIONS OF THE AUTOMATIC PHASE CONTROL

In order to investigate the mechanism of automatic phase control more closely, it will be useful to distinguish two stages of the regulating process. The regulation may be either in a static condition, the relaxation frequency being exactly equal to the synchronizing frequency, or a sudden disturbance may cause one of the quantities to change, which will bring about a change from one static condition to another via a transient condition. The static conditions will be dealt with first.

The static condition of the regulation process is given by eqs. (105) and (106). Eq. (106) may be rewritten by dividing both members by V_b , which gives:

$$\frac{V_c}{V_b} = 1 - \frac{IR}{V_b} \cdot \tau f_{\text{sync}}, \dots (106a)$$

in which f_{sync} is the synchronizing frequency. The ratio V_c/V_b has been denoted by γ , and since I is obviously proportional to V_b , the term IR/V_b may be replaced by a constant ζ , so that eq. (106a) becomes:

$$\gamma = 1 - \zeta f_{\text{sync}} \tau, \dots (106b)$$

whilst eq. (105) was:

$$f = \frac{k}{T_d} \cdot (\gamma + \gamma_0) \dots \dots \dots (105)$$

In the static condition f_{sync} is obviously equal to the relaxation frequency f . A representation of this condition is given in the graph of fig. 95, in which eq. (105) is represented by the straight line 1 and eq. (106b) by the line 2.

According to eq. (105), when the synchronizing frequency is f_{sync} , the relaxation frequency will adjust itself to point *A* of the line 1 at which the corresponding (relative) control voltage is γ_A . According to eq. (106b) and the line 2, a phase difference τ_A corresponds to this value of the control voltage.

Variation of the time constant

When the time constant T_d is now decreased, for example by reducing the grid leak R , eq. (105) will be represented by the line *1a* instead of by the line 1. After having passed through the transient stage of the regulation, the relaxation frequency finally reaches another static condition at $f = f_{sync}$, as represented by point *B* of the line *1a*. The phase difference corresponding to this point is τ_B .

The frequency f of the relaxation signal is thus maintained at the synchronizing frequency, but this involves a change of the phase relation between the two signals. This is manifest in a displacement of the image on the screen of the picture tube.

Such a displacement is in fact typical for a time-base generator with automatic phase control. Unless special measures are taken to counteract this effect, the image is displaced horizontally over the screen when the horizontal frequency control of a television receiver equipped with such a generator is operated. This displacement may be possible within wide limits,

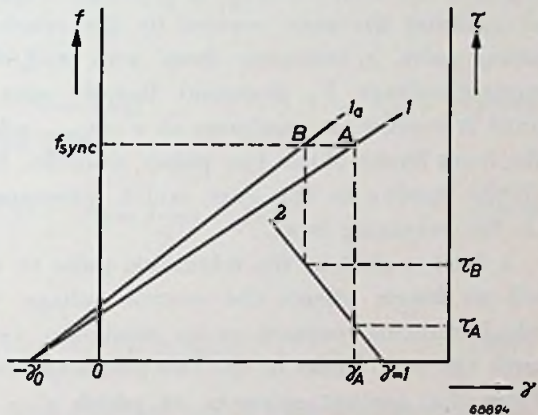


Fig. 95.

Representation of automatic phase control. The line 1 represents the frequency of the relaxation signal as a function of the relative control voltage γ ; the line 1a applies to a different (smaller) time constant of the relaxation oscillator. The line 2 represents the phase difference α between the relaxation and synchronizing signals as a function of the relative control voltage.

of τ has been represented in a graph similar to that of fig. 95.

Assume the normal adjustment of the relaxation oscillator to be situated at point A , to which the (relative) control voltage γ_1 and the phase difference τ_1 correspond. It is obvious that the time-constant T_d can be varied within the retaining zone, i.e. within the limits corresponding to the lines $1a$ and $1b$, without synchronization being disturbed. The corresponding values of T_d , which will be denoted by T_{da} and T_{db} , are then given by eq. (105), viz.

$$f = f_{\text{sync}} = \frac{k}{T_{da}} \cdot (1 + \gamma_0) \cdot \dots \dots \dots (105a)$$

and

$$f = f_{\text{sync}} = \frac{k}{T_{db}} \cdot (\gamma_2 + \gamma_0) \cdot \dots \dots \dots (105b)$$

whilst, according to eq. (106b):

$$\gamma_2 = 1 - \zeta t_{\text{sync}} f_{\text{sync}} \cdot \dots \dots \dots (106c)$$

Hence, from eqs. (105b) and (106c):

$$T_{db} = \frac{k}{f_{\text{sync}}} \cdot (1 - \zeta t_{\text{sync}} f_{\text{sync}} + \gamma_0) \cdot \dots \dots \dots (200)$$

and from eq. (105a):

$$T_{da} = \frac{k}{f_{\text{sync}}} \cdot (1 + \gamma_0) \cdot \dots \dots \dots (201)$$

The range within which the time constant can be varied without the retaining zone being exceeded, i.e. without the synchronization being upset, is therefore:

$$\Delta T_d = T_{da} - T_{db} = k \zeta t_{\text{sync}} \cdot \dots \dots \dots (202)$$

The values which k and ζ assume in practice will as a rule not differ considerably from unity, so that ΔT_d is approximately equal to t_{sync} . In other words, the retaining zone will be so situated that a certain variation of the time constant of the relaxation oscillator is possible without risk of its frequency being no longer governed by the synchronization, the permissible variation being of the same order as the width of the synchronizing pulses applied to the phase detector.

In fig. 96 it was assumed that the relaxation pulses are wider than the synchronizing pulses, which is generally the case in practice. When, however, t_0 is smaller than t_{sync} , the values $\tau = t_0$ and $\tau = t_{\text{sync}}$ in fig. 97 are interchanged, and eq. (202) becomes:

$$\Delta T_d = k \zeta t_0 \cdot \dots \dots \dots (202a)$$

Variation of the synchronizing frequency

In the previous section a representation was given of the static condition and the retaining zone for the case in which the time constant T_d of the relaxation oscillator is changed. It will now be investigated how a relaxation oscillator with automatic phase control responds to variations of the synchronizing frequency. The graphic representation corresponding to that of fig. 97 then becomes as depicted in fig. 98.

Assume point A to be the normal adjustment of the relaxation frequency at a synchronizing frequency f_{sync} , eq. (106b) being represented by the curve 2. The (relative) control voltage is then γ_A and the corresponding phase difference is τ_A .

When the synchronizing frequency is decreased to the value f_{sync1} , eq. (106b) will be represented by the curve 2a instead of 2. This is a boundary case, viz. the lower limit of the retaining zone, at which $\gamma = \gamma_1$ and $\tau = t_{sync}$.

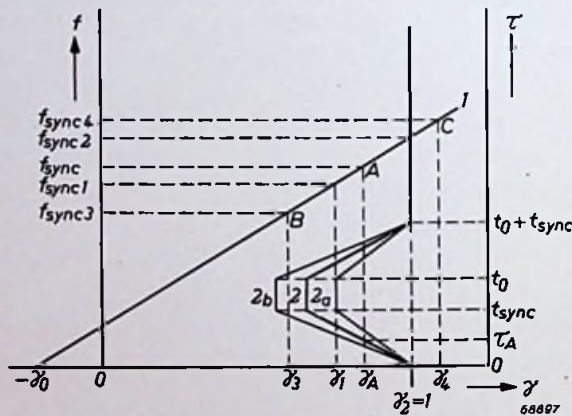


Fig. 98.

Representation similar to that of fig. 97, showing the influence of a variation of the synchronizing frequency on a relaxation oscillator with automatic phase control.

When, on the other hand, the synchronizing frequency is raised to the value f_{sync2} , the representation of eq. (106b) will be as shown by curve 2b, i.e. the upper limit of the retaining zone at which $\gamma = \gamma_2 = 1$ and $\tau = 0$.

The synchronizing frequencies f_{sync3} and f_{sync4} , which lie beyond the retaining zone, correspond to the points B and C on the line l , at which the (relative) control voltages are γ_3 and γ_4 respectively. It is obvious that these control voltages cannot be supplied by the automatic phase control unless γ_3 and γ_4 correspond to real values of τ situated respectively on curves 2 located to the right of curve 2a and to the left of curve 2b. This proves to be impossible, the retaining zone being situated between the synchronizing

frequencies f_{sync1} and f_{sync2} to which the curves 2a and 2b correspond.

The values of f_{sync1} and f_{sync2} can be calculated as follows. From eq. (105):

$$f_{\text{sync2}} = \frac{k}{T_d} \cdot (1 + \gamma_0) \dots \dots \dots (105c)$$

and

$$f_{\text{sync1}} = \frac{k}{T_d} \cdot (\gamma_1 + \gamma_0) \dots \dots \dots (105d)$$

According to eq. (106b):

$$\gamma_1 = 1 - \zeta t_{\text{sync}} f_{\text{sync1}} \dots \dots \dots (106d)$$

Hence, from eqs. (105d) and (106d):

$$f_{\text{sync1}} = \frac{k}{T_d} \cdot \frac{1 + \gamma_0}{1 + \frac{k}{T_d} \cdot \zeta t_{\text{sync}}} \dots \dots \dots (203)$$

and from eqs. (105c) and (203):

$$\Delta f_{\text{sync}} = f_{\text{sync2}} - f_{\text{sync1}} = \frac{k}{T_d} \cdot (1 + \gamma_0) \cdot \frac{k\zeta \cdot \frac{t_{\text{sync}}}{T_d}}{1 + k\zeta \cdot \frac{t_{\text{sync}}}{T_d}} \dots \dots (204)$$

T_d is of the same order of magnitude as the periodic time T of the synchronizing pulses. The width of these pulses is roughly one tenth of T . t_{sync} is the duration of the pulses which are derived from the synchronizing pulses, for example, by differentiation, and are applied to one of the control grids of the phase detector. As a rule t_{sync} will therefore be even smaller than $0.1 T$. As already stated, k and ζ are approximately equal to unity, so that eq. (204) may be simplified to:

$$\Delta f_{\text{sync}} \approx \frac{k}{T_d} \cdot (1 + \gamma_0) \cdot \frac{t_{\text{sync}}}{T} \dots \dots \dots (205)$$

From eqs. (205) and (105c):

$$\frac{\Delta f_{\text{sync}}}{f_{\text{sync2}}} \approx \frac{t_{\text{sync}}}{T} \dots \dots \dots (206)$$

Eq. (206) signifies that the synchronizing signals will maintain control of the relaxation signals so long as the relative frequency range within which the synchronizing signals fluctuate does not exceed the ratio of the duration of the synchronizing pulses at the grid of the phase detector to the periodic time of the synchronizing signals.

The above comments apply to the case in which t_0 is larger than t_{sync} . If t_0 is smaller than t_{sync} , eq. (206) becomes:

$$\frac{\Delta f_{sync}}{f_{sync2}} = \frac{t_0}{T} \dots \dots \dots (206a)$$

6.4.3. TRANSIENT CONDITIONS OF THE AUTOMATIC PHASE CONTROL

Three quantities are interrelated by the automatic phase control, viz. the frequency of the relaxation oscillator to be synchronized, the phase relation of the relaxation pulses to the synchronizing pulses, and the control voltage supplied by the phase detector.

In the static condition the relaxation frequency is equal to the synchronizing frequency, so that, for determining the three quantities, only two more equations suffice. Recapitulating, the following three equations are valid in the static condition:

$$f = f_{sync}, \dots \dots \dots (207)$$

$$f = \frac{k}{T_d} \cdot (\gamma + \gamma_0), \dots \dots \dots (105)$$

and:

$$\gamma = 1 - \zeta f_{sync} \tau \dots \dots \dots (106b)$$

γ and τ are expressed in known quantities, viz.

$$\gamma = f_{sync} \cdot \frac{T_d}{k} - \gamma_0, \dots \dots \dots (208)$$

and:

$$\tau = \frac{1 + \gamma_0}{\zeta f_{sync}} - \frac{T_d}{\zeta k} \dots \dots \dots (209)$$

When the static condition comes to an end owing to a disturbance by which, for example, f_{sync} or T_d are changed, the three above-mentioned quantities vary with time and the control system passes, via the transient condition, to a new static condition.

During this transient condition the three static equations (207), (105) and (106b) are no longer valid in their entirety. Eq. (105) remains valid since there is no noticeable variation of the control voltage within the periodic time of the relaxation voltage because of the large time constant of the filter circuit. Eq. (207), however, becomes void and eq. (106b) assumes a more complex form.

To determine the new form of eq. (106b), the term $\zeta f_{sync} \tau$ will be examined more closely. ζ represents the ratio IR/V_b , where I is the

amplitude of the anode-current pulse of the phase detector and R is the load resistance of this valve. The product $I f_{\text{sync}} \tau$ is the mean value of the anode-current pulses, assuming these to have a constant frequency f_{sync} and a constant width τ . This mean anode-current flows through the load resistance R shunted by a capacitance C . In the static condition the mean value of the voltage across the network of the R and C connected in parallel is calculated by simply multiplying the mean current by R , i.e. the D.C. impedance of the RC network.

When the mean value of the anode current is subject to fluctuations, for example owing to variations of f_{sync} or of τ , the mean value of the voltage across the RC network is found by multiplying the mean current by the operational impedance of this network instead of by its D.C. impedance R .

For an R and C connected in parallel, this operational impedance is given by:

$$Z(p) = \frac{R}{1 + RCp}, \dots \dots \dots (210)$$

in which p is the symbol for a differentiation with respect to time. For the deduction of this expression see Appendix II, p. 146.

In the transient condition the mean value of the voltage across the RC network is therefore:

$$\bar{V} = \frac{R}{1 + RCp} \left[I \tau f_{\text{sync}} \right], \dots \dots \dots (211)$$

instead of $R I \tau f_{\text{sync}}$ in the static condition. The square brackets indicate that the differential operator (210) must be applied to the quantity within these brackets, this quantity being a function of time.

The change to which eq. (106b), valid for the static condition, is subject, thus amounts to the replacement of the impedance R by the operational impedance (210), so that eq. (106b) now becomes:

$$\gamma = 1 - \frac{\zeta}{1 + RCp} \left[\tau f_{\text{sync}} \right], \dots \dots \dots (212)$$

I being assumed to be constant.

It is now necessary to find a third relation between the three variable quantities, which enables two variables to be eliminated from the three equations. In this way one equation with one unknown remains, viz. a differential equation the solution of which gives the variation of the unknown as a function of time. The two remaining unknowns can then

be solved from the two other equations. In the solution of the differential equation the integration constants will have to be determined from the initial and final conditions to which the static equations apply.

The third dynamic equation is given by the relation consisting between the phase difference τ and the frequency difference $f - f_{sync}$. When the frequency of the relaxation voltage is equal to that of the synchronizing signal, τ is obviously constant, but when f varies with time, τ also changes. The relation between these variations may be determined as follows.

In fig. 62 the width of the anode current pulses (fig. 62c) of the phase detector, which is a measure of the phase difference between the relaxation and synchronizing signals, is determined by the rear flank of the synchronizing pulses and the front flank of the relaxation pulses. In fig. 99 these flanks have been merely indicated as reference points on the time axis.

The arrow heads pointing upwards represent the rear flanks of the synchronizing pulses, and those pointing downwards the front flanks of the relaxation pulses. The positions of these arrow heads are fixed by the points at which the descending lines of the two sinusoidal curves S_1 and S_2 pass through zero. These sine functions have the same frequency as the syn-

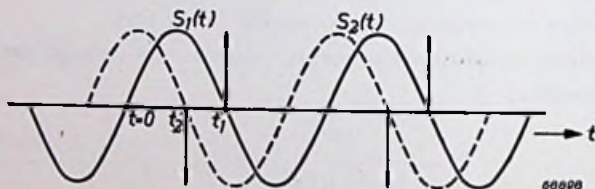


Fig. 99.

Auxiliary sine functions $S_1(t)$ and $S_2(t)$ for calculating the phase difference $\tau = t_1 - t_2$ between two pulsatory signals. The arrow heads pointing upwards represent the rear flanks of the synchronizing pulses and those pointing downwards the front flanks of the relaxation pulses.

chronizing and relaxation pulses respectively. The zero point $t = 0$ of the time axis has been so fixed that the synchronizing pulses are determined by the sine function:

$$S_1(t) = \sin(2\pi f_{sync}t), \quad \dots \dots \dots (213)$$

whilst the relaxation pulses are assumed to be determined by a sinusoidal curve shifted in phase, viz.

$$S_2(t) = \sin(2\pi ft + \varphi) \dots \dots \dots (214)$$

The first point beyond $t = 0$ at which S_1 passes through zero is at $t = t_1$. This point is given by the condition:

$$2\pi f_{\text{sync}} t_1 = \pi,$$

whence:

$$t_1 = \frac{1}{2 f_{\text{sync}}} \dots \dots \dots (215)$$

Similarly, the first point at which S_2 passes through zero is at $t = t_2$, this being given by the expression:

$$2\pi f t_2 + \varphi = \pi,$$

whence:

$$t_2 = \frac{1}{2f} - \frac{\varphi}{2\pi f} \dots \dots \dots (216)$$

In the static conditions, $f = f_{\text{sync}}$, so that from eqs. (215) and (216):

$$t_1 - t_2 = \frac{\varphi}{2\pi f_{\text{sync}}},$$

or, since $t_1 - t_2$ corresponds to the phase difference τ in fig. 162:

$$\tau = \frac{\varphi}{2\pi f_{\text{sync}}} \dots \dots \dots (217)$$

When f differs from f_{sync} , φ changes according to the expression:

$$\frac{d\varphi}{dt} = 2\pi (f - f_{\text{sync}}), \dots \dots \dots (218)$$

so that τ from eq. (217) also changes with time, which gives:

$$\frac{d\tau}{dt} = \frac{f - f_{\text{sync}}}{f_{\text{sync}}} \dots \dots \dots (219)$$

This is the third equation, which determines the transient condition of the regulation. Recapitulating, the three equations by which this condition is completely determined, are:

$$f = \frac{k}{T_d} (\gamma + \gamma_0) \dots \dots \dots (105)$$

$$\gamma = 1 - \frac{\zeta}{1 + RC_p} \left[\tau f_{\text{sync}} \right], \dots \dots \dots (212)$$

and

$$p\tau = \frac{f - f_{\text{sync}}}{f_{\text{sync}}}, \dots \dots \dots (220)$$

in which p stands again for d/dt , i.e. differentiation with respect to time.

When γ and f are eliminated from these equations, a differential equation with respect to τ remains, viz.

$$\frac{d^2\tau}{dt^2} + \frac{1}{RC} \cdot \frac{d\tau}{dt} + \frac{k\zeta}{T_d RC} \cdot \tau = \frac{k}{T_d RC} \cdot \frac{1 + \gamma_0}{f_{sync}} - \frac{1}{RC} \quad \dots (221)$$

6.4.3.1. Influence of disturbances

The influence of various disturbances can now be investigated. The two principal possibilities will be dealt with below.

First the variation of τ will be investigated when at the instant $t = 0$ a sudden change of the time constant T_d of the relaxation oscillator takes place. It will be assumed that at $t < 0$ the time constant had the constant value T_{d1} , so that the static equations apply, viz.

$$\left. \begin{aligned} f &= f_{sync} \\ f &= \frac{k}{T_{d1}} \cdot (\gamma_1 + \gamma_0) \\ \gamma_1 &= 1 - \zeta f_{sync} \tau_1 \end{aligned} \right\} \dots \dots \dots (222)$$

When at the instant $t = 0$ the time constant suddenly changes from T_{d1} to the value T_{d2} and maintains this value for all times beyond $t = 0$, a new static condition is reached theoretically after an infinitely long time, the three following equations then being valid:

$$\left. \begin{aligned} f &= f_{sync} \\ f &= \frac{k}{T_{d2}} \cdot (\gamma_2 + \gamma_0) \\ \gamma_2 &= 1 - \zeta f_{sync} \tau_2 \end{aligned} \right\} \dots \dots \dots (223)$$

The initial and final conditions are fixed by eqs. (222) and (223). The variation of τ (and thus also of f and γ) beyond the instant $t = 0$ is now determined by the differential equation (221), which can be solved by substituting for τ the following expression:

$$\tau = Ke^{qt} + \frac{1 + \gamma_0}{\zeta f_{sync}} - \frac{T_{d2}}{k\zeta} \dots \dots \dots (224)$$

In the differential equation (221), which is valid for $t > 0$, the value of T_{d2} must now be substituted for T_d . From eqs. (224) and (221):

$$q^2 + \frac{1}{RC} \cdot q + \frac{k\zeta}{T_{d2}RC} = 0, \dots \dots \dots (225)$$

from which q can be solved. There are two roots, viz.

$$q_1 = -\frac{1}{2RC} + \sqrt{\frac{1}{4(RC)^2} - \frac{k\zeta}{T_{d_2}RC}}, \dots \dots \dots (226)$$

and

$$q_2 = -\frac{1}{2RC} - \sqrt{\frac{1}{4(RC)^2} - \frac{k\zeta}{T_{d_2}RC}}, \dots \dots \dots (227)$$

Combined with eq. (224) this gives the general solution:

$$\tau = K_1 e^{q_1 t} + K_2 e^{q_2 t} + \tau_2, \dots \dots \dots (228)$$

in which:

$$\tau_2 = \frac{1 + \gamma_0}{\zeta f_{sync}} - \frac{T_{d_2}}{k\zeta}, \dots \dots \dots (229)$$

i.e. the value assumed by the phase difference after an infinitely long time. This is in agreement with the conditions (223) which apply to the final static condition.

The frequency f is given by eqs. (228) and (220):

$$\frac{f - f_{sync}}{f_{sync}} = K_1 q_1 e^{q_1 t} + K_2 q_2 e^{q_2 t} \dots \dots \dots (230)$$

For an infinitely long time, f becomes equal to f_{sync} , which is again in agreement with eqs. (223).

The relative control voltage γ is calculated from eqs. (230) and (105):

$$\gamma + \gamma_0 = \frac{T_{d_2} f_{sync}}{k} \cdot (1 + K_1 q_1 e^{q_1 t} + K_2 q_2 e^{q_2 t}), \dots \dots \dots (231)$$

which, for an infinitely long time is once again in agreement with eqs. (223).

The integration constants K_1 and K_2 can be determined from the consideration that, at $t = 0$, τ is continuous (cf. eq. (220)), whilst γ is continuous owing to the integrating action of the filter circuit (cf. eq. (212)).

For $t = 0$, according to eq. (209):

$$\tau = \tau_1 = \frac{1 + \gamma_0}{\zeta f_{sync}} - \frac{T_{d_1}}{k\zeta}, \dots \dots \dots (232)$$

whilst, according to eq. (228):

$$\tau_1 = K_1 + K_2 + \tau_2,$$

which gives:

$$K_1 + K_2 = \tau_1 - \tau_2 \dots \dots \dots (233)$$

For $t = 0$, according to eq. (208):

$$\gamma + \gamma_0 = \gamma_1 + \gamma_0 = \frac{T_{d_1} f_{sync}}{k}, \dots \dots \dots (234)$$

whilst, according to eq. (231):

$$\gamma_1 + \gamma_0 = \frac{T_{d2} f_{sync}}{k} (1 + q_1 K_1 + q_2 K_2),$$

or

$$q_1 K_1 + q_2 K_2 = \frac{k}{T_{d2} f_{sync}} \cdot (\gamma_1 + \gamma_0) - 1 = \frac{\gamma_1 + \gamma_0}{\gamma_2 + \gamma_0} - 1 = \frac{\gamma_1 - \gamma_2}{\gamma_2 + \gamma_0}. \quad (235)$$

From eqs. (233) and (235):

$$K_1 = \frac{-q_2(\tau_1 - \tau_2) + \frac{\gamma_1 - \gamma_2}{\gamma_2 + \gamma_0}}{q_1 - q_2}, \dots \dots \dots (236)$$

and:

$$K_2 = \frac{q_1(\tau_1 - \tau_2) - \frac{\gamma_1 - \gamma_2}{\gamma_2 + \gamma_0}}{q_1 - q_2} \dots \dots \dots (237)$$

Now:

$$\tau_1 - \tau_2 = \frac{1}{k\zeta} \cdot (T_{d2} - T_{d1}),$$

in which $T_{d2} - T_{d1}$ is the surge of T_d at the instant $t = 0$. When this is represented by ΔT_d , then:

$$\tau_1 - \tau_2 = \frac{\Delta T_d}{k\zeta} \dots \dots \dots (238)$$

Furthermore:

$$\frac{\gamma_1 - \gamma_2}{\gamma_2 + \gamma_0} = -\frac{\Delta T_d}{T_{d2}} \dots \dots \dots (239)$$

By means of eqs. (238) and (239) K_1 and K_2 may therefore also be expressed by:

$$K_1 = \frac{-q_2 \cdot \frac{\Delta T_d}{k\zeta} - \frac{\Delta T_d}{T_{d2}}}{q_1 - q_2} \dots \dots \dots (240)$$

and:

$$K_2 = \frac{q_1 \cdot \frac{\Delta T_d}{k\zeta} + \frac{\Delta T_d}{T_{d2}}}{q_1 - q_2} \dots \dots \dots (241)$$

As a second case of a disturbance in the regulating system, the influence of a sudden variation of the synchronizing frequency will be in-

vestigated. At all times prior to $t = 0$, the synchronizing frequency is assumed to be $f_{\text{sync}1}$; at the instant $t = 0$ the synchronizing frequency suddenly changes from $f_{\text{sync}1}$ to $f_{\text{sync}2}$ and remains constant at the latter value for all times beyond $t = 0$. In a similar way as in the previous case the following final results are obtained:

$$\tau = K_1 e^{q_1 t} + K_2 e^{q_2 t} + \tau_2, \dots \dots \dots (242)$$

in which τ_2 now is:

$$\tau_2 = \frac{1 + \gamma_0}{\zeta f_{\text{sync}2}} - \frac{T_d}{\zeta k},$$

whilst:

$$\frac{f - f_{\text{sync}2}}{f_{\text{sync}2}} = K_1 q_1 e^{q_1 t} + K_2 q_2 e^{q_2 t}, \dots \dots \dots (243)$$

$$\gamma + \gamma_0 = \frac{T_d f_{\text{sync}2}}{k} \cdot (1 + K_1 q_1 e^{q_1 t} + K_2 q_2 e^{q_2 t}), \dots \dots \dots (244)$$

$$K_1 = \frac{-q_2(1 + \gamma_0) \cdot \frac{\Delta f_{\text{sync}}}{\zeta f_{\text{sync}1} f_{\text{sync}2}} - \frac{\Delta f_{\text{sync}}}{f_{\text{sync}2}}}{q_1 - q_2}, \dots \dots \dots (245)$$

and:

$$K_2 = \frac{q_1(1 + \gamma_0) \cdot \frac{\Delta f_{\text{sync}}}{\zeta f_{\text{sync}1} f_{\text{sync}2}} + \frac{\Delta f_{\text{sync}}}{f_{\text{sync}2}}}{q_1 - q_2}, \dots \dots \dots (246)$$

in which Δf_{sync} represents the surge $f_{\text{sync}2} - f_{\text{sync}1}$ of the synchronizing frequency and q_1 and q_2 are the roots of the characteristic equation (225), which are represented by eqs. (226) and (227). In this case T_{d2} can be replaced by T_d , because this quantity is now assumed to remain constant at $t = 0$.

It will be useful to investigate more closely the roots q_1 and q_2 of eq. (225), as they largely determine the transient phenomenon. According to eqs. (226) and (227) there is a possibility of q_1 and q_2 becoming complex, namely when the term under the root sign is negative. This will be the case when:

$$\frac{1}{4RC} < \frac{k\zeta}{T_d} \cdot \dots \dots \dots (247)$$

After the occurrence of a disturbance in the regulation, τ then varies as a damped oscillation, the angular frequency of which is given by:

$$\omega = \sqrt{\frac{k\zeta}{T_d RC} - \frac{1}{4(RC)^2}} \dots \dots \dots (248)$$

Such a disturbance will be manifest in an undulation of the vertical edges of the picture. Disturbance of the control voltage of the relaxation oscillator is often caused by disturbances such as the equalizing pulses broadcast during the frame blanking and synchronizing signals. The damped oscillatory variation of the phase disturbance will then distort the picture as shown in fig. 100 if the condition given by eq. (247) is satisfied.

When, on the other hand, the condition

$$\frac{1}{4RC} \geq \frac{k\zeta}{T_d} \dots \dots \dots (249)$$

is satisfied, the roots q_1 and q_2 of eq. (225) will be real, and the variation of the phase difference τ resulting from a disturbance will be damped aperiodically. A television picture suffering from interference by the equalizing pulses will then assume a form as shown in fig. 101.

If this interference cannot be eliminated, the distorted picture of fig. 101 will be preferred to that of fig. 100, so that, generally speaking, an endeavour will be made to satisfy eq. (249).



Fig. 100.

Distortion of a television picture as caused by equalizing pulses when in a line time-base generator with automatic phase control the condition of eq. (247) is satisfied.

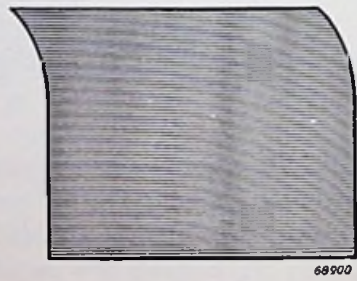


Fig. 101.

As fig. 100, but when the condition of eq. (249) applies.

As pointed out previously, k and ζ will not differ considerably from unity, so that eq. (249) may be simplified to:

$$RC \leq \frac{1}{4} T_d \dots \dots \dots (249a)$$

The condition of eq. (249a), however, conflicts with the requirements

imposed on efficient smoothing of the control voltage, since the periodic time of the current pulses from which this control voltage is derived in the RC network is equal to the periodic time of the synchronizing pulses, whilst the time constant T_d is of the same order of magnitude.

6.4.3.2. Use of a special smoothing filter

It is obvious that, when the control voltage contains excessive pulsatory components, the frequency of which is equal to that of the synchronizing pulses, there is a risk of the time-base generator being synchronized direct by these components, so that automatic phase control is out of question. It will therefore be impossible to obtain the aperiodic regulation aimed at by means of a simple RC smoothing filter, and it will be necessary to use a more complicated filter, which does permit such regulation.

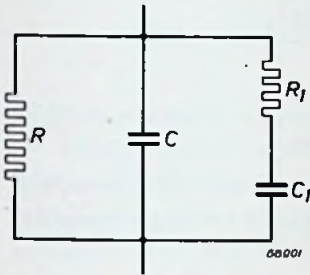


Fig. 102.

Improved filter circuit across which the voltage for the automatic phase control is produced.

This filter may be as depicted in fig. 102. The formulae which determine the transient condition of the automatic phase control are now changed, in so far as the operational impedance given by eq. (210) must be replaced by a different expression. As a result only eq. (212) is modified.

The operational impedance of the filter shown in fig. 102 is given by:

$$Z(p) = R \frac{1 + R_1 C_1 p}{1 + (C_1 R + C_1 R_1 + CR)p + C_1 R_1 C R p^2} \dots (250)$$

By substitution of

$$R_1 = nR, \dots (251)$$

$$C_1 = mC \dots (252)$$

and

$$RC = x, \dots (253)$$

eq. (250) becomes:

$$Z(p) = \frac{1 + nmxp}{1 + (1 + m + nm)xp + nm x^2 p^2} \dots (254)$$

Hence, the equations by which the transient condition of the regulation is given now become:

$$f = \frac{k}{T_d} \cdot (\gamma + \gamma_0), \dots (105)$$

$$\gamma = 1 - \zeta \cdot \frac{1 + nm\alpha p}{1 + (1 + m + nm)\alpha p + nm\alpha^2 p^2} \cdot \left[f_{sync} \tau \right], \dots (255)$$

and

$$p\tau = \frac{f - f_{sync}}{f_{sync}} \dots \dots \dots (220)$$

If the two variables f and γ are eliminated, a differential equation of the third degree remains, with τ as the time variable, viz.

$$nm\alpha^2 p^3 \left[\tau \right] + (1 + m + nm) \alpha p^2 \left[\tau \right] + \left(1 + nm\alpha \cdot \frac{k\zeta}{T_d} \right) p \left[\tau \right] + \frac{k\zeta}{T_d} \cdot \tau = \frac{k}{T_d f_{sync}} (\gamma_0 + 1) - 1. \dots (256)$$

When the solution of this expression is again represented as a sum of terms of the form Ke^{qt} , the characteristic equation from which the quantity q can be solved becomes:

$$nm\alpha^2 q^3 + (1 + m + nm)\alpha q^2 + \left(1 + nm\alpha \cdot \frac{k\zeta}{T_d} \right) q + \frac{k\zeta}{T_d} = 0. \dots (257)$$

A new variable $\varrho = qx$ is now introduced, which can be solved from the equation:

$$nm\varrho^3 + (1 + m + nm)\varrho^2 + \left(1 + nm\alpha \cdot \frac{k\zeta}{T_d} \right) \varrho + x \frac{k\zeta}{T_d} = 0. \dots (258)$$

There is no general rule for obtaining an explicit solution of this equation of the third degree. To investigate whether the roots are real or complex, the left-hand member is split into two functions of ϱ , viz.

$$\Psi_1(\varrho) = nm\varrho^3 + (1 + m + nm)\varrho^2 + \varrho, \dots \dots \dots (259)$$

and

$$\Psi_2(\varrho) = -\frac{xk\zeta}{T_d} \cdot (nm\varrho + 1). \dots \dots \dots (260)$$

For the roots of eq. (258) Ψ_1 will be equal to Ψ_2 . If, therefore, Ψ_1 and Ψ_2 are graphically plotted, the points of intersection will correspond to the roots of eq. (258).

$\Psi_1(\varrho)$ is zero at:

$$\varrho = \varrho_1 = 0,$$

at:

$$\varrho = \varrho_2 = -\frac{1 + m + nm}{2nm} \cdot \left\{ 1 - \sqrt{1 - \frac{4nm}{(1 + m + nm)^2}} \right\},$$

and at:

$$\rho = \rho_3 = -\frac{1 + m + nm}{2nm} \cdot \left\{ 1 + \sqrt{1 - \frac{4nm}{(1 + m + nm)^2}} \right\}.$$

$\Psi_1(\rho)$ has a minimum at:

$$\rho = \rho_4 = -\frac{1 + m + nm}{3nm} \cdot \left\{ 1 - \sqrt{1 - \frac{3nm}{(1 + m + nm)^2}} \right\},$$

and a maximum at:

$$\rho = \rho_5 = -\frac{1 + m + nm}{3nm} \cdot \left\{ 1 + \sqrt{1 - \frac{3nm}{(1 + m + nm)^2}} \right\}.$$

$\Psi_2(\rho)$ is zero at $\rho = \rho_6 = -1/nm$. $\Psi_2(\rho)$ is a straight line which intersects the vertical axis at a point which is situated an amount $xk\zeta/T_d$ below the horizontal axis. When $xk\zeta/T_d$ changes, the line rotates around the point ρ_6 .

Fig. 103 gives the general form of the functions $\Psi_1(\rho)$ and $\Psi_2(\rho)$. It can be seen that these will have only real points of intersection when:

$$\frac{xk\zeta}{T_d} \leq \left(\frac{xk\zeta}{T_d} \right)_1 \dots \dots \dots (261)$$

or when:

$$\left(\frac{xk\zeta}{T_d} \right)_2 \leq \frac{xk\zeta}{T_d} \leq \left(\frac{xk\zeta}{T_d} \right)_3 \dots \dots \dots (262)$$

The region of real roots given by eq. (261) corresponds to the case already discussed of the simple RC filter and leads to inconveniently small values of the time constant of the filter, so that the smoothing of the control voltage will be insufficient. On the other hand, the new region of real roots

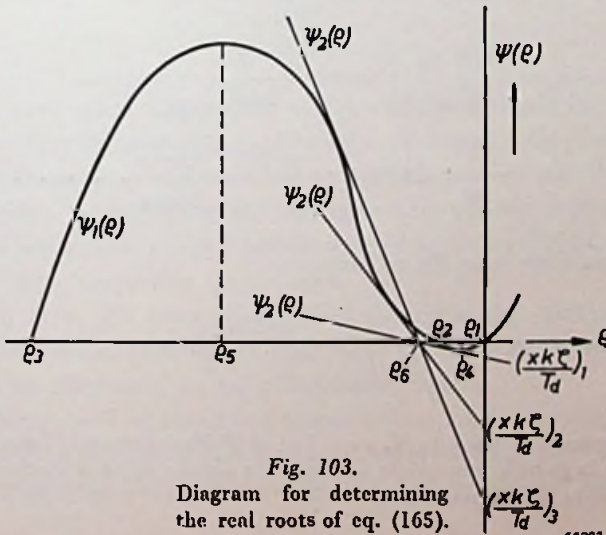


Fig. 103.
Diagram for determining the real roots of eq. (165).

given by eq. (262), due to the more complex form of the filter, gives very suitable conditions for aperiodic regulation.

The region given by eq. (261) is always present in contrast to the second region, i.e. that given by eq. (262), the availability of which depends on the choice of m and n , which also determines the extent of this region ¹⁶⁾.

6.4.3.3. Damped oscillatory transient condition versus overcritically damped transient condition

It will be useful to work out in greater detail the previously mentioned case where a discontinuity of the synchronizing frequency influences the regulation, a simple RC smoothing filter being used. To that end eq. (242), which gives the variation of the phase difference τ between the synchronizing and the relaxation signal during the transient condition of the regulation, will be investigated more closely. It will be assumed that the time constant RC of the smoothing filter largely exceeds the time constant T_d of the relaxation oscillator, so that the condition given by (247) is satisfied and both q_1 and q_2 are complex. Using the notation of eq. (248):

$$q_1 = -\frac{1}{2RC} + j\omega, \quad \dots \dots \dots (263)$$

and:

$$q_2 = -\frac{1}{2RC} - j\omega. \quad \dots \dots \dots (264)$$

Substitution of these values in eqs. (245) and (246) and of K_1 and K_2 in eq. (242) gives the following expression for τ :

$$\tau - \tau_2 = \left\{ \frac{1 + \gamma_0}{\zeta f_{sync1}} \cdot \left(\cos \omega t + \frac{1}{2\omega RC} \cdot \sin \omega t \right) - \frac{1}{\omega} \cdot \sin \omega t \right\} \cdot e^{-t/2RC} \cdot \frac{\Delta f_{sync}}{f_{sync2}} \dots \dots \dots (265)$$

This equation may also be written:

$$\tau - \tau_1 = (\tau_2 - \tau_1) \cdot \left\{ 1 - e^{-t/2RC} \left(\cos \omega t + \right. \right.$$

¹⁶⁾ Acknowledgment is made to M. van Tol of Philips' Research Laboratory, whose cooperation in gaining this insight and carrying out the required mathematical operations proved to be of great value.

$$\left. + \frac{1}{2\omega RC} \cdot \sin\omega t - \frac{\zeta f_{\text{sync}1}}{\omega(1 + \gamma_0)} \cdot \sin\omega t \right\} \dots \dots \dots (266)$$

$\tau - \tau_1$ represents the deviation of τ from its value τ_1 in the initial static condition (for times $t \leq 0$). This deviation is zero for $t = 0$ and $\tau_2 - \tau_1$ for an infinitely long time. The latter value in the final static condition is reached via a damped oscillatory transient condition.

The time constant of the damping is $2RC$ and the frequency of the oscillation is $\nu = \omega/2\pi$, so that, according to eq. (248):

$$\nu = \frac{1}{2\pi} \cdot \sqrt{\frac{k\zeta}{T_d RC} - \frac{1}{4(RC)^2}} \dots \dots \dots (267)$$

It is now assumed that RC is so much larger than T_d that the second term under the root sign is negligible compared with the first term, which gives:

$$\nu \approx \frac{1}{2\pi} \cdot \sqrt{\frac{k\zeta}{T_d RC}} \dots \dots \dots (268)$$

or, assuming RC to be x times T_d ($x \gg 1$), and taking into account that in practice $k\zeta$ is in the order of unity:

$$\nu \approx \frac{1}{2\pi T_d} \cdot \sqrt{\frac{1}{x}} \dots \dots \dots (269)$$

The time constant T_d is, moreover, almost equal to the periodic time of the synchronizing signal, hence $1/T_d \approx f_{\text{sync}}$, so that it may also be stated that:

$$\nu \approx \frac{f_{\text{sync}}}{2\pi\sqrt{x}} \dots \dots \dots (270)$$

Since x is very much larger than unity, ν must certainly be smaller than the synchronizing frequency f_{sync} . As shown previously, the damped oscillations which occur in τ are manifest as undulations of the vertical edges of the television picture when the line time-base generator is synchronized by means of automatic phase control. According to eq. (270) one complete undulation then comprises $2\pi\sqrt{x}$ lines.

Expressed in x , the time constant of the damping, $2RC$, is $2xT_d$, i.e. about $2x$ line cycles. This means that after $2x$ lines the amplitude of the undulation has decreased to $1/e$ of its initial value.

In an experimental circuit x was about 100, so that one complete undulation of the frame comprised 20π lines, i.e. about $1/10$ of the total height of the frame, whilst the amplitude of the undulation had not decayed to $1/e$

of its original value until 200 lines or about 1/3 of the frame had been scanned.

This result will now be compared with that obtained when the filter of fig. 102 is used. To determine the variation of τ after a sudden change Δf_{sync} of the synchronizing frequency, the differential equation (256) must be solved.

The solution in the form of the sum of three exponential time functions contains three integration constants which are determined by the initial conditions according to which the phase difference τ , the control voltage V_c and the voltage across the capacitor C_1 are continuous when the change of the synchronizing frequency occurs. Moreover, values must be found for m and n (see eqs. (252) and (251)), for which the region given by eq. (262), containing three real roots of eq. (258), is present. For $m = 20$ and $n = 1/20$, this region appears to cover the range from 78 to 132, in other words, the ratio $xk\zeta/T_d$ must be so chosen that:

$$78 \leq \frac{xk\zeta}{T_d} \leq 132 .$$

In the experimental circuit, $xk\zeta/T_d$ was given a value of 100, which means that $x (= RC)$ had the same value as in the case of the simple filter dealt with above, where RC was assumed to be xT_d and x was finally chosen to be 100. The result is then:

$$\Delta\tau = \tau - \tau_1 = (1 + 42.181e^{-0.0137\vartheta} + 3.144e^{-0.1613\vartheta} - 46.325e^{-0.045\vartheta})\Delta T, \dots (271)$$

where $\Delta T = T_2 - T_1$ denotes the sudden variation of the periodic cycle of the synchronizing pulses and $\vartheta = t/T_1$, i.e. the time expressed in the duration of the periodic time of the synchronizing pulses. In a line time-base generator with automatic phase control, ϑ is therefore a measure of the number of lines scanned after the instant at which the disturbance has commenced. The term $(1 + \gamma_0)/\zeta$ which occurs in eq. (265) is assumed to be unity, which is indeed practicable. If this assumption is also introduced in eq. (265) and it is moreover taken into account that:

$$\frac{\Delta f_{sync}}{f_{sync1} f_{sync2}} = \frac{f_{sync2} - f_{sync1}}{f_{sync1} f_{sync2}} = T_1 - T_2 = -\Delta T ,$$

the following expression is obtained for eq. (265):

$$\tau - \tau_2 = -\Delta T e^{-t/2RC} \left(\cos \omega t + \frac{1}{2\omega RC} \cdot \sin \omega t - \frac{f_{sync1}}{\omega} \cdot \sin \omega t \right), \dots (272)$$

which, for $t = 0$, becomes:

$$\tau_1 - \tau_2 = -\Delta T. \quad \dots \dots \dots (273)$$

The difference between eqs. (272) and (273) is:

$$\tau - \tau_1 = \Delta T \left\{ 1 - e^{-t/2RC} \left(\cos \omega t + \frac{1}{2\omega RC} \cdot \sin \omega t - \frac{f_{sync1}}{\omega} \cdot \sin \omega t \right) \right\}. \quad (274)$$

(cf. eq. (266)).

Since, according to eq. (270), $\omega = 2\pi\nu \approx f_{sync1}/\sqrt{x}$ and $RC = x T_d \approx x/f_{sync1}$, the two sine functions of eq. (274) may be written:

$$\frac{1}{2\omega RC} \cdot \sin \omega t = \frac{1}{2\sqrt{x}} \cdot \sin \omega t,$$

and

$$\frac{f_{sync1}}{\omega} \cdot \sin \omega t = \sqrt{x} \sin \omega t.$$

The value of x was taken to be 100, so that the first sine function is negligible compared to the second sine function and also compared to the cosine function, so that eq. (274) may therefore be simplified to:

$$\Delta\tau = \tau - \tau_1 = \left\{ 1 - e^{-\frac{\vartheta}{200}} \left(\cos \frac{\vartheta}{10} - 10 \sin \frac{\vartheta}{10} \right) \right\} \Delta T, \quad \dots \dots \dots (275)$$

in which ωt has been replaced by $t/T_1 \sqrt{x}$ and RC by xT_1 .

By means of eqs. (275) and (271) a comparison can be made of the response of the two filters to a sudden variation of the synchronizing frequency. In figs. 104a to 104d these expressions have been represented, the fully drawn lines applying to eq. (275) and the broken lines to eq. (271).

From top to bottom has been plotted the number of line periods ϑ which have elapsed since the disturbance commenced, whilst, horizontally, the ratio $\Delta\tau/T$ has been plotted for the two sides of a television picture with a ratio of 5 : 4. To simplify the calculations, the number of lines was taken to be 200π . The disturbance is assumed to occur when the scanning of these frames commences and to consist of a sudden variation of the synchronizing frequency in all cases.

In fig. 104a this variation Δf_{sync} (or ΔT of the periodic cycle of the synchronizing pulses) occurs at the instant $\vartheta = 0$. In fig. 104b one variation Δf_{sync} occurs at $\vartheta = 0$, and another equal but negative variation $-\Delta f_{sync}$ occurs at $\vartheta = 5\pi$; in other words: the synchronizing frequency varies according to an impulse having an amplitude Δf_{sync} and a duration of $\frac{1}{2}$ undulation of the frame edge. In figs 104c and d the amplitude of the impulse is also Δf_{sync} , but in fig. 144c its duration is 10π line times or one half of the un-

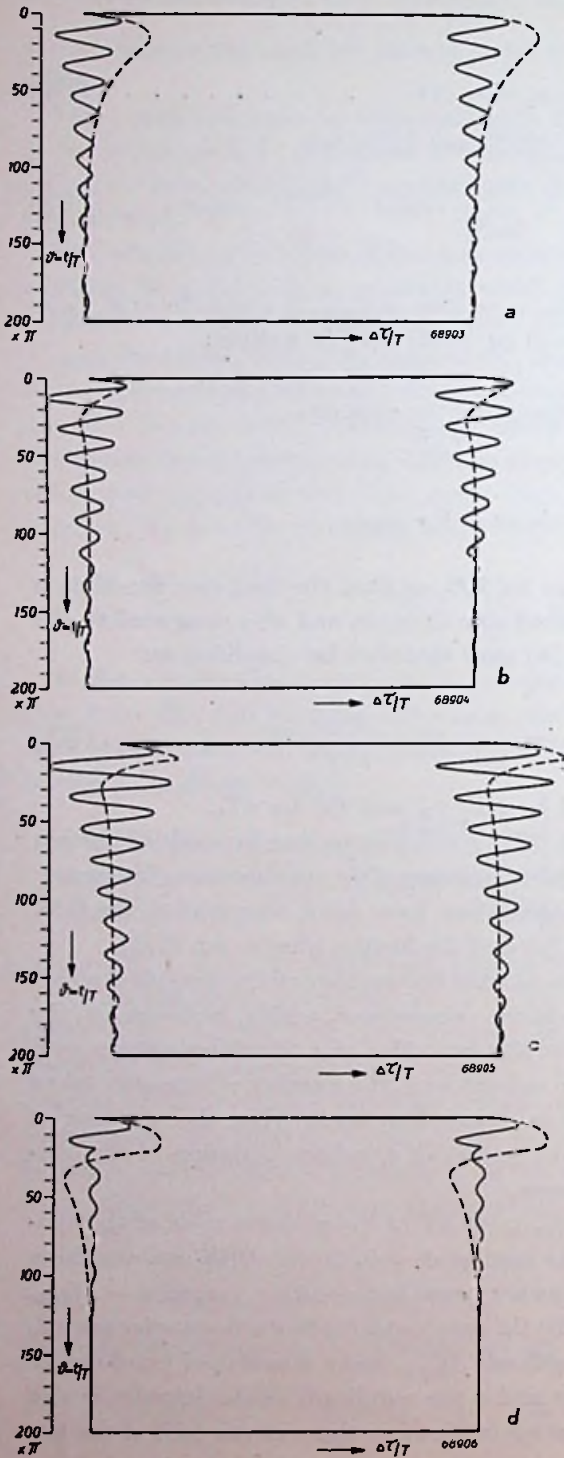


Fig. 104.

Television pictures P_0^* as obtained when in the automatic phase control a filter circuit satisfying eq. (182) (fully drawn lines) or, eq. (178) (broken lines) is used, a disturbance consisting of a sudden variation of the synchronizing frequency occurring at the commencement of the scanning. In (a) the variation Δf_{sync} occurs at $\vartheta = 0$, in (b) one variation Δf_{sync} occurs at $\vartheta = 0$, and another equal but negative variation $-\Delta f_{\text{sync}}$ occurs at $\vartheta = 5\pi$; in (c) the duration of the variation Δf_{sync} is 10π , and in (d) this duration is 20π .

dulation, whilst in fig. 104d the duration is 20π line times or one complete undulation of the frame edge.

When the duration of the impulse is 15π line periods, the variation $\Delta\tau$ will not differ appreciably from that depicted in fig. 104b for the damped oscillatory transient condition.

It is seen that, in the case of the damped oscillatory transient condition, the disturbance is much more troublesome than in the case of the over-critically damped condition. In this respect the case of fig. 104d is least serious, whereas that of fig. 104c is most objectionable. This difference is due to the particular relation between the duration of the disturbance and the modulation of the frame edge.

6.4.4. APPLICATION OF AUTOMATIC PHASE CONTROL

6.4.4.1. Deviations from the fundamental circuit

In practice the fundamental circuit for automatic phase control as outlined above will not always be strictly adhered to, and it will be useful first of all to discuss briefly some of the possible variants.

The filter circuit shown in fig. 102, for example, is not the only means for obtaining the aperiodic regulation aimed at. The same effect can be achieved with a different network consisting of capacitors and resistors.

Neither is it essential to use an EQ 80 valve for phase detection. This valve was taken as an example when discussing the problem of automatic phase control only because it provides a simple and easily explained method of converting phase differences between two pulsatory signals into a signal consisting of pulses whose amplitude is constant and whose duration is a direct measure of the phase difference. This effect may, however, be obtained with any conventional mixer valve.

A somewhat different method of phase detection which is also frequently employed consists in modifying one of the two pulsatory input signals into a signal which has a waveform with a fairly steep slope, the other pulsatory input signal being added to the modified signal, so that it is displaced along its slope¹⁷). This is again done in a mixer valve, which then supplies pulses of constant duration (i.e. equal to that of the pulsatory input signal), but of amplitude depending on the position of the pulsatory signal on the slope of the modified input signal.

When this current pulse of varying amplitude is fed to the filter of fig. 102,

¹⁷) See for example D. Kleis and M. van Tol, Experimental Transmitting and Receiving Equipment for high-speed Facsimile Transmission, Part V: Synchronization of Transmitter and Receiver, Philips Techn. Review 10, p. 325, 1949 (No. 11), in particular fig. 5.

a voltage is obtained the average value of which is again proportional to the content of the current pulses. It is in fact immaterial whether this content varies as a result of the amplitude or of the duration of the pulses being affected by the phase variation.

Suitable waveforms with a steep slope into which one of the signals could be modified are the saw-tooth and sine functions. With a view to obtaining flywheel action, the sine function is to be preferred, because this can easily be generated by exciting a resonant circuit with a pulsatory signal. In this way advantage is taken not only of the smoothing action of the filter, but also of the flywheel action due to the inertia effect of the resonant circuit.

It will further be useful to discuss the use of a multivibrator with cathode coupling as relaxation oscillator. Both the blocking oscillator and the multivibrator have been mentioned as examples of frequently used relaxation oscillators, and it was assumed that the effect of the control voltage at the grid of the self-blocking valve which produces short anode current pulses is such that the frequency of the relaxation signal increases with increasing control voltage and vice versa.

As far as the multivibrator is concerned, this is always the case in the conventional type as described in section 6.4.4.1. In this circuit the positive feedback is obtained by means of a capacitance between the anode of the second and the control grid of the first valve. Feedback may, however, also be obtained by including a common impedance in the cathode circuit of the two valves. In such a multivibrator with cathode coupling, the frequency of the output voltage is sometimes inversely proportional to the control voltage applied to the grid of one of the valves; in other words, the frequency decreases as the control voltage increases and vice versa. This necessitates modification of the circuit of the automatic phase control, the basic principle being, however, maintained.

An obvious solution is to reverse the polarity of the control voltage supplied by the phase detector, e.g. by means of a D.C. amplifying valve the output voltage of which decreases as the input voltage increases and vice versa. This output

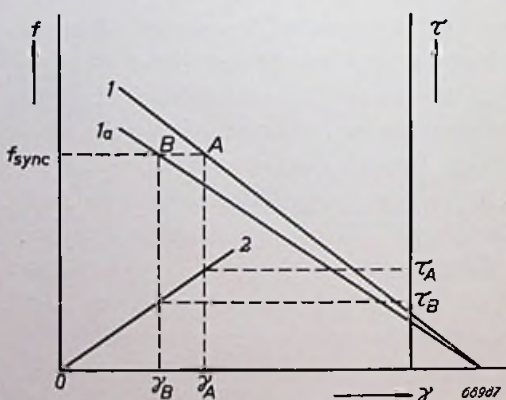


Fig. 105.

Automatic phase control in the static condition when a multivibrator with cathode coupling is used.

voltage is then used for controlling the multivibrator.

Another method of reversing the variation of the control voltage consists in including the smoothing filter in the cathode circuit rather than in the anode circuit of the phase detector. The voltage at the cathode is then used directly for controlling the multivibrator. The static condition of the automatic phase control thus obtained is represented in fig. 105 (cf. fig. 95).

A third possibility is to arrange the automatic phase control system so

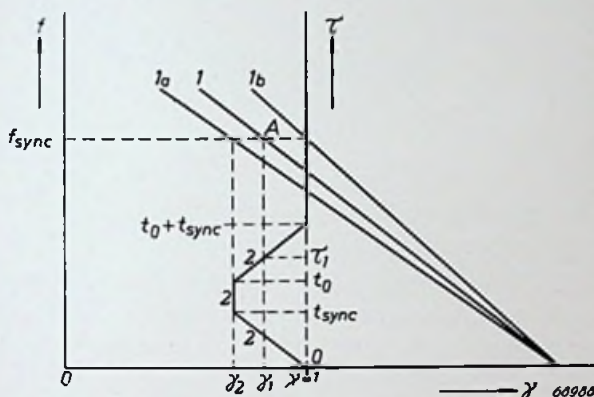


Fig. 105.

Retaining zone when a multivibrator with cathode coupling is used in an automatic phase-control system.

that the positions of the relaxation and synchronizing pulses of fig. 162, section 6.4.1, are interchanged. In this figure it was assumed that within the retaining zone each relaxation pulse is produced just after the corresponding synchronizing pulse, but now this sequence must be reversed, the relaxation signals thus leading with respect to the synchronizing signals. In this case τ is taken to be the interval between the front flank of the synchronizing pulses and the rear flank of the relaxation pulses.

Eq. (106) is then again valid, and it is seen that τ increases as the relaxation frequency decreases. Consequently the control voltage also decreases with frequency.

This means, in effect, that the retaining zone of the regulation is now determined by the uppermost inclined part of curve 2 of fig. 97. In analogy to this figure the retaining zone has been indicated in fig. 106 for this new situation.

6.4.4.2. Practical circuit

Before discussing practical circuits of line time-base generators with automatic phase control used in television receivers, it will be useful to

study the block diagram, fig. 107, which shows the general principles of automatic phase control.

The block D in fig. 107 represents a phase detector in which the signals derived from the synchronizing pulses and from the saw-tooth voltage are compared from the point of view of their mutual phase difference. The amplitude and/or the width α , speaking more generally, the "content" (time integral) of the output voltage V_D of the phase detector depends on this phase relation.

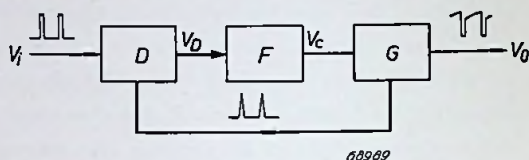


Fig. 107.

Block diagram of an automatic phase control system. D - phase detector, F - filter circuit which smooths the output signal V_D supplied by D , thus producing a control voltage V_C which governs the frequency of the time-base generator G . V_i - synchronizing input voltage; V_o saw-tooth output voltage.

The filter F converts the pulsatory voltage V_D into an average voltage V_C which fluctuates with slow variations of the phase difference, and so influences the time-base generator G that any tendency of the time-base frequency to depart from the synchronizing frequency is corrected.

An example of such a circuit is given in fig. 108. The synchronizing signal is applied to the control grid of the triode section of the ECH 42 valve; this grid is internally connected to the third grid of the hexode section.

In the triode section grid rectification takes place, so that the third grid of the hexode section is at cathode potential during the synchronizing pulses and strongly negative during the intervals between these pulses.

In the hexode section, therefore, anode current can flow only during the synchronizing pulses. Part of the alternating voltage occurring across the primary of the line output transformer is, however, applied to the first grid of the hexode section. The flyback pulses of this voltage are positively directed, so that grid rectification again takes place and the hexode section is consequently blocked during the intervals between the flyback pulses also. The hexode section is therefore conductive only when both the synchronizing and the line flyback pulses occur simultaneously. The average value of the anode current is obviously determined by the extent to which these pulses overlap.

The voltage drop across the anode resistor R_1 as a result of the anode current pulses is smoothed by the filter circuit consisting of R_1 , C_1 , C_2 and R_6 (cf. fig. 108).

The control voltage across this filter circuit is applied to the first grid of the pentode section of the ECL 80 valve via the adjustable resistor R_5 . This valve is connected as a multivibrator with the flywheel circuit $L_1 C_3$,

tuned to the line frequency, incorporated in the anode circuit of the triode section.

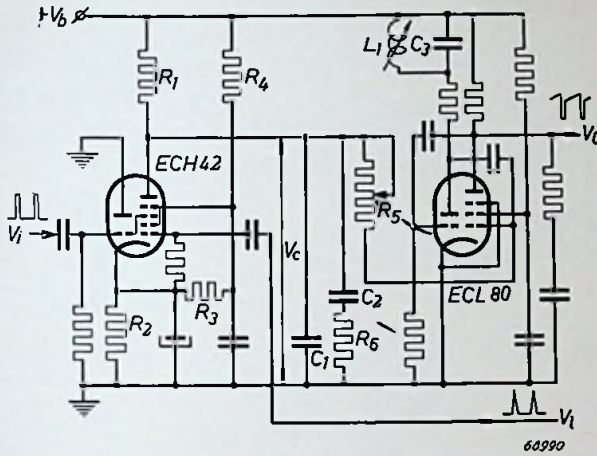


Fig. 108.

Automatic phase control system in which the hexode section of the ECH 42 valve is used as a phase detector. The filter circuit is formed by R_1 , C_1 , C_2 , R_6 . The ECL 80 acts as a multivibrator and is controlled by the voltage V_c applied to the first grid of the pentode section via the resistor R_5 . V_i - positive synchronizing pulses; V_1 - positive pulses taken from the line output transformer; V_0 - saw-tooth output voltage.

It is obvious that, when the frequency of the multivibrator increases, i.e. when in fig. 109 the flyback pulses b move to the left with respect to the synchronizing pulses a , the average anode current of the hexode section of the ECH 42 also increases. This results in a higher voltage drop across R_1 , as a consequence of which the frequency deviation of the multivibrator is reduced. The same reasoning can be applied for the case where the frequency of the multivibrator decreases. The anode current of the ECH 42 then decreases, which results in a lower voltage drop across R_1 and tends to reduce the frequency deviation. The frequency of the multivibrator is thus kept constant and equal to that of the synchronizing pulses.

On closer examination of fig. 109 it is seen that the synchronizing pulse a starts before the flyback pulse b , so that the time available for the flyback of the line output circuit is reduced. This is less serious than might appear at first sight. Actually, the shape of the flyback pulse b is approximately sinusoidal (see dotted line) and its amplitude is very large. The hexode section of the ECH 42 can therefore draw current only during the peak of the sinusoidal pulse, so that R_5 can very well be so adjusted that the commencements of the flyback and synchronizing pulses coincide.

Moreover, an integrating network may be included between the line

output transformer and the first grid of the hexode section of the ECH 42, providing a time delay in the arrival of the peak of the flyback pulse at the hexode grid. The value of the capacitor forming part of this integrating circuit can best be determined experimentally.

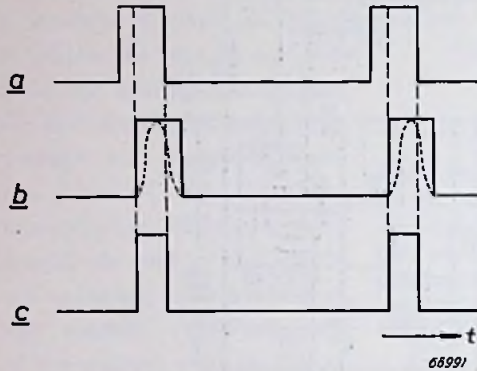


Fig. 109.

a - Synchronizing pulses applied to the third grid of the hexode section of the ECH 42 valve in the circuit of fig. 108; *b* - Pulses derived from the line output transformer and applied to the first grid of the hexode section; *c* - Resulting anode current pulses. The shape of the pulses *b* is actually as indicated by the dotted lines.

This valve must be at least a pentode, the cathode and first and second grids of which, combined with the triode T_2 , act as a multivibrator¹⁸⁾ whilst the third grid is employed for controlling the anode current.

Assume the first grid, g_1 , to be at cathode potential during a short interval. In addition to the current pulse flowing towards g_2 , an anode current pulse will also occur, provided the third grid, g_3 , is also

¹⁸⁾ Instead of a multivibrator a blocking oscillator could also be used.

Since the frequency of the multivibrator should be maintained if the synchronizing signal fails for some time in the absence of a signal or if the signal is disturbed by an interference, the resistors R_2 , R_3 and R_4 must be so chosen that the anode current is about the same, with or without synchronizing signal.

A circuit in which a valve of the time-base signal generator is used both for phase detection and for generating the time-base signal, is given in fig. 110.

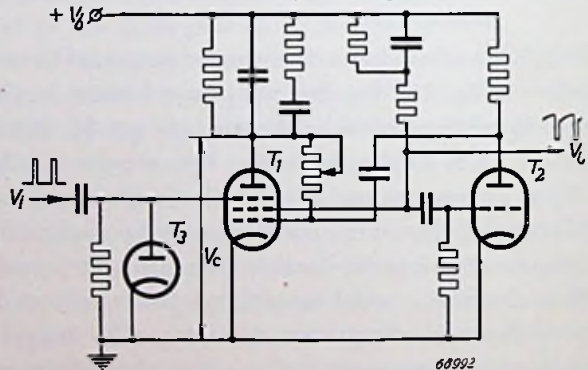


Fig. 110.

Basic circuit of an automatic phase control system, in which the cathode and first and second grids of T_1 , combined with the triode T_2 , are used as a multivibrator. T_1 also acts as a phase detector, the synchronizing pulses being applied to its third grid. The control voltage V_c at the smoothing filter in the anode circuit of T_1 is applied to the first grid of the same valve.

The diode T_3 provides for peak detection of the input signal, the negative potential of the third grid of T_1 thus being obtained automatically.

at cathode potential. These anode current pulses can be gradually decreased and even entirely suppressed by rendering g_3 more negative with respect to the cathode. When g_3 is maintained at this highly negative potential and short positive pulses derived from the synchronizing signal are superimposed thereon, anode current will flow only when a synchronizing pulse coincides partly or entirely with a relaxation pulse at the first grid g_1 .

The content of the anode current pulses is, here again, a measure of the phase difference between the synchronizing and relaxation pulses. It now suffices to include a smoothing filter in the anode circuit of the self-blocking valve: the voltage between anode and cathode can then serve as the control voltage V_c to be applied to the first grid of the same valve.

In the circuit of fig. 110 a multivibrator is used for generating the time-base voltage. The negative potential at g_3 is obtained automatically by means of an additional diode with an RC network. In this way peak detection of the input pulses is obtained, which offers the advantage that the control voltage V_c drops considerably, should the synchronizing pulses happen to fail. The relaxation pulses can then again give rise to anode current pulses, g_3 now being no longer negative. The frequency of the multivibrator then decreases with the control voltage, and as soon as the synchronizing pulses reappear, g_3 again becomes negative, and the control voltage, and thus the time base frequency, increase until the latter approaches the synchronizing frequency sufficiently to enable normal synchronizing control to be re-established.

If the negative voltage at g_3 were given a fixed value instead of being obtained automatically, the control voltage would increase to a value equal to the anode supply voltage $+ V_b$ on failure of the synchronizing pulses. The frequency of the multivibrator would then assume such a high value that it would come to lie beyond the collecting zone. In these circumstances synchronization would not be restored automatically when the synchronizing pulses reappear, and it would be necessary to readjust the frequency of the multivibrator by means of a variable grid leak in order to restore synchronization. Since this phenomenon is likely to occur each time the synchronization of the multivibrator is upset, irrespective of the cause, special measures, such as the above-mentioned diode circuit, are essential.

Finally, a circuit in which there is no risk of the relaxation frequency coming to lie beyond the collecting zone on a failure of the synchronizing signal, is given in fig. 111. In this circuit the synchronizing signal is first converted into a signal which is symmetrical with respect to a zero axis and contains a steeply descending flank, for example a saw-tooth or sine function. This signal is applied to the third grid of the combined phase detector and relaxation oscillator, this valve being so adjusted that anode

current does not drop to zero so long as the potential of the first grid is equal to that of the cathode; in other words, the symmetrical signal lies entirely within the "grid base" of g_3 .

A relaxation pulse at the first grid, no matter at what instant it occurs, will now always give rise to an anode current pulse, the amplitude of which,

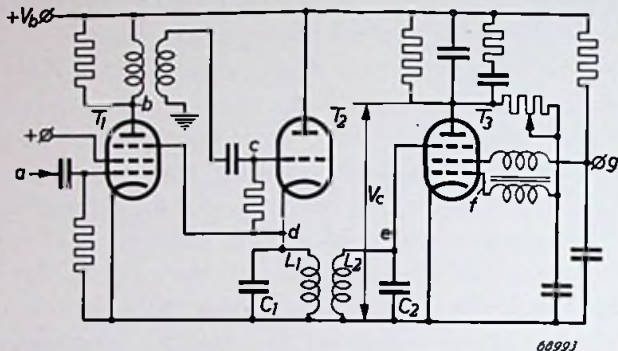


Fig. 111.

Basic circuit of an automatic phase-control system in which the cathode and first and second grids of T_3 are used as blocking oscillator. A sinusoidal signal of synchronizing frequency, derived from the video signal by means of the valves T_1 and T_2 , is applied to the third grid of T_3 , so that this valve also provides the required phase detection. The control voltage V_c is applied to the first grid of the valve T_3 .

however, depends on the value of the signal at the third grid at that particular instant, that is to say, on the phase difference between the two signals.

The adjustment should normally be such that the relaxation pulse at g_1 coincides with the centre of the descending flank of the sinusoidal or saw-tooth signal applied to g_3 .

The time-base signal is generated by a blocking oscillator formed by the cathode and the first and second grids of valve T_3 ¹⁹⁾, fig. 111. A sinusoidal voltage derived from the synchronizing signal is applied to the third grid of this valve, which thus acts as a phase detector also.

The various signals and their relationship can be seen by reference to the circuit of fig. 111 and the oscillograms depicted in fig. 112.

In the valve T_1 the first grid operates as a peak detector, so that the synchronizing pulses are separated from the complete video signal a . These pulses give rise to anode current pulses which flow through the differentiating network in the anode circuit consisting of an inductor shunted by a resistor.

In the resulting anode voltage b , only the differentiated line synchronizing pulses remain. The polarity of this signal is now reversed by transformation (signal c), and the resulting short current pulses are fed to the

¹⁹⁾ Instead of a blocking oscillator a multivibrator could also be used.

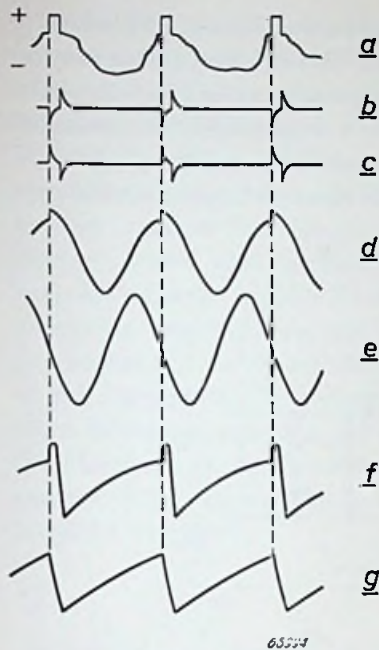


Fig. 112.

Oscillograms of the various signals occurring at the points *a* to *g* of the circuit of fig. 111, showing their shapes and phase relations.

resonant circuit L_1C_1 by the valve T_2 , the grid of which is adjusted for peak detection by the positive, differentiated leading edges of the line synchronizing signal.

The circuit L_1C_1 is tuned to the line frequency, as is also circuit L_2C_2 which is critically coupled to L_1C_1 . In this way the almost sinusoidal signal *d* is shifted 90° in phase (signal *e*) and applied to the third grid of the valve T_3 .

The saw-tooth output signal of this tube is shown in fig. 112*g*, whilst the control grid voltage is depicted in fig. 112*f*.

It should be noted that the sinusoidal signal *d* is fed back to the third grid of the valve T_1 . This is necessary only because of the equalizing pulses contained in the synchronizing signal. During the occurrence of these equalizing pulses the third grid of T_1 is forced negative by the sinusoidal signal *d*, so that these pulses cannot give rise to anode

current pulses and the signal *c* contains only pulses of line frequency.

Should the synchronization of the saw-tooth signal generated by the valve T_3 and the sinusoidal signal at the third grid of this valve be disturbed, the average value of the anode current remains nevertheless practically unchanged. This is due to the fact that, on the average, the number of relaxation pulses at g_1 , which coincide with the peaks of the sinusoidal signal at g_3 , will be equal to the number of pulses which coincide with the "valleys". The frequency of the time-base generator will therefore not deviate appreciably from the line frequency, and after the disturbance has ceased, the line frequency can easily be caught again by the synchronizing signal.

In this respect the circuit of fig. 111 is to be preferred to that of fig. 110, but its sensitivity to interference, particularly to noise interference, is usually greater. In fact, in the so-called "gate circuit" of fig. 110, interference can give rise to anode current variations only during the short intervals when a relaxation pulse is applied to the first grid of the phase detector.

In the circuit of fig. 111 it is mainly the flywheel circuit L_1C_1 which is relied upon to reduce the effect of interference. This flywheel circuit may be considered as a filter which passes only frequencies which do not differ greatly from the synchronizing frequency. If it were permissible to make the bandpass of this filter extremely narrow, it would be possible to obtain results which are as good as or even better than those obtained with the gate

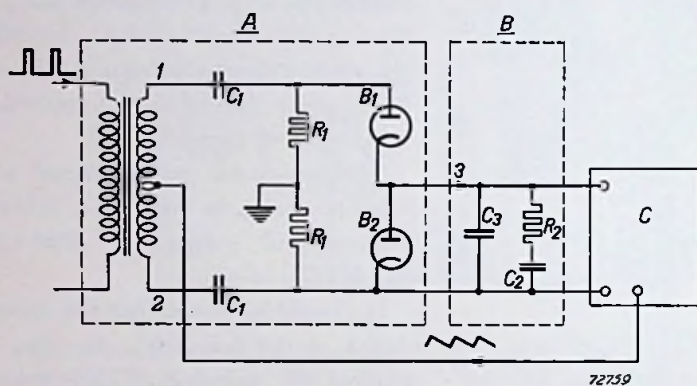


Fig. 113.

Phase discriminator circuit with two diodes. Dotted block *A* contains the phase discriminator proper, block *B* the filter circuit that feeds the control voltage to the line saw-tooth generator *C*.

circuit of fig. 110. As explained above, however, in view of the frequency fluctuations of the mains, the quality of the circuit L_1C_1 cannot be increased beyond a certain limit.

In practice the phase detector can assume various forms, and may, for example, consist of a mixer circuit with four or with two diodes, or of a single mixer valve. For particulars of these circuits the reader is referred to the literature on this subject, published mainly in the U.S.A. and including the articles quoted below²⁰).

The principle of the double-diode system will be briefly discussed. Fig. 113 represents the fundamental circuit diagram.

The first dotted block comprises the phase detector, which compares the synchronizing signal balanced via the transformer with the saw-tooth signal generated in the line time base. (The synchronizing pulse is thus applied to the phase detector in push-pull, and the saw-tooth in push-push.)

²⁰) K. R. Wendt and G. L. Fredendall, Automatic Frequency and Phase Control of Synchronization in T.V. Receivers, Proc. I.R.E. 31, p. 7, 1943.

E. L. Clark, Automatic Frequency Phase Control of Television Sweep Circuits, Proc. I.R.E. 37, p. 497, 1949.

Milton S. Kiver, Modern T.V. Receivers, Radio and Telev. News 43, p. 50, 1950.

The operation of the phase detector is as follows: Fig. 114 shows the voltages at points 1 and 2 and fig. 115 those at the anode of the diode B_1 and at the cathode of the diode B_2 . For the sake of simplicity the synchronization pulses have been represented by vertical dotted lines. The diodes B_1 and B_2 are top detectors and draw current only at the moments when synchronization pulses occur. The potential at point 3 (fig. 113) will assume the average value of the voltages depicted in fig. 115. With the phase relation between pulses and saw-tooth as represented in fig. 115 this average potential is zero. A phase shift between pulses and saw-tooth results in a positive or negative potential at point 3 with respect to earth, according to whether the pulses are shifted to the left or right along the steep flank of the saw-tooth. The voltage at point 3 is smoothed by means of the filter circuit contained in the second dotted block, the output voltage of the filter being used as automatic control voltage of the line saw-tooth generator. If necessary, the control voltage can be inverted by a D.C. amplifier.

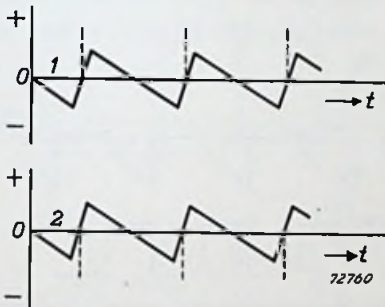


Fig. 114.

Representation of the voltages at points 1 and 2 of fig. 113 as functions of time. Synchronization pulses are schematically indicated by dotted vertical lines.

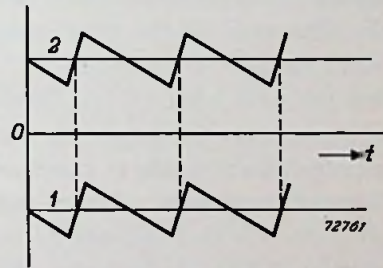


Fig. 115.

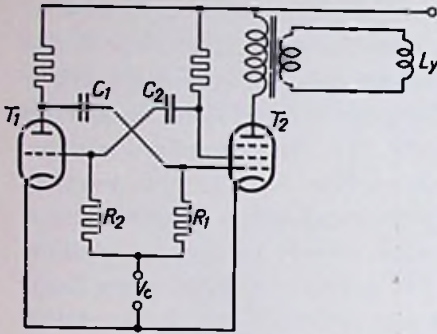
1 represents the voltages at the anode of diode B_1 , 2 the voltage at the cathode of diode B_2 .

The average voltage at point 3 is zero for the case drawn. Shifting of the synchronization pulses to the left or to the right results in the average voltage of point 3 assuming a positive or a negative value respectively.

The last practical application to be considered here is a self-oscillating line saw-tooth current generator which, contrary to most other types, can be adapted for automatic phase control as well as for any kind of direct synchronization.

As already mentioned elsewhere, most saw-tooth current oscillators have the drawback of being rather difficult to synchronize, but this can be overcome by applying a combination of the principle of a multivibrator with that of a saw-tooth current generator as depicted in fig. 116.

T_1 may be any triode, preferably with a low internal resistance. T_2 is a normal line-output valve, with a normal output transformer in the anode



72762
Fig. 116.

Self-oscillating saw-tooth current generator. L_y = line deflection coils.

circuit, possibly containing also a booster diode and an EHT-rectifier diode or whatever circuit is required. The lower part of T_2 — cathode, control grid and screen grid — acts as another triode functioning together with the triode T_1 as a multivibrator circuit. The frequency of this multivibrator may be influenced by applying a control voltage V_c in the manner shown; V_c may be obtained by means of any of the automatic phase control systems described in the foregoing pages. In the case of direct synchroniza-

tion it is possible to apply the synchronization pulses direct to the grid of T_1 . The ratio of the time constants C_1R_1 and C_2R_2 may be so chosen as to make the cut-off period and the conducting period in both valves almost equal. If there were no losses in the output circuit (ideal transformer and coils, zero internal resistance of the valve T_2), these two periods should be equal (cf. section 2.2.1). In practice the cut-off period of the valve T_2 must be somewhat shorter than its conducting period. The shape of the voltages on grids 1 and 2 of T_2 is given in fig. 117.

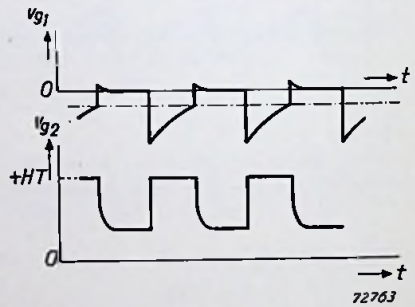


Fig. 117.

The voltages at the first grid (V_{g1}) and the second grid (V_{g2}) of the valve T_2 of fig. 116. Dash-dot line represents cut-off level of the tube.

APPENDIX I

When a constant current pulse I of duration τ with a periodic time T flows through a resistance R , the mean value of the voltage across the resistance is:

$$V = IR \cdot \frac{\tau}{T}, \dots \dots \dots (a)$$

whilst for current pulses which are not constant this voltage is:

$$V = \frac{R \int I dt}{T}, \dots \dots (b)$$

in which $\int I dt$ is the content of the current pulse.

When the duration of the pulse is short compared with its periodic time and the ripple voltage is disregarded, this mean value will be produced across the resistance R , if it is shunted by a smoothing capacitance C .

It will be useful to give the deduction of this familiar fact here, because the result also gives information about the variation of the voltage across the RC combination as a function of time when the periodic time of the pulses (or, what amounts to the same thing, their frequency) is changed. This is particularly important for investigating the transient conditions (see Appendix II).

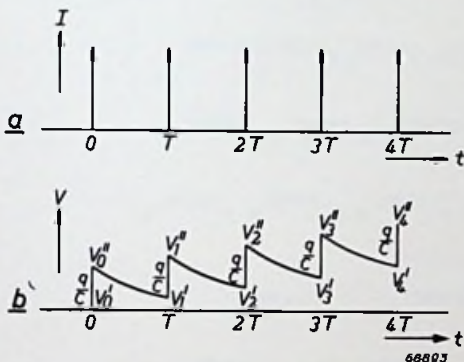


Fig. 118.

a-Idealized current pulses occurring at 0, T , $2T$, etc. b-Corresponding variation of the voltage across a filter circuit consisting of a resistance shunted by a capacitance.

In fig. 118a a graphical representation is given of the idealized pulses with an infinitely small width and an infinitely large amplitude, their content being a finite amount $q = \int I dt$.

The first current pulse at $t = 0$ results in a charge $q = \int I dt$ being supplied to the capacitor, so that the voltage V suddenly assumes the value q/C (see fig. 118b). The lowest value of the voltage surge at $t = 0$ is therefore $V_0' = 0$, whilst the top value is $V_0'' = q/C$.

During the interval between the first and the second current pulse, the charge of the capacitor C leaks away across the resistance R with a time constant RC , so that the variation of V between $t = 0$ and $t = T$ is given by:

$$V = \frac{q}{C} \cdot e^{-t/RC}.$$

After an interval T , this voltage has dropped to:

$$V_1' = \frac{q}{C} \cdot e^{-T/RC}.$$

At the instant $t = T$, another current pulse is applied and the voltage V increases with a surge q/C to:

$$V_1'' = \frac{q}{C} (1 + e^{-T/RC}).$$

When for the subsequent variation of V the instant T is denoted by $t = 0$ in a new time scale, this variation will be:

$$V = \frac{q}{C} (1 + e^{-T/RC}) e^{-t/RC}.$$

After T seconds, this voltage has dropped to:

$$V_2' = \frac{q}{C} (1 + e^{-T/RC}) e^{-T/RC},$$

which coincides with the instant $2T$ of the original time scale. At this instant, another current pulse, and thus also another voltage surge q/C , occur, and V becomes:

$$V_2'' = \frac{q}{C} \left\{ 1 + (1 + e^{-T/RC}) e^{-T/RC} \right\}.$$

Following this argument, the values of V at the bottom of the voltage surges (V') and at the top of these surges (V'') become:

$$V_3' = \frac{q}{C} \left\{ 1 + (1 + e^{-T/RC}) e^{-T/RC} \right\} e^{-T/RC},$$

$$V_3'' = \frac{q}{C} \left[1 + \left\{ 1 + (1 + e^{-T/RC}) e^{-T/RC} \right\} e^{-T/RC} \right],$$

$$V_4' = \frac{q}{C} (e^{-T/RC} + e^{-2T/RC} + e^{-3T/RC} + e^{-4T/RC}),$$

$$V_4'' = \frac{q}{C} (1 + e^{-T/RC} + e^{-2T/RC} + e^{-3T/RC} + e^{-4T/RC}),$$

and, finally:

$$V_n' = \frac{q}{C} (e^{-T/RC} + e^{-2T/RC} + \dots + e^{-nT/RC}),$$

$$V_n'' = \frac{q}{C} (1 + e^{-T/RC} + e^{-2T/RC} + \dots + e^{-nT/RC}).$$

The sums of these geometric series are:

$$V_n' = \frac{q}{C} \cdot e^{-T/RC} \cdot \frac{1 - e^{-nT/RC}}{1 - e^{-T/RC}}, \dots \dots \dots (c)$$

and:

$$V_n'' = \frac{q}{C} \cdot \frac{1 - e^{-(n+1)T/RC}}{1 - e^{-T/RC}} \dots \dots \dots (d)$$

The mean value of the voltage between two current pulses, for example between $(n-1)T$ and nT , is given by:

$$\bar{V} = \frac{\int_0^T V_{n-1}'' \cdot e^{-t/RC} dt}{T} = \frac{1}{T} \int_0^T \frac{q}{C} \cdot \frac{1 - e^{-nT/RC}}{1 - e^{-T/RC}} \cdot e^{-t/RC} dt =$$

$$\begin{aligned}
 &= -\frac{q}{C} \cdot \frac{RC}{T} \cdot \frac{1 - e^{-nT/RC}}{1 - e^{-T/RC}} \cdot (e^{-T/RC} - 1) = \frac{qR}{T} (1 - e^{-nT/RC}) = \\
 &= \frac{R \int I dt}{T} \cdot (1 - e^{-nT/RC}) \dots \dots \dots \quad (e)
 \end{aligned}$$

For $n \rightarrow \infty$, the mean value of the voltage approaches:

$$\bar{V} \rightarrow \frac{R \int I dt}{T},$$

or, for constant current-pulses having a width τ :

$$\bar{V} \rightarrow \frac{RI\tau}{T} = IR \cdot \frac{\tau}{T} \dots \dots \dots \quad (f)$$

This corresponds to the second term in the right-hand member of eq. (106), which represents the voltage across the RC filter in the anode circuit of the phase detector.

APPENDIX II

It has been shown in Appendix I that, when current pulses are fed to a resistance and capacitance connected in parallel, the mean value of the voltage across the resistance between the $(n - 1)^{\text{th}}$ and n^{th} pulse is given by:

$$\bar{V} = \frac{R}{T} \int Idt \cdot (1 - e^{-nT/RC}). \dots \dots \dots \quad (c)$$

or

$$\bar{V} = Rf(1 - e^{-nT/RC}) \int Idt \dots \dots \dots \quad (g)$$

Substitution of nT by the time t gives the time function:

$$\bar{V}(t) = Rf(1 - e^{-t/RC}) \int Idt \dots \dots \dots \quad (h)$$

On this time function the integers from eq. (g) are situated, which are obtained by substituting for t :

$$t = nT \quad (n = 0, 1, 2, 3, \dots).$$

When, at the instant $t = 0$, a series of current pulses with frequency f is suddenly fed to the RC filter, in other words when the frequency is suddenly changed from 0 to f , the mean value \bar{V} is built up according to eq. (h).

When, at the instant $t = 0$, after current pulses with a frequency f have been applied for a considerable length of time, so that \bar{V} has practically reached the constant value $Rf \int Idt$, the frequency is suddenly changed from f to f_1 , then the mean value of the voltage will reach its final value

$$\bar{V} = Rf_1 \int Idt,$$

according to the time function:

$$\bar{V} = R \left\{ f_1 + (f - f_1) e^{-t/RC} \right\} \int Idt \dots \dots \dots \quad (i)$$

This may also be expressed by stating that sudden changes of the frequency will cause the mean value of the voltage to change according to the unit function response curve:

$$U(t) = R(1 - e^{-t/RC}) \dots \dots \dots \quad (k)$$

The Laplacian transformation of this expression is given by:

$$Z(p) = R \frac{\frac{1}{RC}}{p + \frac{1}{RC}},$$

or

$$Z(p) = R \frac{1}{1 + RCp} \dots \dots \dots \quad (l)$$

For an arbitrary frequency change $f = f(t)$ the variation of the mean value of the voltage is determined by:

$$\bar{V} = R \frac{1}{1 + RCp} \left[f(t) \right], \dots \dots \dots \quad (m)$$

when the content of the current pulse is $\int Idt = 1$.

ADDITIONAL LITERATURE LIST

A. BLOCKING OSCILLATOR

1. L. Fleming: "The Blocking Oscillator as a Variable-Frequency Source" (Correspondence).
Proc. I. R. E. **37** (Nov. 1949), p. 1293.
2. J. Racker and P. Selvaggi: "Television Synchronizing Circuits" Part 1.
Radio and Television News **45** (Jan. 1951), p. 70.
3. A. F. Giordano: "Blocking-Tube Oscillator Design for Television Receivers"
Electrical Engineering **70** nr. 12 (Dec. 1951), p. 1050

B. MULTIVIBRATOR

1. H. Abraham and E. Bloch: "Mesure en Valeur Absolue des Périodes des Oscillations Electriques de Haute Fréquence"
Ann. de Physique **12**, 1919, p. 237.
2. F. C. Williams and A. Fairweather: "A 'chopped-signal' Vacuum Tube Generator with good Voltage Regulation"
Post Office Elect. Engs. J., **32**, 1939, p. 104.
3. E. H. B. Bartelink: "A Wide-band Square-wave Generator".
A. I. E. E. Trans., **60**, (June 1941), p. 371.
4. A. E. Abbot: "Multivibrator Design by Graphical Methods"
Electronics **21** (June 1948), p. 118.
5. R. Feinberg: "On the Performance of the Push-Pull Relaxation Oscillator (Multivibrator)".
Phil. Mag. **39**, (April 1948) p. 268.
6. D. Sayre: "Generation of Fast Waveforms"
Chapter V of "Waveforms".
M.I.T. Radiation Lab. Series nr. 19, edited by B. Chance. (Mac. Graw. Hill, 1949).

C. SELF-OSCILLATING SAW-TOOTH CURRENT GENERATOR

1. E. A. W. Spreadbury: "Television Servicing"
Part. 11: "The Line Output Stage" Wireless and Electrical Trader, October 27, 1951, p. 263.

D. FLYWHEEL SYNCHRONIZATION

1. J. Racker and P. Selvaggi: "Television Synchronizing Circuits" Part 2.
Radio and Television News **45**, (Febr. 1951), p. 58.
2. G. Howitt: "Evaluating AFC Systems for Television Receivers"
Electronics **25**, nr. 11 (Nov. 1952), p. 132.
3. W. L. Stephenson: "Automatic Frequency and Phase Control of Television Line Timebases for Negative Modulation Transmissions".
Mullard Techn. Communications **1** nr. 1 (May 1952), p. 18.
4. C. A. Marshall, K. E. Martin, B. R. Overton: "A Television Receiver for Use on the European (C.C.I.R.) 625-line Transmissions".
Mullard Techn. Communications **1**, nr. 3 (Jan. 1953), p. 57.
5. B. T. Gilling: "Flywheel Synchronization".
Wireless World **59**, nr. 3 (March 1953), p. 137.

LIST OF SYMBOLS

- A* voltage amplitude (expression 60); arbitrary constant (expr. 6).
- a* damping factor or reciprocal time-constant of an exponential function (expr. 6); damping constant of a tuned circuit (expr. 36); factor, dependent upon the properties of a blocking transformer (expr. 30).
- B* general notation of an electronic valve (fig. 38).
- b* ratio of periodic time of pulse cycle to natural periodic time of a resonant circuit (expr. 55).
- C* capacitance.
- C_p* stray capacitance (fig. 23).
- D* general notation of a diode (fig. 49); ratio of cut-off voltage of a valve to the H.T. supply voltage (page 74).
- d* ratio of a small time-difference τ between a pulse period and the natural periodic time of a tuned circuit to this natural periodic time, detuning measure (expr. 65); ratio of discharging- to charging time-constant of a multivibrator (expr. 129).
- e* base of natural logarithm (2.71828 . . .).
- F* arbitrary function (expr. 89, 90); ratio of frequency to minimum frequency of a multivibrator when a control voltage V_r is applied to the grids of the tubes (expr. 185).
- f* frequency.
- f₀* resonant frequency of a tuned circuit; frequency of a multivibrator for zero grid-bias control voltage (expr. 184).
- f₁* frequency of a multivibrator when using the H.T. supply voltage V_b as grid-bias control voltage V_r . (expr. 186).
- I, i* current.
- I_a, i_a* anode current of a valve current.
- I_b* current, generated by a current source, derived by application of Thévenin's theorem from a battery- or H.T. supply voltage source (fig. 10).
- I_d* current through a diode (fig. 25).
- I_g, i_g* grid current of a valve.
- I_k, i_k* cathode current of a valve.
- I_L* current through an inductance (figs. 21 and 22).
- I_s* current through a switch (fig. 25).
- I₀* initial current of a transient phenomenon (expr. 24).
- j* square root of minus one.

K	arbitrary constant (expr. 33); general indication of a network (fig. 36).
k	constant (expr. 105); ratio of discharging- to charging time-constant of a multivibrator (expr. 167, 168).
L	inductance.
\ln	natural logarithm.
\log	decimal logarithm.
m	arbitrary whole number (section 6.3.2.3); ratio of discharging time constants of an asymmetrical multivibrator (expr. 169); ratio of two capacitances (expr. 252).
n	arbitrary whole number (expr. 54); ratio of two resistances (expr. 251); number of turns of a coil or transformer (fig. 32).
p	damping factor or reciprocal time constant of an exponential function (expr. 33); operator $\frac{d}{dt}$, i.e. differentiation with respect to time.
Q	quality factor of a resonant circuit.
q	electric charge (expr. 3); damping factor or reciprocal time constant of an exponential function (expr. 224).
R	resistance.
R_i	internal resistance.
R_p	peaking resistance (fig. 43).
R_s	internal resistance of an open switch (fig. 15).
r	internal resistance, e.g. between the anode and cathode (index a), between the grid and cathode (index g) of a valve, or of a closed switch in general (fig. 4).
S	a switch (fig. 9); arbitrary complex expression (expr. 68).
$S_1(t), S_2(t)$	auxiliary sine functions for calculating the phase difference between two pulse signals (fig. 99).
T	general notation of an electronic valve (fig. 13); transformer (figs. 37, 38); repetition time of a periodical signal (fig. 35); time constant.
T_c	charging time constant of a capacitance (expr. 118).
T_d	discharging time constant of a capacitance (expr. 115).
t	time.
V	general indication of a voltage or potential difference between two points of a network.
\bar{v}	vector notation in complex plane (fig. 53).

V_a	anode voltage of a valve with respect to negative H.T. terminal.
V_{ak}	voltage between the anode and cathode of a valve.
V_b	battery- or H.T. supply voltage.
V_c	voltage across a capacitance; control voltage, variable by hand-control or automatically (fig. 61, 108, 110, 111).
$V_{c/o}$	cut-off grid voltage of a valve (fig. 39; expr. 28, 29, 30).
V_{g,v_g}	grid voltage of a valve with respect to negative H.T. supply terminal.
V_{gc}	cut-off grid voltage of a valve (expr. 117).
V_{gk}	voltage between grid and cathode of a valve.
V_k	cathode voltage of a valve with respect to negative H.T. supply terminal.
V_L	voltage across a selfinductance (figs. 21, 22).
V_R	voltage across a resistance.
V_r	control voltage, variable by hand-control or automatically (figs. 44, 45, 71, 72, 73).
V_o	initial voltage of a transient phenomenon (expr. 9).
\bar{w}	vector notation in complex plane (fig. 54).
x	time constant (expr. 253) ; abbreviated representation of an exponential function (expr. 121, 159).
y	abbreviated representation of an exponential function (expr. 160).
α	phase angle (expr. 69, 70, fig. 53).
β	phase angle (expr. 73, fig. 53).
γ	ratio of a control voltage to the H.T. supply voltage (expr. 105, 150).
Δf	difference of two frequencies (expr. 92).
Δt	time difference (fig. 58, expr. 96).
$\Delta \omega$	difference of two angular frequencies (page 63).
ε	phase angle (expr. 79, fig. 54).
ζ	a constant (expr. 106 b).
ϑ	time variable for a limited time interval (page 49); relative time variable, expressed in periodic time of synchronizing pulses (expr. 271).
ν	frequency (expr. 267).
π	ratio of circumference to diameter of a circle (3. 14159).
ρ	auxiliary variable for solving equation (257).
τ	pulse duration time or pulse width (expr. 106, fig. 62); small time difference between pulse period and natural periodic time of a tuned circuit (expr. 63).

φ	phase angle (expr. 79, 214, fig. 54).
ψ_1, ψ_2	auxiliary functions for solving equation (258) (expr. 259, 260).
Ω	ohm.
ω	angular frequency (radn./sec).
ω_0	resonant angular frequency of an undamped tuned circuit (expr. 37).
∞	infinite.

PHILIPS' TECHNICAL LIBRARY comprises 4 series of books:

- a. Electronic Valves
- b. Light and Lighting
- c. Miscellaneous
- d. Popular series

The series a, b and c published in 6" × 9" are cloth bound, gilt. The dimensions of the popular series are 3 $\frac{3}{4}$ " × 8 $\frac{1}{4}$ " bound in coloured "integral" binding.

These books are mostly published in 4 languages: English, French, German and Dutch.

a. Series on ELECTRONIC VALVES:

- Book I "Fundamentals of Radio-Valve Technique", by J. Deketh
Book II "Data and Circuits of Receiver and Amplifier Valves"
Book III "Data and Circuits of Receiver and Amplifier Valves",
1st Suppl.
Book IIIA "Data and Circuits of Receiver and Amplifier Valves", 2nd
Suppl., by N. Markus and J. Otte
Book IIIB "Data and Circuits of Receiver and Amplifier Valves", 3rd
Suppl., by N. Markus
Book IIIC "Data and Circuits of Television Receiver Valves", by
J. Jager
Book IV "Application of the Electronic Valve in Radio Receivers and
Amplifiers", Volume I, by B. G. Dammers, J. Haantjes,
J. Otte and H. van Suchtelen
Book V Idem, Volume 2
Book VI Idem, Volume 3
Book VII "Transmitting Valves", by P. J. Heyboer and P. Zijlstra
Book VIIIA "Television Receiver Design" 1, by A. G. W. Uitjens
Book VIIIB "Television Receiver Design" 2, by P. A. Neeteson

Books IIIB and VI are in preparation.

b. Series "LIGHT AND LIGHTING"

1. "Physical Aspects of Color", by P. J. Bouma
2. "Gas Discharge Lamps", by J. Funke and P. J. Oranje
3. "Fluorescent Lighting", by Prof. C. Zwikker c.s.
4. "Artificial Light and Architecture", by L. C. Kalf
5. "Artificial Light and Photography", by G. D. Rieck and L. H. Verbeek

6. "Manual for the Illuminating Engineer on Large-Size Perfect Diffusors", by H. Zijl
7. "Calculation and Measuring of Light", by H. A. E. Keitz
8. "Light technique", by Joh. Jansen
9. "Airport Lighting", by J. Stap
10. "Germecidal Lamps", by J. Hemerik
11. "Infrared Lamps", by M. Bierman and S. J. W. Zandvoort

The books 4 and 7 exist in German only. The English edition of the books 7, 8, 9, 10 and 11 is in preparation.

c. Series "MISCELLANEOUS"

- a. "Television", by Fr. Kerkhof and W. Werner
- b. "Low-Frequency Amplification", by N. A. J. Voorhoeve
- c. "Metallurgy and Construction", by E. M. H. Lips
- d. "Strain Gauges", by Prof. J. J. Koch
- e. "Introduction to the study of Mechanical Vibrations", by G. W. v. Santen
- f. "Data for X-Ray Analysis" I, by W. Parrish and B. W. Irwin
- g. "Data for X-Ray Analysis" II, by W. Parrish, M. G. Ekstein and B. W. Irwin
- h. "X-Rays in Dental Practice", by G. H. Hepple
- i. "Industrial Electronics", by R. Kretzmann

Book c is in preparation.

"POPULAR SERIES"

The books of Philips' Technical Library are on a rather high level. Again and again we received requests for technical books on a somewhat lower level. It was decided to comply with these requests and to bring such books in a "popular" series. Popular does not mean here superficial, but intelligible to a larger group of readers.

1. "Remote Control by Radio", by A. H. Bruinsma
2. "Electronic Valves for L.F. Amplification", by E. Rodenhuis
3. "The Odes and Trons Family", by J. Haantjes
4. "Battery Receiving Valves", by E. Rodenhuis
5. "Germanium Diodes", by J. Jager
6. "Cathode-Ray Tubes for Oscilloscopes", by Harly Carter

The books 3, 4, 5 and 6 are in preparation.



INDEX

	Page		Page
Application, automatic phase control —	131/142	Ferroxcube application in line output transformers	35
capacitive saw-tooth generator —	22/29	flashover	34
electronic valves in saw-tooth generators	33/37	flyback	2, 11, 38
ferroxcube —	35	flywheel resonant circuits, application of —	63/66, 138/140
flywheel resonant circuits —	63/66, 138/140	flywheel synchronization	42/146
frame deflection saw-tooth current generator —	30	filter network, special smoothing—	123/131
inductive saw-tooth generator	29/33	forward stroke	2, 9, 11, 38
line deflection saw-tooth current generator —	30/33	frame deflection	30
asymmetrical multivibrator	83/93, 98/99	free running transmitter	44, 64
automatic phase control	66/69, 108/142	frequency, blocking oscillator	27, 28, 103, 104, 106/108
Blocking oscillator	24/25, 28/29, 103/108	frequency, multivibrator	27, 28, 99/102
blocking oscillator frequency	27, 28, 103, 104, 106/108	fringe area	42
booster diode	19/20, 34	Inductive saw-tooth generator	10/21
Capacitive saw-tooth generator	4/10	inductive saw-tooth generator, application of —	29/33
Deflection, — coils	14	Linearization of saw-tooth voltage	7/10, 38
electrostatic —	3, 29	linearization of saw-tooth current	13
frame —	30	line deflection	30/33
line —	30/33	line deflection saw-tooth current generator, application of—	30/33
magnetic —	3, 29	line output transformer	14
Efficiency diode	16/19	line output valve	34
EHT, — diode	20/21, 34	literature list	147
— generation	20/21	lock-in zone	110/114
electronic valves for use in saw-tooth generators	33/37	Magnetic deflection	3, 29
electrostatic deflection	3, 29	multivibrator	25/28, 69/102, 104/108
equalizing pulses	65/139	multivibrator, asymmetrical —	83/93, 98/99
		multivibrator, frequency	27, 28, 99/102
		multivibrator, symmetrical —	72/83, 93/98

	Page		Page
Noise effects	42	scan	38
Operational impedance	115, 123	scanning	1, 2
Peaking resistance	26/27	scanning systems	2
phase detector	68, 110, 131, 135, 136, 138, 140, 141	secondary booster circuit	35
phase discriminator	68, 110, 131, 135, 136, 138, 140, 141	self-oscillating line saw-tooth current generator	33, 141, 142
primary booster circuit	34/35	stray capacitance effects	14/20
Radiation-heated booster diode	35, 36	stray oscillations	15/21
resonant circuit	43/66	switching devices	9/10
retaining zone	110/114	symmetrical multivibrator	72/83, 93/98
Saw-tooth function	2	synchronization	38/41
saw-tooth generator	3/34	synchronization, flywheel —	42/146
saw-tooth generator, capacitive —	4/10, 22/29	synchronization pulses	39
saw-tooth generator, inductive —	10/21, 29/33	synchronizing pulses	39
		Transformer, line output —	14
		transients with automatic phase control	114/131
		Valves for use in saw-tooth generators	34/37

